2011

Development and validation of a fatigue-modified, EMG-assisted biomechanical model of the lumbar region

Omid Haddad
Iowa State University

Development and validation of a fatigue-modified, EMG-assisted biomechanical model of the lumbar region

by

Omid Haddad

A dissertation submitted to the graduate faculty

in partial fulfillment of the requirements for the degree of

DOCTOR OF PHILOSOPHY

Major: Industrial Engineering

Program of Study Committee:
Gary A. Mirka, Major Professor
Max Morris
Jason C. Gillette
Matthew Frank
Richard Stone

Iowa State University

Ames, Iowa

2011

DEDICATION

I would like to dedicate this thesis to the people of Iran. To my mother and my late father, who made it possible for me to pursue this educational path. To my siblings, for the invaluable emotional support they provided me. To the many teachers and educators that inspired me along the way.

TABLE OF CONTENTS

LIST OF FIGURES

LIST OF TABLES

ABSTRACT

EMG-assisted biomechanical modeling is a well-established modeling technique for estimating muscle forces in biomechanical models of the lumbar spine. Fatigue, however, creates a problem in that fatigue alters the relationship between the EMG signal generated by the muscle and the amount of force being generated. The aim of this study was to evaluate the impact of fatigue on EMG-related components in an EMG-assisted biomechanical model: the gain factor (i.e. maximum muscle stress value in N/cm^2), force-length modulation factor, and force-velocity modulation factor. This is a particularly relevant research topic in that fatigue is considered a potential risk factor for musculoskeletal disorders, and being able to quantify muscle forces and joint reaction forces in these fatigued conditions would be helpful to understand the underlying risk factors in these types of exertion. The present study can inform and guide efforts in determining safety criteria in task design to decrease incidences of musculoskeletal disorders. This study was conducted in two phases: the isometric extension phase (1) and the isokinetic extension phase (2). Each was designed to provide the data necessary to evaluate the hypothesis that either the length-force modulation factor (Phase 1) or force-velocity modulation factor (Phase 2) need to be dependent on the level of fatigue experienced by the extensor muscle of the lumbar region.

Four subjects participated in each of these phases, performing trunk extension exertions at a level of 50% of their maximum force generation capacity to generate muscular fatigue in the trunk extensor muscles. In the isometric phase subjects performed controlled, isometric trunk extension test contraction exertions at 10^o, 20^o, and 30^o angles

of trunk flexion on three different days. In the isokinetic phase, subjects performed controlled, isokinetic trunk extension test contraction exertions at 5 and 15 degrees/sec angular velocity (concentric range of motion) on two separate days. As they performed these exertions, EMG data were collected from the longissimus, iliocostalis, multifidus, latissimus dorsi, external obliques, internal obliques, and rectus abdominis muscles.

The EMG results of the trunk extensors (the fatigued muscles) obtained from the isometric and isokinetic phases of this study indicate that the force-length and force-velocity modulation factors are independent of fatigue for the levels of trunk flexion angle and trunk extension velocity considered. The results showed that, while there were strong effects of fatigue, trunk flexion angle, and trunk extension velocity as main effects, there was no significant interaction between trunk angle and fatigue in the Phase 1 study and there was no significant interaction between the trunk extension velocity and fatigue in the Phase 2 study. Significant interactions of these variables would imply that the fatigue was differentially affecting these responses. These non-significant results imply that there is no need to adjust the force-length and force-velocity modulation factors in an EMG-assisted biomechanical model in the range of the levels of the independent variables tested.

The third hypothesis considered in this experiment focused on the need to have a fatigue-dependent gain factor in an EMG-assisted biomechanical model. It is well known that the onset of fatigue leads to a decline in the force generation capability in fatigued muscle, and it is therefore a reasonable hypothesis that the gain factor of this muscle would differ as a function of fatigue level. Using regression analysis, the ratio of pre-fatigue gain factor and fatigued gain factor was shown to be correlated well with the ratio

of the pre-fatigue and fatigued median frequency values of the primary trunk extensor muscles. This led to formal modification of the gain of the extensor muscles based on the apparent decrease in median frequency and its pre-fatigue gain factor. The results of this analysis revealed that mean normalized error between predicted and measured internal moments improved from 17.5% error to 9.6% error via the implementation of this modified, fatigue-dependent gain factor. When used to calculate spine reaction forces, the modified EMG-assisted model output shows that the compression force on L5/S1 doesn't change during fatigue development while anterior-posterior shear force increases.

To provide some validation of this new model, two new subjects were recruited to perform different fatiguing lifting exertions. These subjects performed lifting tasks for 20 and 25 trunk flexion angles on two different days in the isometric extension phase, as well as 5 and 10 degrees/sec angular velocity (concentric range of motion) in the isokinetic extension phase on two separate days. Mean normalized error between predicted and measured internal moments affirms that model accuracy improved significantly from 21.4 to 12.9%. Again, applying these results in the calculation of the spine reaction forces, the model with invariant gain factor leads to increases in estimated compression force as fatigue develops, while the modified model shows that the compression forces on L5/S1 are effectively constant. Use of this newly-developed EMG-assisted model could lead to more accurate estimates of spine loading in a manner that requires only gain factor modification without alteration of force-length and force-velocity modulation factors.

The results are particularly important for ergonomists interested in understanding spinal loading and injury risk under fatiguing conditions. This improved EMG-assisted

biomechanical modeling technique may help in the establishment of better safety criteria for occupations that generate significant low back muscle fatigue.

ACKNOWLEDGEMENTS

First and foremost, I would like to express my sincerest gratitude to my advisor Dr. Gary Mirka. Dr. Mirka displayed great patience, while challenging me to expand my horizons. Dr. Mirka's approach to graduate education has been a tremendous aid in my development as a researcher. I would also like to thank Drs. Morris, Gillette, Frank, and Stone for the constructive advice they provided as members of my doctoral committee. My research path was greatly enriched by other students in the laboratory. Xiaopeng Ning and Sangeun Jin provided thoughtful advice and involved themselves in useful discussions pertaining to my work. I would like to thank the many subjects who devoted time to this cause, as without them this would not have been possible. Lastly, I would like to thank Mostafa Zamanian for his help in editing this document.

CHAPTER 1. INTRODUCTION

1.1 Epidemiology studies

Lower-back disorders (LBD's) are recognized as the most frequently occurring and costly occupational musculoskeletal disorders. In addition to pain and stress, workers often must tolerate medical costs and loss of wages as a consequence of such disorders. Furthermore, industries are required to invest money on both the direct and indirect costs associated with LBD's. These costs include compensation, employee medical treatment, and costs related to hiring and training new staff. Epidemiological studies on this issue reveal that approximately 29.5% of claims by manual material handlers are related to the lower back area, and the majority of these are associated with overexertion (Dempsey and Hashemi 1999). Over the past several decades, researchers have attempted to control disorders associated with manual material handling (MMH) since studies of this type could bring about many physical, psychological, and economic benefits for society, employees, and employers.

1.2 Spinal biomechanical models

Previous studies have shown that biomechanical stresses on the lumbar spine have a direct relationship with risk of injury (Marras et al. 1993; Kumar 2001). The purpose of biomechanical approach in this area is to determine acceptability of each task in the range of potential activities. To achieve a quantitative understanding of compression or shear force between two spinal vertebrae, the use of biomechanical spinal models is more acceptable than making direct measurements on living human bodies. Accordingly, mathematical

models of the lumbar spine for estimating the relevant loads during various postures have been developed. The development of more accurate models will serve to ascertain knowledge of lumbar spine biomechanics, improve the ability to predict the cause and risk of injury during MMH, and provide a better basis for assessing recommendations for reducing risk factors during MMH.

Early researchers used simple static, single muscle models for predicting loads on the lumbar spine, but later studies showed that dynamic lifting leads to a 30-40% increase in the moment on the lumbar spine compared to that found in a static posture (McGill and Norman 1985) and muscle coactivation (i.e. multiple muscles) plays a considerable role in the true loading of the lumbar spine (Marras and Sommerich 1991). To overcome problems and errors associated with these simplified models, researchers have employed what is called the EMG-assisted modeling technique that captures empirical data directly from a human subject performing a lifting task and then uses these data to estimate muscle force.

1.3 EMG-assisted modeling

In EMG-assisted models, muscle forces are predicted with empirical EMG data and the accuracy of the predications may be checked by comparison of the true external moment and predicted muscle moments. To increase the accuracy of these EMG-assisted models, several other physiological factors are considered by developing muscle length and muscle shortening velocity modulation factors. It is important to note that all previous validated EMG-assisted models have considered fresh (i.e. unfatigued) muscles.

The impact of fatigue on EMG signals, previously explored by many studies, shows that EMG-force relationship is altered by fatigue and this must be addressed when employing

the EMG-assisted model for fatigued muscles. Previous studies have shown that the EMG signal of a muscle, undergoing either prolonged constant or repetitive force exertion, gradually increases while maintaining a constant force level, due to both a recruitment of new motor units as well as an increase in firing rate of those already recruited. Although it is fairly accurate for unfatigued muscles, the EMG-assisted modeling technique proves to be problematic because of this artifact when applied in conditions involving muscle fatigue.

Sparto and Parnianpour (1999) attempted to address this challenge by employing frequent maximum voluntary (MVC) exertions to compensate for this changing EMG-force relationship. The major weakness of that method, however, is relying on multiple MVC exertions, which is potentially risky for subjects and can influence the level of fatigue in the subjects. Furthermore, muscles during fatiguing recruit slow twitch fibers instead of fast twitch fibers to increase endurance. This might lead to different EMG responses at various contraction lengths and velocities in comparison to those of fresh muscles because of different mechanical features used by slow and fast twitch fibers to provide a given force. This phenomenon may lead to the deceptive interpretation of EMG-assisted models, since it relates to derivation of force-length and velocity modulation factors.

1.4 Purpose of the study

The goal of this study is to develop an EMG-assisted model that is able to accurately assess spinal loads during fatiguing exertions. This will require a detailed investigation of the impact of muscle fatigue on the maximum muscle stress value, the effect of fatigue on the force-length relationship and the effect of fatigue on the force-velocity relationship. In the

end, this methodology could help to develop task design criteria and duty cycles precisely geared towards avoidance of low-back injuries during fatiguing work tasks.

CHAPTER 2. BACKGROUND

2.1 Prevalence of low back disorders

Throughout a variety of industrial work environments, the percentage of LBD's over the whole range of work-related disorders is estimated to be between 30 and 40% (Verhaak et al. 1998; Hüppe et al. 2007, Manchikanti et al. 2009). "More than 26 million Americans in the age range 20-64 and almost 6 million more of age 65 and older experience frequent lower-back pain" (Lawrence et al. 1998. p. 796). Statistics have shown that the total direct and indirect cost for LBD's has exceeded $100 billion in the United States (Katz 2006). Accordingly, work-related LBDs in ergonomics and other relevant fields have become a major topic of focus. One of the most hazardous work-related activities in terms of inducing LBD's is manual material handling (Bernard 1997; McGill 1997; Hoogendoorn et al. 1999; Marras 2000, Punnett and Wegman 2004). Between 23.4% and 30% of work-related pain and injuries were due to manual material handling, with 57% of claims attributed to overexertion. Strains and sprains in the lower-back region result in the most expensive treatments and account for 68.5% of the costs associated with MMH injuries (Dempsey and Hashemi 1999).

2.2 Basic biomechanical models of the spine

Several different epidemiology studies have made it clear that the highest risk factors of LBD's related to unsafe distribution of spinal loads in compression, shear, and torsion forces depend on posture, time, and exertion level in MMH (Punnett et al. 1991; Marras et al. 1993; Marras and Granata 1995; Bernard 1997; Hoogendoorn et al.1999). Therefore

ergonomists employ biomechanical models to quantitatively analyze the reaction forces and moments within particular joints in order to design safe tasks and workstations for manual material handlers. The principal goal of these researchers is to develop more precise and accurate models of joint loading for determining safe workplace criteria. Due to the importance of the lower back, biomechanical spinal models have attracted special attention by investigators.

There are many different choices of spinal biomechanical models to be considered, including two-dimensional vs. three-dimensional, static vs. dynamic, or single muscle vs. multiple muscle characterizations (e.g. Schultz et al. 1982; Schultz and Andersson 1981, Chaffin 1969; Gracovetsky and Farfan 1986; Aspden 1989; Mirka and Marras 1993; Granata and Marras 1993; Granata and Marras 1995; Bean et al. 1988; McGill and Norman 1996; Cholewicki and McGill 1994; Cholewicki et al. 1995; Fathallah et al. 1997). During the past several decades, researchers have attempted to advance these models to consider much more realistic elements and boundaries as well as more reasonable assumptions to support more accurate internal load calculation.

To develop each spinal biomechanical model, the following items must be considered:

1) Defining the model based on static or dynamic assumptions
2) Identifying border and other element such as muscle, ligament, or bones
3) Quantifying all external loads
4) Calculating internal loads relying on model assumptions

The first spinal biomechanical model was developed by Morris et al. (1961). They employed a single-force vector and calculated internal muscle and spinal forces under static

equilibrium conditions. The only unknown in this model was the erector spinae force, which could be calculated by taking the moment arm of the erector spinae from fulcrum (a distance of about 2 inches) and the external moment generated by upper-body weight. This represents a very simple initial model that is still used for rough calculation of the internal force experienced at the L5/S1 intervertebral joint.

Later Chaffin and colleagues (Chaffin 1969; Freivalds et al.1984) divided the whole human body into seven solid segments consisting of upper arms, lower arms, hands, trunk (with neck and head), upper legs, lower legs, and feet. They then used the maximum voluntary torques of all joints considered in this sagittal static model, along with anthropometry data related to each segment and its posture, to predict maximum force-generation capacity during lifting in different postures. Their model, like that of Morris et al. (1961), considered the internal trunk force generator (a muscle) as a single vector and did not model antagonist muscles.

A modeling approach in which only one muscle is employed against the external load can be used to calculate muscle force and joint reaction force using simple algebra. With the addition of other muscles, the system becomes indeterminate from the standpoint of mechanical equilibrium and requires other solution methods. Some investigators have employed linear or nonlinear programming techniques (optimization) to overcome this problem. For example, Schultz and Andersson (1981) used an optimization technique by considering five major bilateral-trunk muscles (erector spinae, latissimus dorsi, internal oblique, external oblique and rectus abdominis) (Figure 1).

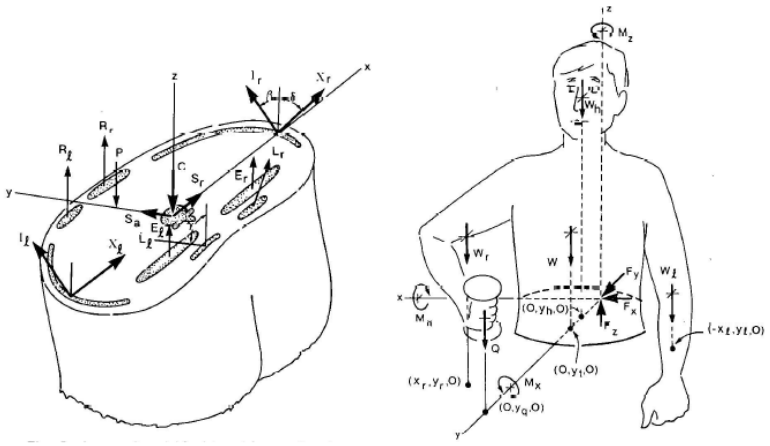

Figure 1. Schematic of the five bilateral trunk muscles (left side) and net reaction components (right side) (Schultz and Andersson 1981).

When using optimization techniques, the choice of objective function is a principal matter. Schultz and Andersson (1981) selected "minimization of compression on the lumbar vertebra as the objective function. The three equations of moment equilibrium, the ten requirements that the muscle tensions not be negative, and the ten requirements that the muscle contraction intensities not exceed a reasonable level (100 N/cm^2) were used as constraints" (Schultz and Andersson 1981. p. 81). Using this approach they were able to estimate the internal muscle forces and spine reaction forces but recognized that these were a lower bound on the true muscle and spine reaction forces, because antagonist muscle activity did not result from these optimal solutions. Bean et al (1988) and Hughes (1995) have used a double linear programming model to predict the load while handling dynamic and asymmetry load (Bean et al., 1988; Hughes 1995). In this setup, the first model determines the minimal intensity value allowing for feasible solutions, and the second linear selects the solution that minimizes spinal compression. This approach outputs sensitivities that can be used to

calculate the trade-off between spine compression and muscle intensity. As with the Schultz and Andersson formulation antagonist co-contraction was still underestimated.

Two weaknesses of the optimization modeling approach are that these models do not correctly represent the actual coactivation of antagonist muscles and these models do not accurately characterize the inherent variability in the muscle activation levels. Optimization methods have not been able to accurately predict muscle coactivity that contributes to trunk stability (Gagnon et al. 2001; Van Dieën and Kingma 2005). Marras and Mirka (1992) have demonstrated significant antagonist coactivity of abdomen muscles as a function of external load, trunk angle, and velocity. When computing the spinal load distribution, determining the impact of muscle coactivity is necessary because of its role in changing load distribution that depends on each cardinal axis, so if optimization methods estimate antagonistic muscle forces inaccurately, they would obviously be unable to accurately compute antagonistic muscle force. Optimization models are also deterministic in that they are not able to predict muscle force variability within and between subjects. Given a certain lifting task they will always find the same optimal solution and this is contrary to the reality of the variable muscle coactivation patterns observed (Mirka and Marras, 1993; Gagnon et al. 2001; Cholewicki and McGill 1994; Cholewicki et al. 1995). Another modeling approach intended to overcome the indeterminacy of spinal biomechanical models through the use of empirical data collected directly from the lifter is the EMG-assisted model (McGill and Norman 1986, Reilly and Marras 1989; Marras and Sommerich 1991, Granata and Marras 1993 and 1995; Davis and Mirka 2000). In this modeling technique, investigators estimate individual muscle tensile forces by recording the myoelectric signals of the muscles directly. These models are described in greater detail in the following sections.

2.3 EMG-assisted models

The basic technique underlying all EMG-assisted models is that the contraction force generated by a muscle can be estimated by multiplying force-generation capacity of the muscle tissue (~55 N/cm^2) (also often called the gain factor), by the muscle's cross-sectional area and its level of contraction (expressed in terms of percent of maximum). For example, when performing a lifting task, the EMG signals of the low back muscles are measured and then normalized to the maximum voluntary contraction (MVC) EMG signals for that muscle. They thus represent a percentage of maximum level and can also be presented as a percentage of maximum force exerted by the muscle. This allows the force to be estimated from this measurement. Researchers have found that other basic muscle physiological factors must also be modulated, such as force-length relationship and force-shortening velocity relationship. A brief description of the evolution of these models is presented in the following subsections.

2.3.1 McGill's model

An early EMG-assisted model was developed by McGill and Norman (1986). They employed a sagittally symmetric three-dimensional dynamic model in which skeletal muscles (active tissue) and passive tissues tolerate external moments and calculate the forces acting on L4/L5. The most important features of this model in comparison with older models are:

1) Reliance on detailed studies of spine anatomy to define relatively accurate insertion and origin points of trunk muscles to observe their orientation during lifting.

2) Monitoring markers placed on pelvis and ribcage locations using film coordinate data to improve the tracking of vertebrae motion unit to assist in computing their kinematic data.
3) Considering the cross-sectional area of each muscle and the underlying physiology of the force-length and force velocity relationships when computing the trunk muscle's tensile force.
4) Considering the effect of passive tissues in calculation of provided internal loads, leading to the discovery that passive tissues do provide a small amount of internal force compared to muscle forces.

The two major inputs to this model are:

1) EMG signals recorded by using six bilateral surface electrodes on trunk muscles.
2) Kinematic data gathered by tracking markers placed on pelvis and ribcage and computing net external moment (body weight and load-handled moment) exerted on L4/L5.

The net external moment is allocated to passive tissues (disc bending, ligament strain, and passive muscle elements) and active tissues (active elements of muscles). The internal moments provided by passive tissue are determined first, because these moments depend only on trunk flexion angle. The muscles therefore provide the remaining moments. The tensile contraction force exerted by a specific muscle is computed as the product of the maximum muscle stress value and the normalized EMG value, and is regulated by length modulation, and velocity modulation factors. Accordingly, the cross product of each muscle force and its moment arm generates a three-dimensional moment vector, and summation of these vectors gives the resultant internal moment provided by active tissue. To adjust the

total net internal moment to be equal to the net external moment at each time, a gain value is calculated, which describes the maximum stress (force per unit cross-sectional area) of the muscles. This same gain value is subsequently used for the force calculation for all muscles in this step.

In conclusion, after finding individual tensile forces produced by different elements, we can calculate the resultant distribution of loads such as compression, torsion, and shear on the lumbar spine. This model indicated that the passive tissue moment amounted to less than 1% of the total, and active tissues were the dominant elements used to tolerate the net external moment.

Although this model had many advantages, it had a major point of weakness:

1) A variable gain factor, requiring modification in each trial (not the same for the same subject across trials) - conflicts with basic physiology that requires that a muscle's contraction force exertion capacity should be directly related to muscular cross-sectional area, because it must be constant for individual (Granata and Marras 1993).
2) Only sagittally symmetry lifting was investigated in this model, whereas they expanded this model to find impact of axial trunk-twisting motions (McGill and Hoodless 1990) and lateral bending- motions (McGill 1992).

2.3.2 Marras's model

A second EMG-assisted model was described by Marras and co-workers, who, over the past 15 years, developed a basic EMG-assisted model very similar to that of McGill and Norman (1986). The first model for the Marras group was presented by Reilly and Marras

(1989). It relied on trunk-muscle EMG activities describing relative changes of load distribution on the spine. However, they didn't consider maximum muscle stress values, and therefore did not present any direct computation of muscle tensile forces. Then Marras and Sommerich (1991) published an EMG-assisted biomechanical model that considered the maximum muscle stress value. It had the same limitations as the early McGill models (applying varied maximum muscle stress value). Furthermore, as the authors pointed out, this model could be improved with more accurate estimates of the force vectors, the muscle cross-sectional areas, and the locations relative to the spine.

Granata and Marras (1993) found that the maximum muscle stress or gain factor values for a given subject did not change significantly during the experimental trials. The fixed maximum muscle stress value in this model had a significant advantage over the McGill and the previous Marras's models that used variable values. This was not only because it was consistent with physiological expectations, but also because it provided a means of validating the models. In this model with constant gain factor, the predicted internal moment should be as close as possible in equilibrium with the external moment. The regression coefficient between the estimated internal moment and the external moment might be used to verify the accuracy of the model. But, like Marras's previous models, this model still employed simplified and insufficiently accurate muscle force vector data. Marras and Granata (1995) addressed this weakness by defining a more accurate anatomical muscle model such that muscle origin and insertion points were defined as three-dimensional locations, coplanar with the iliac crest and 12th rib, respectively. The structure of this anatomical model can be visualized as two "plates" that represent the attachment point of the muscles in the pelvis and the thorax. The muscles and force vectors were represented by a

connecting line between origin and insertion points placed on two plates, instead of at each muscle where orientation changes during trunk flexion or in lateral bending (Figure 2). Using this approach, they could provide new insight to the process of finding each force vector as well as monitoring changing length and velocity of contraction shortening by knowledge of coordination of each attached point in space.

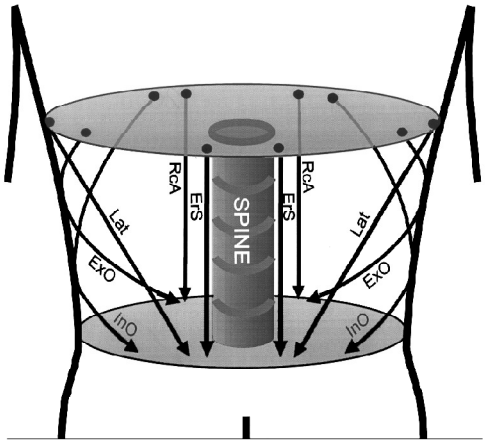

Figure 2. Origin and insertion points of trunk muscles are presented as lines between two defined plates (Marras and Granata 1995).

2.3.3 Davis's model

Davis and Mirka (2000) took another step in developing the EMG-assisted model by using multiple vectors instead of single force vectors for the latissimus dorsi, external oblique, and internal oblique and sampling EMG signals at different locations on these muscles into a transverse –contour model. Furthermore, they used in vivo digitized coordination of origin and insertion points to find more accurate muscle orientation in symmetric and asymmetric trunk flexed angles. With these coordination points, they could compute action line, changed length and velocity of each muscle force vector. Their results revealed that, for both broad and flat muscles, consideration of multiple force vectors rather

than the traditional single vector is necessary in three-dimensional asymmetric lifting tasks to find more precise shear forces. Such forces are recognized as a risk factor in occupational lower-back risk injuries.

2.3.4 Sparto's model

The previous EMG-assisted models described above have primarily focused on non-fatigued muscles, even though repetitive manual material handling is a risk factor for LBDs. A validated biomechanical model under these fatigued conditions could help us to identify biomechanical implications of fatigue and the impact of fatigue on load distribution on the lumbar spine. Sparto and Parnianpour (1999) developed an EMG-assisted model that included repetitive fatiguing trunk exertions. To measure initial maximum dynamic torque exertion, each subject performed three isokinetic (15deg/sec) maximum voluntary contractions (IMVC) from 35 forward flexion angle to the upright posture, during which the average torque was computed for the range 25 to 10 degrees. They recorded EMG signals and torque output for 16 men placed within an isokinetic trunk dynamometer while performing 35% or 70% IMVC isokinetic (15deg/sec) trunk extensions from 35 forward flexion degree to upright posture with two repetition rates of 5 or 10 extensions per minute. The pelvis and lower extremity of subjects were restricted during submaximal exertions. To quantify the decreased capability of IMVC generation, IMVCs were performed once per minute. They showed that latissimus dorsi and trunk flexor EMG signals were less than 15% MVC, meaning that this level of activation didn't cause short-term fatigue using erector spinae as the primary trunk extensor, and an initial activation level of greater than 35% MVC was assumed to be due to fatigue. In this study, they considered two gain factors. One is an

pre-fatigue gain factor (same across all levels of fatigue) called invariant gain factor, like that used in previous models, for latissimus dorsi, rectus abdominis, external oblique, and internal oblique. The second gain factor is a time-varying (i.e. fatigue-varying) gain applied to the fatiguing erector spinae muscles. This time-varying gain factor is modified for each exertion during fatiguing exertion because fatigue artifacts associated with increased EMG signals were recorded from erector spinae. After processing the EMG signals, the amount of tensile force of each muscle was computed using an EMG-assisted model similar to that of Marras. The following equation for calibrating muscle force was derived by considering the two gain factors as follows:

$$\sum \tau_{Ext} =$$

$$Gain_{invariant} \sum (\tau_{Latissimus\ dorsi} + \tau_{Rectus\ Abdominis} + \tau_{External\ Oblique} + \tau_{Internal\ Oblique}) + Gain_{variant} \sum \tau_{Erector\ spinae} \quad (1)$$

They also computed an invariant gain factor for erector spinae to support a qualitative comparison of these two gain factors. Their results revealed that the amount of erector spinae is highly dependent on the assumptions of gain factor selection (Figures 3 and 4). Assuming an invariant gain factor, erector spinae tensile force increases significantly during submaximal exertions. Meanwhile, the results of 35% IMVC using 10 repetitions per minutes showed a 35% reduction in IMVC after three-minute exertions. They also showed that a theoretical reduction of IMVC could be reflected by using a time-variable gain factor. Furthermore, they concluded that, unless the gain factor was modified as a function of time

during repetitive exertions, marked increased compression and shear forces were incorrectly predicted.

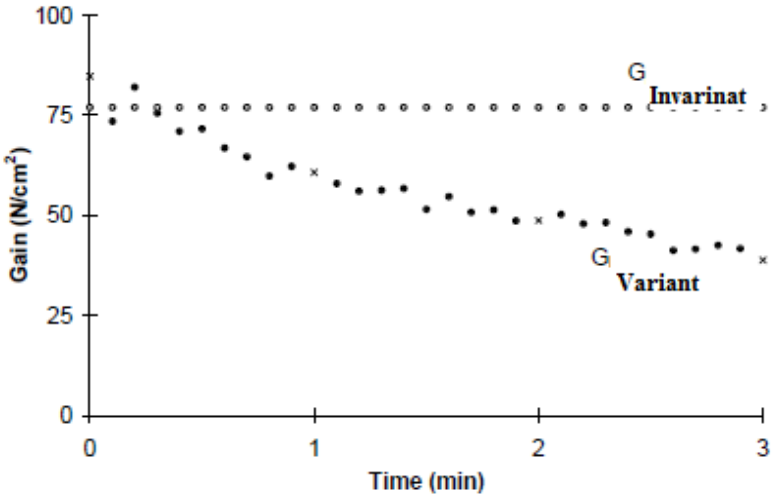

Figure 3. Computed variant ($G_{Variant}$) and invariant ($G_{Invariant}$) gain factor for erector spinae during the exertion of a repetitive isokinetic test at 35% IMVC and 10 repetitions per minute (Sparto and Parnianpour 1999).

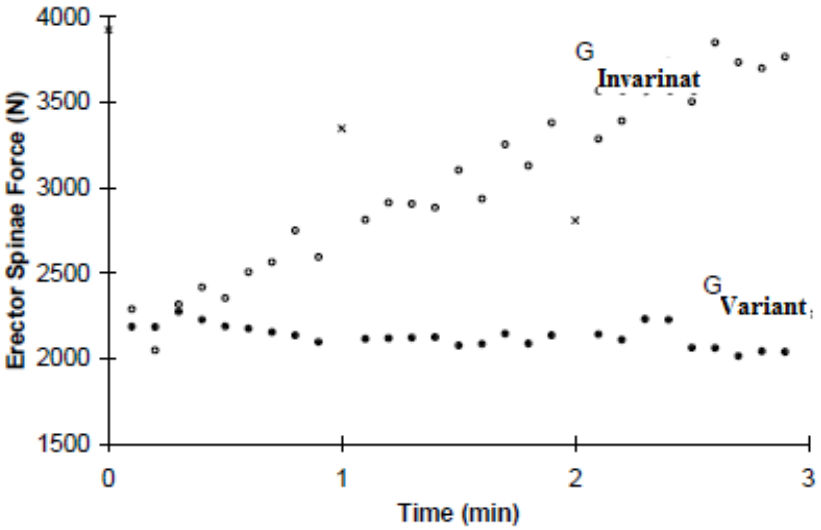

Figure 4. Computed erector spinae tensile force with respect to invariant and variant assumption of gain factor while exertion of a repetitive isokinetic test at 35% IMVC and 10 repetitions per minute (Sparto and Parnianpour 1999).

This study represents the only effort to develop an EMG-assisted model for fatigued muscles. The model was calibrated with subject performing frequent maximum voluntary contractions which can accelerate the development of fatigue, de-motivate the participants and increase the risk of injury. In addition, Sparto and Parnianpour (1999) used same force-length and force-velocity modulation factors for both fresh and fatigued muscle. It is believed that these factors might change under conditions of muscle fatigue, given differences in the mechanical properties of slow and fast twitch fibers. These limitations are the focus of this dissertation research.

2.4 Basic physiology of electromyography

Since electromyography plays such a central role in this research, a brief summary of its development is provided here. I will begin with the basic physiology of the sliding filament theory of skeletal muscle contraction. Inside the muscle cells are two types of protein filaments (actin and myosin) that interact and generate the force during muscle contraction (Figure 5).

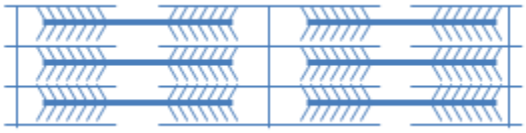

Figure 5. Sliding filament model of muscle contraction.

Their interaction involves the attachment of part of the myosin molecule to an attachment point on the actin filament and a "swiveling" of this myosin head which causes the actin to move relative to the myosin molecule. To contract skeletal muscle, the muscle membrane (sarcolemma) is depolarized. This requires acetylcholine to be released by a motor neuron at the neuromuscular junction. When the sarcolemma has been depolarized, this depolarization will spread to the membrane of the sarcoplasmic reticulum (SR) where the SR releases calcium ions into the interior of the muscle cell. In the presence of these calcium ions the binding site on the actin molecule is revealed allowing the myosin head to attach and swivel (Duggan and Martonosi 1970). In this way, the muscle contracts by pulling the thin actin filaments past the thick myosin filaments (Ebashi 1991).

The physiological basis of surface electromyography is the recording of action potential (depolarization / re-polarization of the sarcolemma) conducted in muscle fibers by surface electrodes at the skin surface (De Luca 1993, De Luca 1997). The sarcolemma is the origin of the electromyographic signal. It is composed of a thin lipid semi-permeable membrane with various channels through which certain ions can move between the intracellular and the extracellular fluid (Lamb and Hobart; 1992). The intracellular fluid has an organic anion (A^-, too large to flow through the membrane) and a high concentration of potassium (K^+, small enough to pass through the channel in the membrane) ions (Merletti and Parker 2004). The interstitial fluid has a high concentration of sodium (Na^+ has difficulty in penetrating the membrane) and chloride (Cl^- is small enough to pass through the membrane) ions. During resting the membrane potential is approximately -70mv. K^+ diffuses into the extracellular fluid due to higher intercellular concentration compared with the outside. Increased positive charge on the extracellular side slows the diffusion of K^+ ions through the membrane. On the other hand, because of the interaction between the Cl^- concentration gradient and potential difference, the Cl^- must to stay in equilibrium. The net resultant effect of K^+ and Cl^- concentrations on extracellular and intracellular concentrations, respectively, creates a positive electrical charge on the outside and a negative electrical charge on the inside of membrane that repel each other.

The presence of K^+ drives Na^+ into the cell, potentially leading to an increase in intracellular positive charge. Sodium-potassium pumps actively maintain the potential difference across the membrane when muscle fibers are in the resting state by using metabolic energy to transfer Na^+ ions to the extracellular side of the membrane. This potential difference remains in equilibrium until receiving either an external or internal

stimulus. Stimulation of the muscle fiber causes a sudden influx of Na^+ into the fiber, leading to rapid depolarization of the membrane until the fiber reverses its polarity. When depolarization of the membrane under the motor endplate occurs, ion current flows between the active and inactive regions. This current flow causes permeability to Na^+ to rapidly increase in the inactive region and an action potential propagates away from the initial active region in both directions along the muscle fiber until it passes through the transverse tubules in the sarcolemma. Accordingly, calcium release by the SR in response to the action potential allows for muscle contraction to occur (Drewes 1999). The EMG technique was first introduced by Adrian and Bronk in 1929 to detect motor unit action potentials of single fibers. It was developed and applied over the past several decades in measuring parameters such as frequency, amplitude, and recruitment threshold of muscle fibers. These measurements directly provide valuable insights into recruitment patterns of different motor unit types during single contractions, on and off the muscle, and aid in computing sub-maximal force generated by muscles under consideration, as well as the development of fatigue in muscles (Arendt-Nielsen and Mills 1985; Adam and De Luca 2003).

2.4.1 EMG-force relationship

Milner-Brown et al. (1973) showed that integrated EMG signals recorded by surface electrodes (after rectifying and smoothing) change linearly with tensile force generated by the muscle. Although some researchers present EMG as a direct index, others have recommended complex equations to estimate muscle contraction tensile force (Redfern 1992). Previous studies have shown an enhancement in force in pre-fatigued muscle assigned to the recruitment of regularly larger and faster twitch fibers with larger conduction velocity

(Heckathorne and Childress 1981). Clearly, we might expect this relationship to be dependent on both motor unit recruitment as well as firing rate during high level force exertion. To find a reliable EMG-force relationship, we must identify the impact of muscle length, contraction velocity, and fatigue on EMG signals to avoid some physiological artifacts created by these parameters and to develop a much more accurate model (Redfern 1992).

2.4.1.1 Impact of muscle length on EMG-force relationship

Tensile force generated by muscle is highly dependent on length (Rassier et al. 1999). Skeletal muscles generally have two major parts that provide force: passive and active. The passive part acts as a rope and correlates to extension of muscle in which greater extension provides more passively tensile force (McGill and Norman 1986; Lloyd and Besier 2003). The active part depends on altered positions of thin and thick filaments compared to the resting length of the muscle. From a physiological standpoint, when the muscle is near its resting length, the opportunity for interaction between the thick and thin filaments will be maximal (Crowninshield and Brand 1981). This means that the maximum active contractile tension occurs at the resting length of the muscle. However, when the muscle shortens, an opposition occurs between the thin filaments on facing sides of the sarcomere. This reduces the opportunity for formation of cross bridges and leads to decreased active contractile force (Chaffin et al. 1999). When the muscle lengthens, the opportunity for interaction between the filaments decreases until there is little chance for the formation of cross bridges, at which point no more active tension can occur. Given that the capacity of force exertion is affected

by muscle length, in order to generate constant force, EMG signals must change for different muscle lengths. At resting length, with greater opportunity of overlap between actin and myosin, smaller-amplitude EMG signals are observed, while in shortened and lengthened muscle, where more motor units are recruited to provide force equivalent to that of the resting length, greater-amplitude EMG signals are observed. This behavior needs to be considered in the EMG-force relationship. Hence, Marras and coworkers experimentally determined the following nonlinear force-length factor to modulate the impact of muscle length on EMG signals (Granata and Marras 1995; Marras and Granata 1997).

$$f(l)= -3.2+10.2l-10.4\ l^2 + 4.6l^3 \qquad (2)$$

While $l= (L\ (t)/L0)$

L (t): Instantaneous length of the muscle

L0: Resting length of the muscle at 20° of trunk flexion.

This force-length modulation factor agrees with the expanded form of a similar factor proposed by McGill and Norman (1986).

2.4.1.2 Impact of shortening velocity on EMG-force relationship

Previous studies have shown that the capacity of force exertion is inversely related to muscle shortening velocity (Wilkie 1950). Huxley (1957, 1974) explained that this phenomenon might be due to increased muscle shortening velocity leading to lower odds for filaments to bind and separate, and therefore to provide the required muscle exertion force. Lippold (1952) showed that only shortening velocity (concentric phase of movement)

and not lengthening velocity (eccentric range of movement) has impact on force generation capacity and that, further, with enhanced shortening velocity during constant tensile force, EMG amplitude increases (Bigland and Lippold 1954). This increase of EMG amplitude is directly related to decrease in the opportunity of cross-bridge formation at higher velocities and the recruitment of more motor units to supply a constant force. Similar to what was determined for changing length, Marras and Granata (1997) determined a new physiological factor for shortening velocity. Accordingly, a unit less factor must be multiplied by relative muscle activity, f (v), to modulate the associated EMG artifact during changing shortening velocity. The following force velocity modulation factor includes the instantaneous contraction velocity of each sampled muscle determined from anthropometry and kinematic data (Marras and Granata 1997).

$$f(v)=1.2-0.99v+0.72v^2 \quad (3)$$

Where v is computed by $\Delta L(t)/L0/sec$

2.4.1.3 Impact of fatigue on EMG-force relationship

In general, fatigue has been associated with enhanced amplitude of EMG signals and declined frequency of surface EMG power spectrum (Sparto et al. 1998; Potvin 1997; Petrofsky et al. 1982) therefore the EMG-force relationship of fresh muscle should differ from that of fatigued muscle. Fatigue causes reduced motor unit action potential since it cannot turn fast twitch fibers on because it cannot reach the stimulation threshold (Allen and Lamb 2008). Therefore, slow-twitch fibers are recruited to provide muscle contraction tensile

force. Because of the decreased ability of slow-twitch fibers compared to fast twitch fibers in generating contraction force (Burke et al. 1973), to provide constant force, a muscle must recruit a greater number of slow-twitch fibers instead of fast–twitch fibers to compensate and maintain the necessary force. Increased amplitude of EMG signal during a fatiguing exertion (Figure 6) results from a greater synchronization of action potentials and a larger population of recruited slower-twitch fibers. Employing slow-twitch fibers instead of fast-twitch fibers during muscle fatigue introduces artifacts on EMG signals used to predict the muscle force generation.

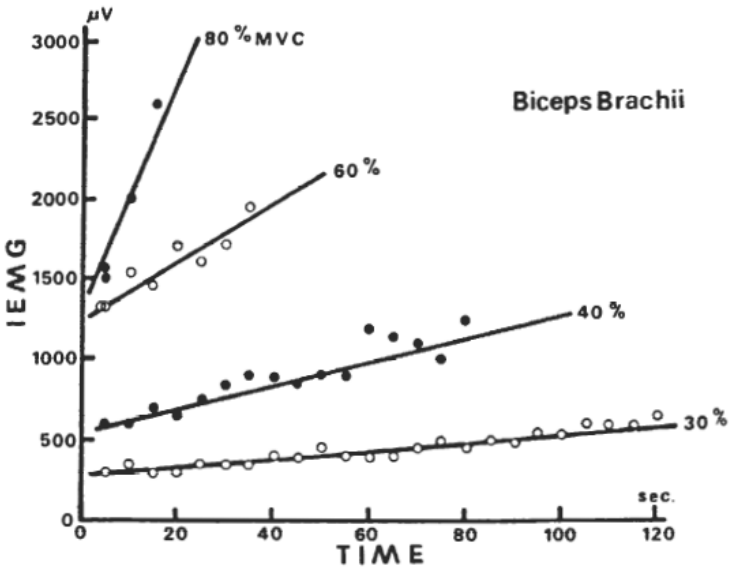

Figure 6. Increased integrated EMG (IEMG) signal for biceps brachii due to fatigue at different levels of MVC (Moritani et al. 1982).

Meanwhile, the median frequency is usually used as indicator of muscle fatigue (De Luca 1993) because the small size of slow-twitch fibers causes a smaller conduction velocity which generates a lower median frequency of the EMG power spectrum.

2.4.1.4 Impact of fatigue on force-length modulation factor

As discussed earlier, changing muscle length produces the physiological artifacts on EMG signals considered in an EMG-force relationship. The opportunity of cross-bridge formation plays a major role on different lengths, and is greatest at resting muscle length. However, whether or not the likelihood of this formation is the same for both slow and fast twitch fibers remains an unanswered question. Accordingly, a recorded EMG signal from fresh muscle produced by employing fast-twitch fiber might be different as compared to fatigued muscle by recruiting more slow-twitch fibers to exert constant force while changing length. Moreover Arendt-Nielson and Mills (1985) found muscle fiber diameter has a direct influence on conduction velocity, which plays a significant role on proportion of median frequency. As muscle length varies, the diameter of muscle fibers must change to be consistent with constant volume of the muscle. As muscle length increases, fiber diameter decreases, resulting in reduced conduction velocity of muscle fiber (Mamaghani et al. 2002). Mannion and Dolan (1996) found that the median frequency of the erector spine in both thoracic and lumbar regions declined with increasing torso flexion angle; however, changes were more pronounced in the lumbar region. Therefore muscle length has a significant impact on median frequency as well as on EMG amplitude (Inbar et al. 1987; Dolan et al. 1995). During post-fatigue, the muscle length-EMG median frequency relationship is substantially altered in comparison with that for pre-fatigue (Doud and Walsh 1995; De Ruiter and De Haan 2001). All of these observations would imply that the relationship shown in Equation 2 may be altered as a function of muscular fatigue.

2.4.1.5 Impact of fatigue on force-velocity modulation factor

Previous studies have shown that maximum power (force×velocity) and maximum shortening velocity are depressed during fatiguing, and force capacity is inversely influenced by shortening velocity (De Ruiter and De Haan 2001; Curtin and Edman 1994). Meanwhile, a muscle must recruit new motor units in order to maintain a given force under developed fatigue, and increased shortening velocity is seen in the increased amplitude of EMG signals. It is believed that the reduction in maximum shortening velocity is due to an alteration in cross-bridge kinetics due to recruiting of slow-twitch fibers rather than fast-twitch fibers in fatiguing muscle (Chaffin 1999) as a result of fast units reaching their peak tension and relaxing more rapidly than slow units.

The exertion of constant torque at a given shortening velocity will lead to the development of fatigue and the recruitment of new motor units. We would expect that their collective EMG signals differ from those of fresh muscle, since their ability to provide the required shortening velocity and force differs from that of fast twitch fibers. Although we can employ the force velocity modulation factor for fresh muscle to compute the EMG-force relationship, we do not know whether or not this factor is valid for fatigued muscle, since it involves the recruitment of different motor units. By reviewing various factors that affect EMG signals, it is apparent that factors that could potentially introduce physiological artifacts need to be recognized and controlled when using EMG signals to compute muscle contraction forces for fatigued muscle. This implies that Equation 3 may need to be adjusted as a function of muscular fatigue level.

2.5 Purpose of study

As EMG amplitude increases for muscles fatigued under constant force, the standing EMG-force relationship outputs incorrect estimates of muscle force as it does not modulate the impact of fatigue. As previously mentioned, the mechanical features of slow and fast twitch fibers differ, and at a given constant force the number of necessary motor units required to generate the force also differs. This has a direct impact on EMG signals, and it is reasonable to expect that length and velocity modulation factors derived from investigation of fresh muscle may be inappropriate for fatigued muscle.

The goal of this study is to investigate the impact of prolonged isometric exertion on the EMG-force relationship applied in the EMG-assisted model. By considering constant external force exertion in pre-fatigue and post-fatigue muscle, we will try to validate the EMG-assisted model for accurate estimation of internal force and spine loading. Accordingly, we will examine the impact of fatigue on three factors:

1. Force-length modulation factor: to identify how recorded EMG signals differ for differing muscle lengths between the pre-fatigue and post-fatigue muscle states.
2. Force-velocity modulation factor: to identify how recorded EMG signals differ for differing shortening velocities at a given length change between the pre-fatigue and post-fatigue muscle states.
3. Gain factor: to find the best way to modify this parameter without requiring frequent MVC exertion by subject.

CHAPTER 3. PILOT WORK

3.1 Objectives

The purposes of these experiments were to observe the impact of fatigue and length, as well as fatigue and shortening velocity, on EMG signals. The results of these experiments may reveal whether new force-length and force-velocity modulation factors need to be developed for the EMG-assisted model when applied to conditions involving repetitive manual material handling or fatigued muscles.

3.2 Methods and Materials

3.2.1 Participant

One male graduate student participated voluntarily in this experiment. The subject was 29 years old, with a height of 172 cm and whole body mass of 82 kg. The subject had no current or past chronic low back disorders.

3.2.2 Apparatus

Electromyography activity of trunk extensors was recorded using six bipolar surface electrodes (Model DE-2.1 Bagnoli™ from Del Sys, Boston, MA). These EMG data were amplified (1000×) and collected at 1024 Hz.

A Kin/Com lumbar dynamometer (Chatanooga Group, Inc., Hixson, TN, USA) (Mirka and Marras, 1993) was used to provide the static resistance and required trunk flexion

angle for collection of the angle-specific maximum voluntary contraction (MVC) EMG data from the lumbar extensors. This dynamometer was also able to provide a measure of trunk flexion angle and the angle-specific moment generated by the subject during isometric and isokinetic contraction, required for computation of the external moment provided by subject. It was further used to restrict the motion of pelvis during the experimental trials.

3.2.3 Experimental design

We divided the experimental design into two phases: isometric extension task and isokinetic extension task.

3.2.3.1 Independent variables

For the isometric extension phase, there were two independent variables: sagittally symmetric trunk flexion angle (15°, 30°, and 45°) and fatigue (pre-fatigue, post-fatigue). The trunk flexion angle was determined as the angle between a vertical reference line and the forward angular deviations from the reference line.

The isokinetic extension phase had two independent variables: angular velocity (0, 5 and 15 degree/sec) and fatigue (pre-fatigue, post-fatigue).

3.2.3.2 Dependent variables

Dependent variables for both phases were the normalized EMG of the muscles of the low back. Since this was a sagittally symmetric lifting task, the bilateral pairs of each muscle were averaged together resulting in three dependent variables: the right-left averages of the multifidus, longissimus, and iliocostalis.

3.2.4 Experimental procedures

3.2.4.1 Procedure of isometric extension phase

After a brief warm up and familiarization with procedures, surface electrodes were placed over bilateral multifidus (1.5 cm to the right and left of the vertebral midline at L5 level), longissimus (3.5 cm to the right and left of the vertebral midline at L3 level), and iliocostalis (4.5 cm to the right and left of the vertebra midline at L3 level). Prior to placement, the electrode placement area was shaved and cleaned with alcohol (Figure 7). The subject then moved into the dynamometer frame (Figure 8).

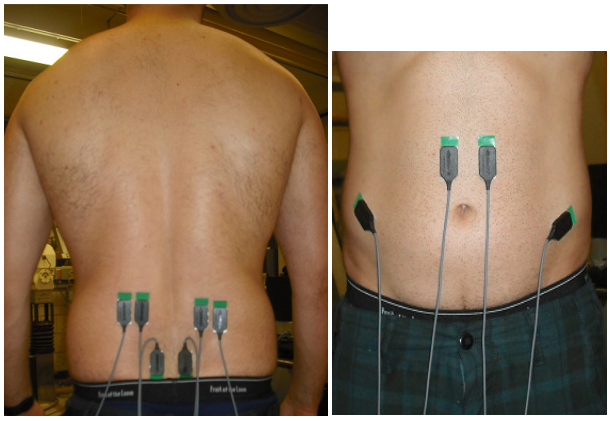

Figure 7. Location of the three pairs of EMG surface electrodes on trunk extensors.

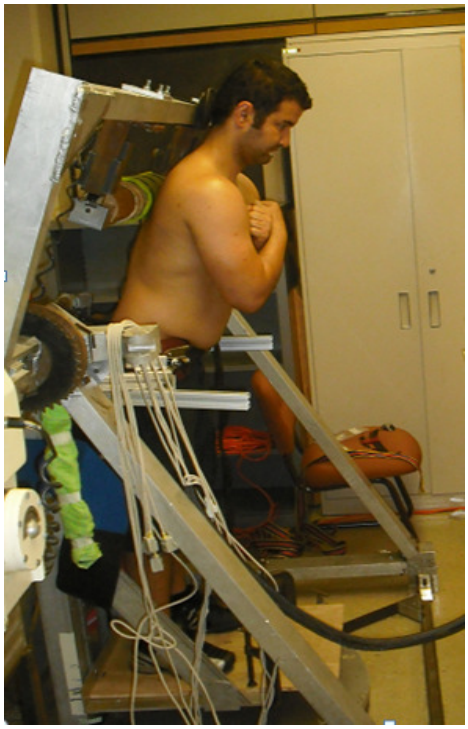

Figure 8. Asymmetric reference frame: Maximal extension of the trunk against a stationary surface.

The subject then completed an isometric maximum voluntary contraction (MVC) for lumbar extensors (attempted trunk extension) against the resistance provided by Kin/Com dynamometer (the subject's pelvis was restrained to the dynamometer with a harness) while the torso angle was set at 15, 30 or 45 degrees (randomized order). During the MVC trial, the EMG signal was recorded for 3 seconds.

The subsequent trials were collected only after the subject completely understood and performed consistent pre-test trials. There was a 2 min rest period provided before the start of the fatiguing protocol. After the MVC trial, the subject's pelvis was restricted to the dynamometer with a pelvic stabilizer (Figure 9), as the subject maintained a standing posture.

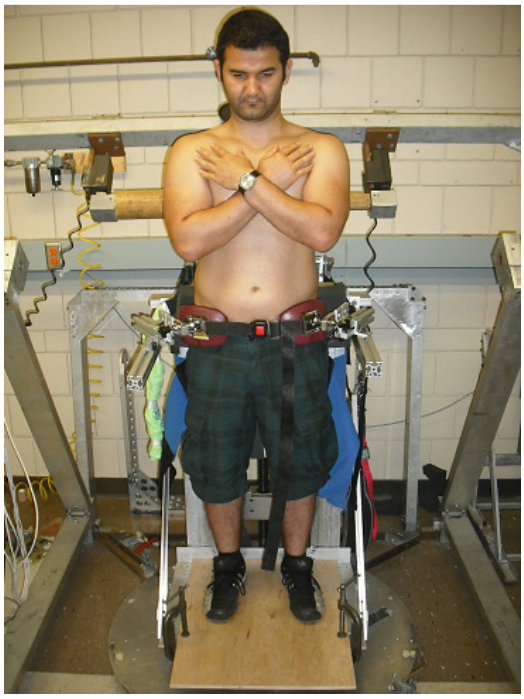

Figure 9. Pelvic stabilizer attached to reference frame, using two lateral pads to restrain pelvic mobility.

In the subsequent trial, the subject was required to generate a continuous isometric extension moment (about L5/S1) equal to 50% of his posture specific force generation capacity until exhaustion while the torso angle was set at 15, 30, 45 degrees. The experimenter recorded EMG data for 4 seconds from initiation of exertion and in subsequent 15 seconds intervals. This 50% condition was accomplished by the subject using a visual feedback display of their force output relative to a target force on a computer monitor (Figure 10).

Figure 10. Visual feedback provided by monitor helps to control the required extension force.

This experiment was repeated for three different flexed angle positions on three separate days, with 5 rest days between each experiment as recovery time.

3.2.4.2 Procedure of isokinetic extension phase

Upon completion of a five minute warm up, EMG electrodes were placed over the sampled muscle detailed in the section 3.2.4.1. The subject then moved into the frame of dynamometer. The subject completed an isometric maximum voluntary contraction (MVCs) for lumbar extensors (attempted trunk extension) against the resistance provided by Kin/Com dynamometer, with the torso maintained at a 30 degree trunk flexion angle. During the MVC

trial, EMG signal was again recorded for 3 seconds. There was a 2 min rest period prior to the start of the fatiguing muscle protocol. After the MVC trials, the subject's pelvis was restricted to the dynamometer by a pelvic stabilizer (Figure 9), as the subject maintained a standing posture.

In the subsequent trial, the subject generated a continuous isometric extension moment (about L5/S1) equal to 50% of his length specific capacity for 15 seconds at a 30 degree flexion angle, followed by a concentric isokinetic exertion from 30 to 10 degree trunk flexion. Selected angular velocities were 0, 5, and 15 degree/sec. This protocol was repeated until exhaustion set in, and the experimenter recorded EMG data during isokinetic concentric contraction. Each angular velocity was selected randomly and performed on 3 separate days, with 5 days of recovery time between experiments.

3.2.5 Data processing

Unprocessed EMG data from all six muscles were transferred into frequency domain and band-pass filtered at a high-pass frequency of 10 Hz and a low-pass frequency of 500 Hz. A notch filter was applied to eliminate 60 Hz, 102.4 Hz and their aliases. The median frequency was computed. The data was then transferred back to time domain for further analysis. Filtered signals were rectified (full-wave) and averaged across the data collection period. This processing occurred for both the data collected during the experimental trials, as well as data collected during the maximum voluntary contractions. The EMG signals from the MVC trials were reduced to $1/4^{th}$ second windows and the peak of the 12 windows (3 seconds exertion) for each muscle in a given each posture were identified and used as the denominator in order to normalize the EMG data from the experimental trials. The EMG

from submaximal exertion of isometric extension phase reduced to 1/4th second windows, and the mean of 16 windows (4 seconds exertion) for each muscle of each posture, were used as the numerator for INEMG. For isokinetic extension phase, the EMG signals between 23 and 18 degrees of trunk flexion were captured, and similar to the numerator of length-force phase, were processed to compute normalized EMG (NEMG) signals. The normalized values of the bilateral pairs were then averaged.

3.3 Results

3.3.1 Isometric extension phase

The purpose of this experiment was to see the influence of fatigue and muscle length on the EMG signals of sampled muscles. Median frequency dropped for all three trunk extensors during isometric trunk extension, which indicates fatiguing occurred for these muscles. Moreover, while exerting constant extension force, two trunk muscles (Figures 17 and 18) showed an increased NEMG signal during developing fatigue. This result is in line with previous studies and supports the need to find fatigued relevant gain factor similar to that developed by Sparto and Parnianpour (1999) for variant gain factor of the erector spinae.

The amount of pre-fatigue normalized EMG for each individual specific length submaximal force generation capacity is close to others, specifically for longissimus. On the other hand, in post-fatigue, Figures 14 and 15 indicated amount of NEMG is different among three angles. The location of EMG electrodes on longissimus in this study was selected to be the same as those used by the EMG-assisted models for erector spinae. This result supports

our hypothesis that the force-length modulation factor may differ between fresh and fatigued muscle.

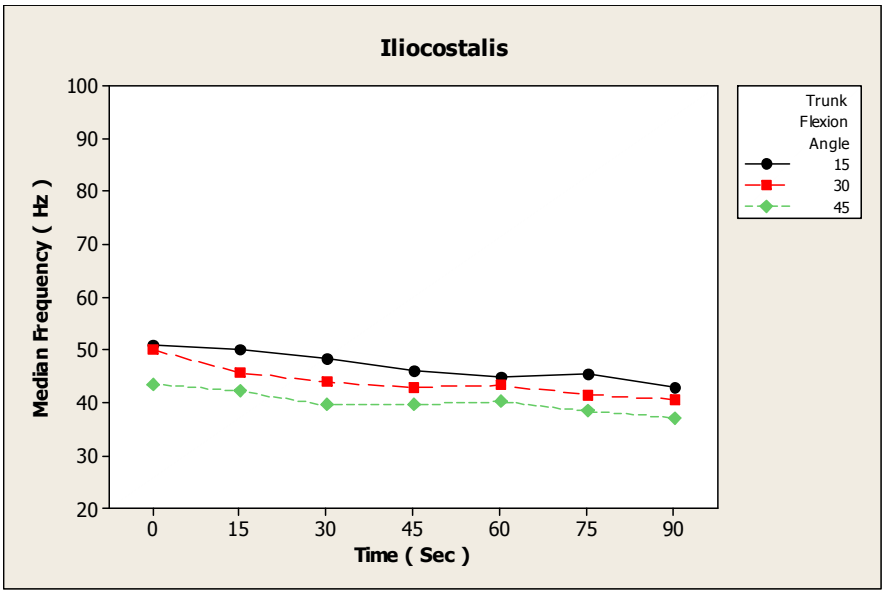

Figure 11. Median frequency of the iliocostalis declined while maintaining 50% MVC until exhaustion (90 seconds).

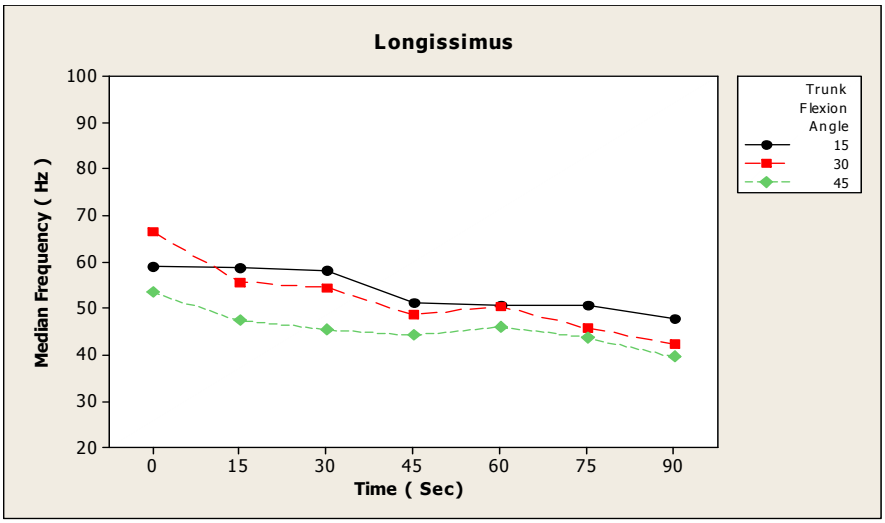

Figure 12. Median frequency of the longissimus declined while maintaining 50% MVC until exhaustion (90 seconds).

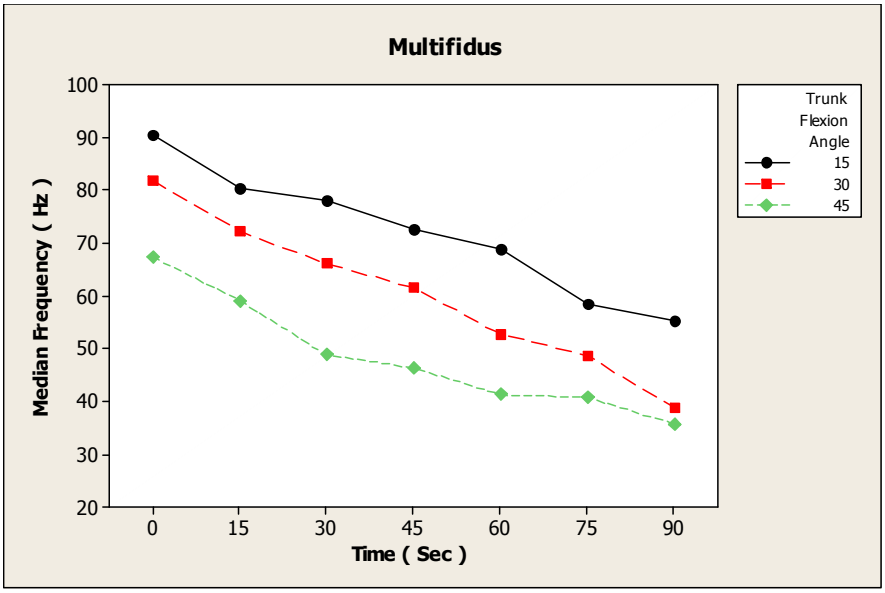

Figure 13. Median frequency of the multifidus declined while maintaining 50% of MVC until exhaustion (90 seconds).

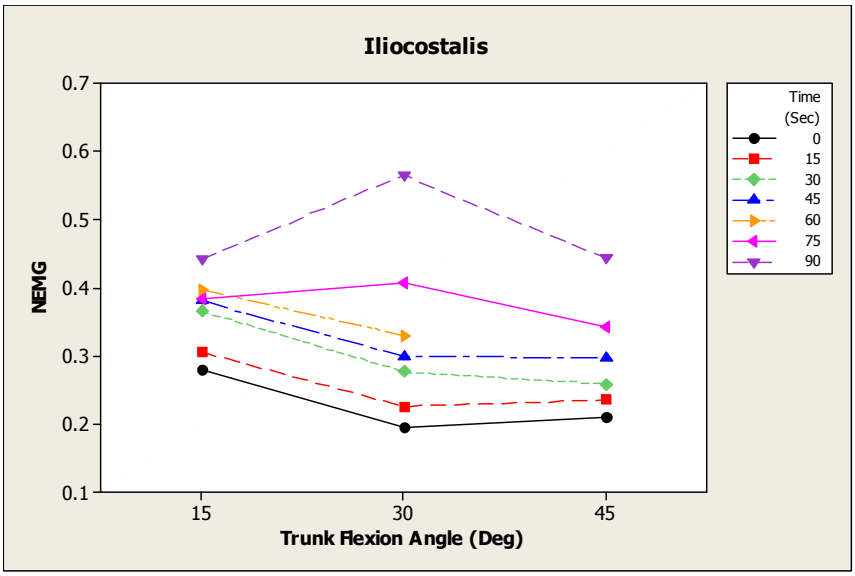

Figure 14. Function of NEMG signal of the iliocostalis with increasing fatigue at different trunk flexion angles.

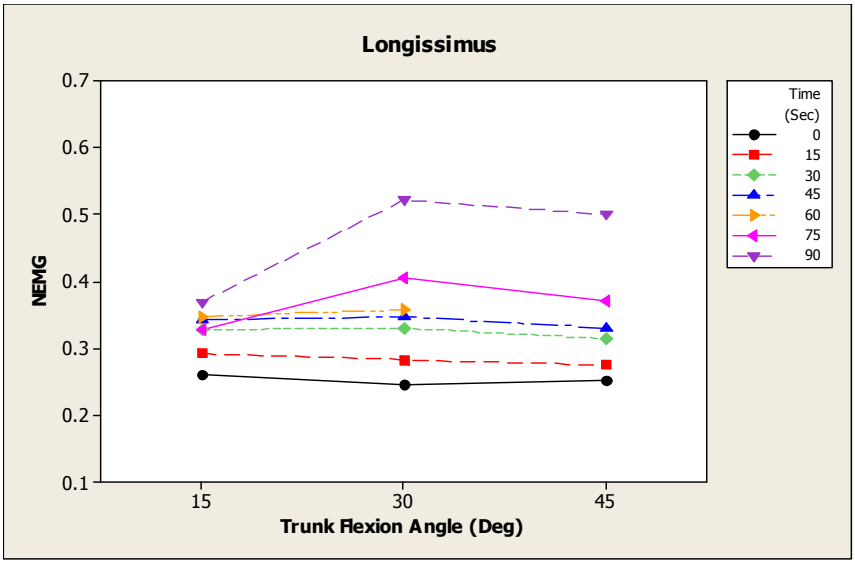

Figure 15. Function of NEMG signal of the longissimus with increasing fatigue at different trunk flexion angles.

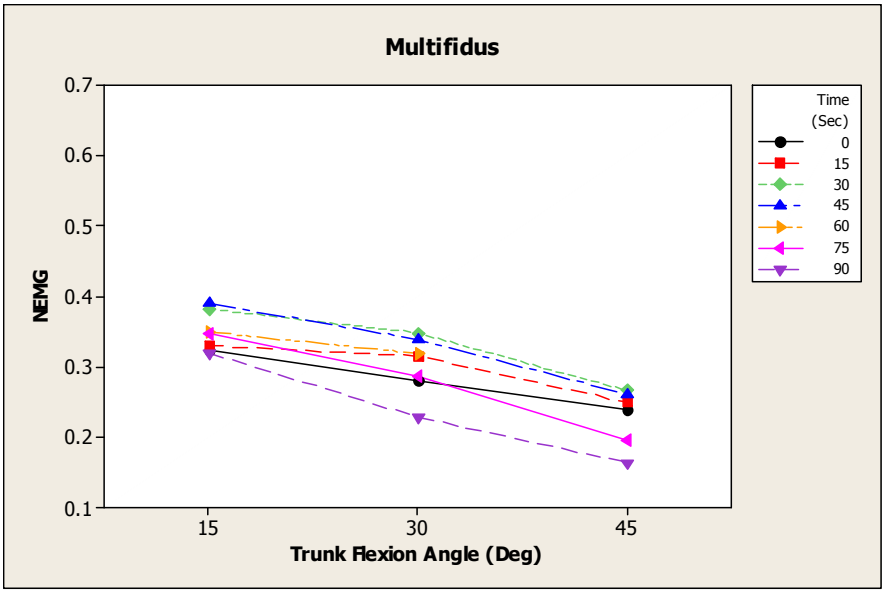

Figure 16. Function of NEMG signal of the multifidus with increasing fatigue in different trunk flexion angle.

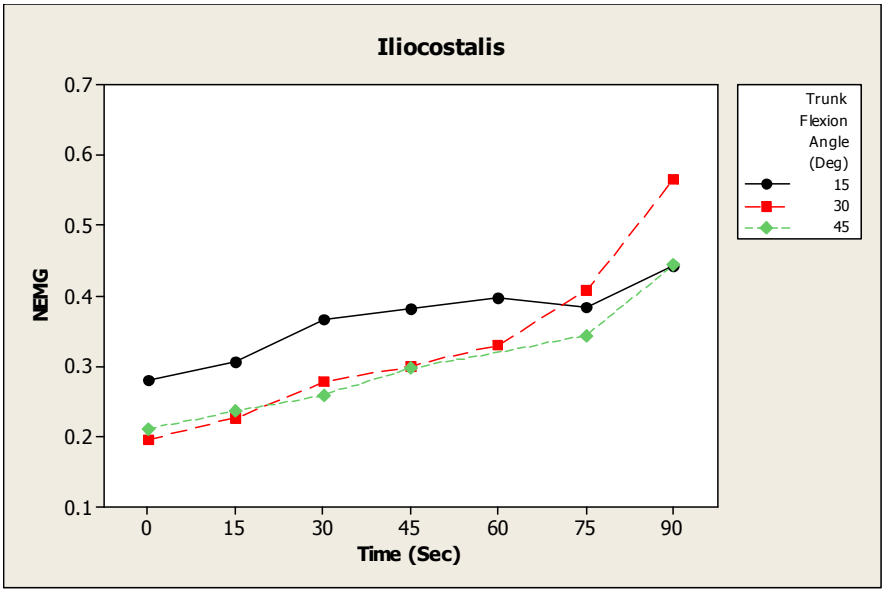

Figure 17. NEMG signals of iliocostalis increased while fatigue proceeds through exerting 50% of maximum length specific force capacity generation.

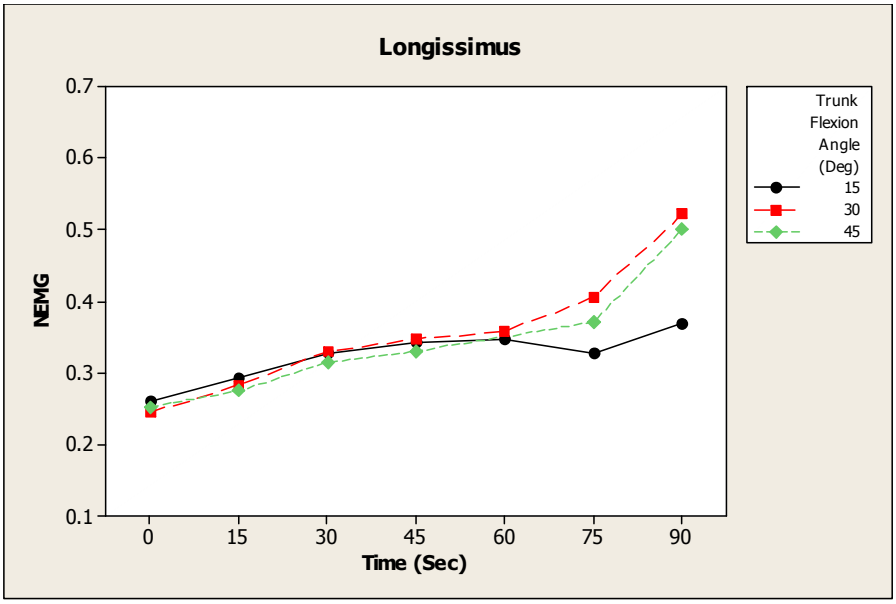

Figure 18. NEMG signals of longissimus increased while fatigue proceed through exerting 50% of maximum length specific force capacity generation.

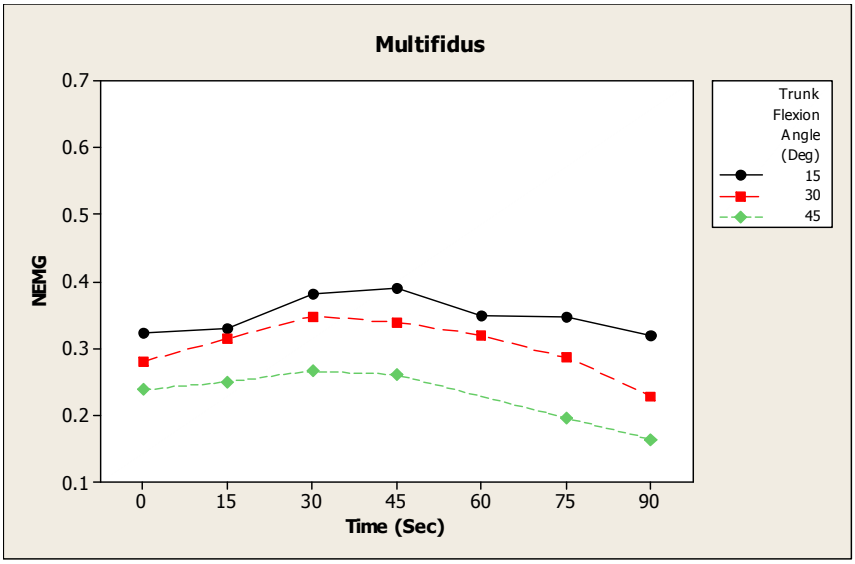

Figure 19. NEMG signals of multifidus decreased while fatigue proceed through exerting 50% of maximum length specific force capacity generation.

3.3.2 Isokinetic extension phase

The purpose of this section was to identify impact of fatiguing on EMG signals of sampled muscles at given force and length, during different shortening velocities. All three muscles showed increased EMG signals between pre-fatigue and post-fatigue, and similar to the isometric extension phase (Figures 20 to 22), reveals the need to look for fatigued relevant gain factor to validate EMG-assisted model under fatigued muscle, given that the trend of changes differed among muscles. This might be the result of the differing functions of each muscle during extension. Whereas the multifidus is known as a stabilizer, the longissimus and iliocostalis are major extensors of the trunk during isometric extension, which is referred to as erector spinae in EMG-assisted models.

Fatigue can presents itself in static, dynamic, intense and intermittent form. The mechanisms behind these various forms of fatigue may differ (refer to the Section 2.4.1.3). In the isokinetic extension phase we are generating isometric intermittent fatigue. Increased

EMG signals between the pre-fatigue and post-fatigue stage are observed for all sampled velocities. Figures 23 to 25 indicated amount of NEMG is different among three velocities. The underlying reason for the disparate 5 degree/sec EMG signal trend is unknown for the longissimus. Given this experiment was conducted for a single subject, interpretation of these results must be done with caution.

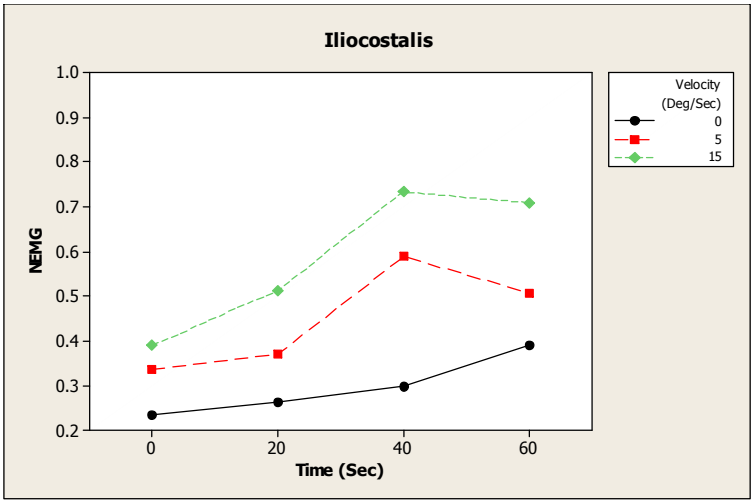

Figure 20. NEMG signals of iliocostalis increased while fatigue proceed through exerting 50% MVC at 30 degree trunk flexion during each shortening velocity

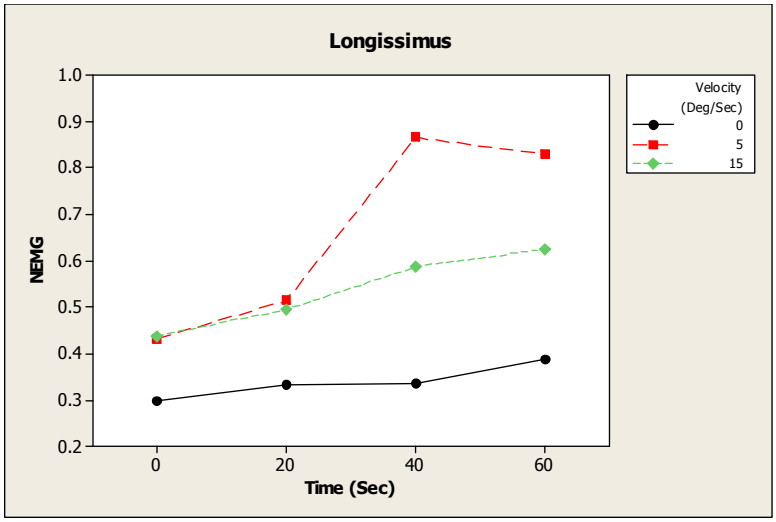

Figure 21. NEMG signals of longissimus increased while fatigue proceed through exerting 50% MVC at 30 degree trunk flexion during each shortening velocity

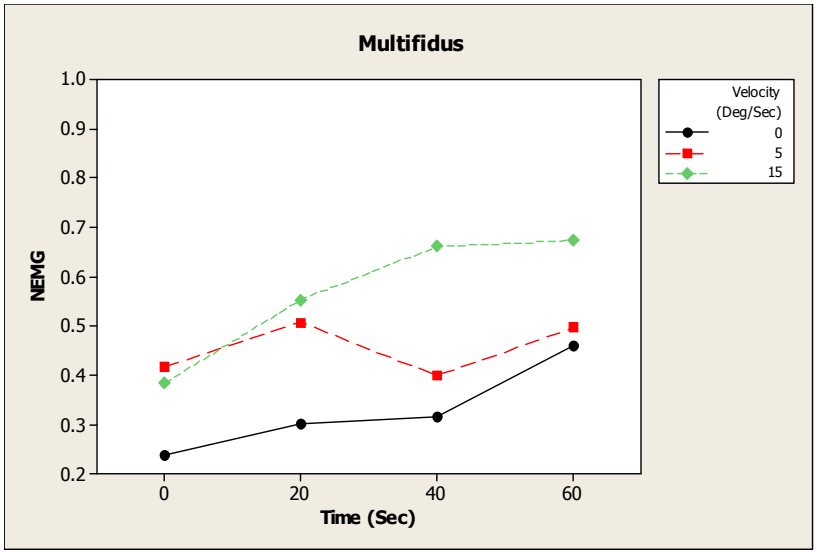

Figure 22. NEMG signals of multifidus increased while fatigue proceed through exerting 50% MVC at 30 degree trunk flexion during each shortening velocity.

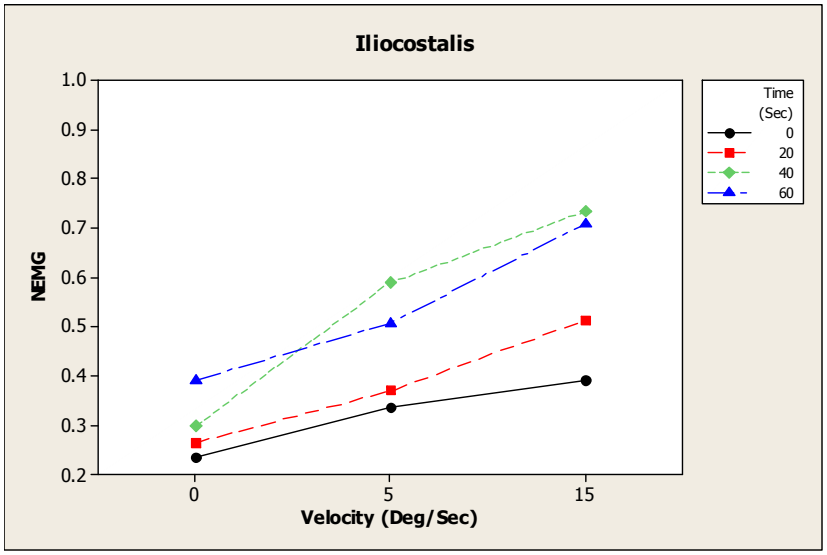

Figure 23. Function of NEMG signal of iliocostalis with increasing fatigue and varied shortening velocity.

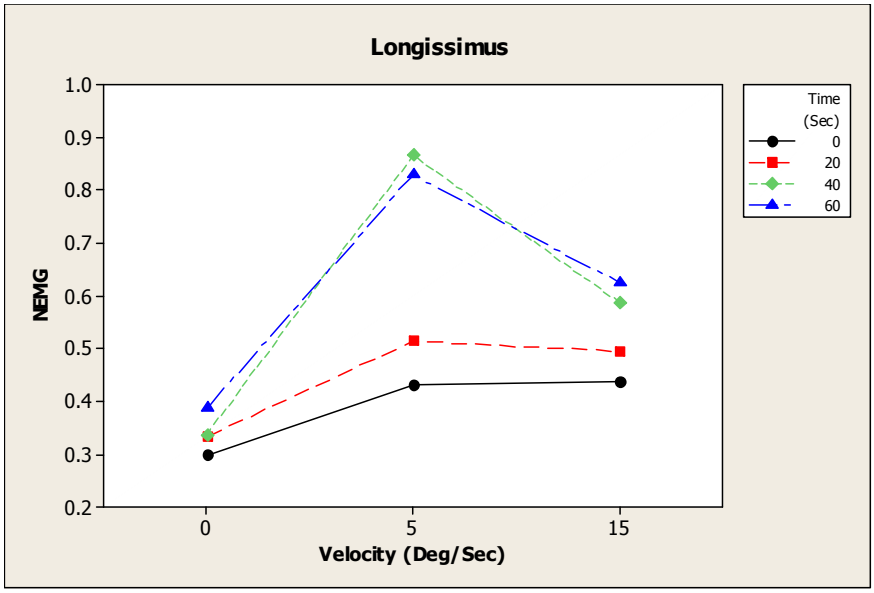

Figure 24. Function of NEMG signal of longissimus with increasing fatigue and varied shortening velocity.

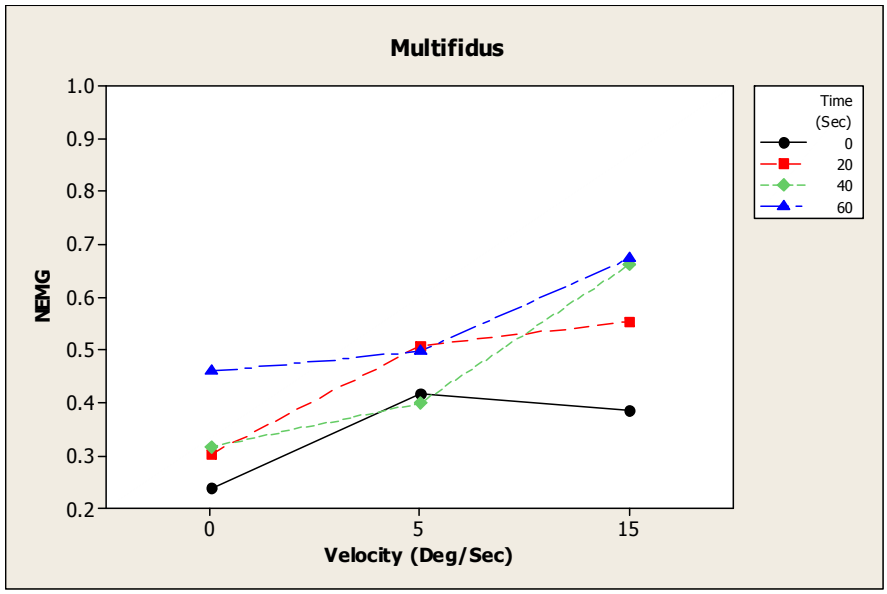

Figure 25. Function of NEMG signal of multifidus with increasing fatigue and varied shortening velocity.

3.4 Summary and hypotheses

Obtaining an accurate estimation of muscle force from the electromyographic signal produced by a muscle is a critical component of the EMG-assisted modeling technique. The literature has shown that for muscles fatigued under constant force generate an increase in EMG signal even though the muscles are generating a constant force and this would lead to an incorrect estimation of muscle force and joint loading using an invariant EMG-force relationship. This result illustrates the need to adjust the gain value (force per unity cross-sectional area of the muscle) for the EMG-force factor in the EMG-assisted modeling technique. Likewise, it is also reasonable to hypothesize that the well-established force-length, and force-velocity relationships (and their corresponding modulation factors in the EMG-assisted modeling technique) may be impacted by muscular fatigue. Moreover, the results of the pilot study illustrated some promising results in terms of the need for adjustments to the gain, length modulation factor and the velocity modulation factors in the EMG-assisted models.

The goal of the current study was to investigate the impact of fatiguing lifting exertions on components of the EMG-force relationship applied in the EMG-assisted model. By considering constant external force exertions in a pre-fatigue and post-fatigue muscle, we hoped to identify appropriate fatigue-dependent modifications to these three important factors in the EMG-assisted modeling technique for accurate estimation of spine loading. Accordingly, we will examine three hypotheses:

First hypothesis: fatigue has an effect on the form of the force-length relationship indicating that the length modulation factor needs to be a function of muscle fatigue level.

Second hypothesis: fatigue has an effect on the form of the force-velocity relationship indicating that the velocity modulation factor needs to be a function of muscle fatigue level.

Third hypothesis: fatigue has an effect on the form of the basic EMG-force relationship indicating that the gain factor needs to be a function of muscle fatigue level.

$$\text{Muscle Force (N)} = \text{Gain (N/cm}^2\text{)} * \text{PCSA}_i\text{(cm}^2\text{)} * \text{NEMG}_i \; *f(l) \; *f(v)$$

Hypothesis 3 Hypothesis 1 Hypothesis 2

CHAPTER 4. METHODS AND MATERIALS

4.1 Study overview

The purpose of the current study was to quantify and validate an EMG-assisted model by considering the influence of fatigue on force-length, force-velocity and gain factor to develop a model capable of estimating spine loading during fatiguing exertions. This study was conducted in two phases. In the first phase, subjects were required to exert prolonged isometric submaximal extension exertions at different trunk flexion angles. While subjects performed the required task, EMG signals of sampled muscle were recorded to find the impact of fatigue on EMG signals of sampled muscles under posture specific submaximal force generation capacity.

In second phase of the study, subjects performed isokinetic trunk extension motions. As subjects performed the required task, EMG signals of sampled muscle were recorded to find the impact of fatigue on EMG signals of sampled muscles under velocity specific submaximal force generation capacity. The combined results of the two phases allowed for the evaluation of each of the four hypotheses an provided the data necessary to estimate the function describing the modification of these factors for an accurate estimate of muscle force under conditions of muscle fatigue.

4.2 Participants

Four participants were recruited from the student population at Iowa State University. None had current/chronic low back or lower extremity problems/discomfort/pain. The basic anthropometry of the subjects (mean (± SD)), was: age 29(± 3.27) years, height 176.5 (± 3.7)

cm, whole body mass 71.5 (± 4.51) kg, trunk depth 21.75 (±1.70) cm, and trunk width 31 (1.82) cm. All provided written informed consent before participation.

Given the exploratory nature of this study, fewer subjects were employed than what is most typical in studies rooted in purely gaining a statistical perspective. Given our primary aim in validating the EMG-assisted model under novel conditions, this allowed a much greater focus on subject training and better ensured subjects perform the required tasks in the correct fashion. Previous such exploratory studies have involved subjects in similar numbers. McGill and Norman (1986), Mirka and Marras (1993) and Davis and Mirka (2000) employed 3, 5, and 7 subjects, respectively.

4.3 Apparatus

Electromyography activity of trunk muscles was recorded using the bipolar surface electrodes (Model DE-2.1 Bagnoli™ from DelSys, Boston, MA). These EMG data were pre-amplified (1000×) and collected at 1024 Hz.

Kin/Com lumbar dynamometer (Chattanooga Group, Inc., Hixson, TN, USA) (Mirka and Marras, 1993) was used to provide computer-recordable isometric and isokinetic resistance force where its bar attached to two load cells. Load cells measured the force exerted by the subject during the isometric and isokinetic extension exertions. Accordingly, the dynamometer was able to provide a computer-controlled measure of trunk flexion angle and the angle-specific moment generated by the subject during the isometric and isokinetic exertions. These data were required to compute of the external moment generated by subject. The angle, velocity, and force of the trunk flexion/extension data were collected from

Kin/Com and were synchronized with the EMG signal at 1024Hz. Furthermore, this apparatus was used to restrict the motion of pelvis during the experimental trials (Figure 8).

FARO Arm (Figure 26) is a portable 3D/6D digitizer and coordinate measurement machine that was used to measure, i.e. digitize, coordinates for the origin and insertion point of erector spinae muscle group by digitizing the bony landmarks while the subjects assumed different trunk flexion angles. Measurement points were collected with a probe located at the end of the arm, placed in perpendicular contact with the skin surface over the bony landmarks.

Figure 26. FARO Arm is a portable 3D/6D digitizer.

4.4 Isometric extension phase

4.4.1 Experimental design

4.4.1.1 Independent variables

There were two independent variables: trunk flexion angles at three levels (ANGLE: 10°, 20°, and 30°), and time into the fatiguing trunk extension exertion protocol (TIME: 0 (pre-fatigue), 15, 30, 45, 60, 75 seconds). The ANGLE was defined as the angle between a vertical reference line and the angular deviation of the dynamometer bar from that vertical position. All exertions were sagittally symmetric trunk extension exertions.

4.4.1.2 Dependent variables

The dependent variables were the normalized (to maximum) EMG (NEMG) of sampled bilateral muscles: multifidus, longissimus, internal oblique, iliocostalis, latissimus dorsi, rectus abdominis and external oblique (Figure 27). These NEMG activities of the trunk muscles were used as inputs for an EMG-assisted biomechanical model for the prediction of spinal reaction forces and moments.

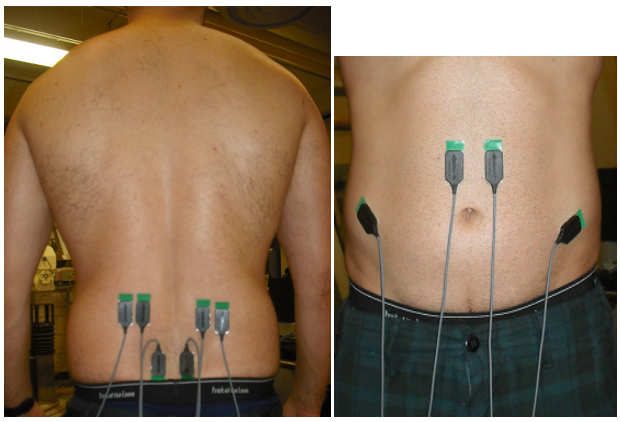

Figure 27. Location of EMG electrodes on trunk flexors.

4.4.2 Experimental procedure

Upon arrival, the experiment was described and the subject was asked to sign an informed consent form. Participants' anthropometric data (height, weight, trunk depth (at umbilicus), and trunk width (at umbilicus)) were recorded. A brief (5 minute) warm up routine was provided in each session to let subjects stretch and warm up the muscles of the low back and lower extremities. Due to the required controlled exertion for this experiment, the first session was used to train the subject to use the video feedback system of the trunk dynamometer (Figure 10). In this first session the subject learned how to use a video feedback device to maintain the required trunk extension force during isometric (static) and isokinetic (dynamic) exertions. They pushed against the dynamometer arm and used the video feedback to match their trunk extension force to a target lifting force, both displayed on the computer monitor. Forces exerted were 50% of the subject-specific maximum values and were maintained for short duration 10-15 seconds. Adequate time was given between exertions to recover and the number of these training exertions was kept less than 20 to avoid fatigue.

Upon completion of the warm up and training, subjects were fitted with seven pairs of bipolar surface electrodes over five bilateral trunk extensors (multifidus, longissimus, internal oblique, iliocostalis and latissimus dorsi) and two bilateral trunk flexors (rectus abdominis and external oblique). A reference electrode was placed over the lateral aspect of iliac crest. Prior to placement, the electrode placement area was shaved and cleaned with alcohol according to established procedures (Marras, 1990). Subjects then stepped into the asymmetric reference frame dynamometer and the subject's pelvis was secured to the dynamometer using a pelvic stabilizer (harness around waist). The participant then

performed a series of trunk extension and flexion maximum voluntary contractions (MVCs) against the static resistance provided by the dynamometer while maintaining one of three levels of ANGLE (10, 20, or 30 degrees, randomly chosen for that day). These data were collected to provide a reference to normalize the EMG activity of each muscle for each subject with respect to their maximum EMG activity. EMG signals were recorded for three seconds during the MVC trial, and the amount of posture specific maximum force generated by the subject was captured from the dynamometer. A two-minute rest period was provided after each maximum voluntary exertion. In the subsequent experimental trials, the subject was instructed to generate a continuous isometric extension force equal to 50% of his maximum until exhaustion. EMG data was collected at time 0 seconds and then recorded every 15 seconds from initiation of the trial (the levels of the variable TIME refer to the time at which each data collection began). The duration of EMG data collection was four seconds. This 50% MVC was exerted by the subject against resistance provided by the dynamometer, and controlled through the visual feedback display on a computer monitor directly in front of the subject. The subject was trained (first session) to control his extension force during each trunk flexion angle so that the blue line (generated force) was as close to the red line (required force) as possible (less than $\mp$ 10 N tolerance was acceptable). After reaching exhaustion, the instrumentation was removed from the subject and he was free to go. Subjects performed this protocol in each of the three levels of ANGLE (10, 20, 30 degrees of trunk flexion) on different days with five days of rest provided between each experimental day for recovery.

4.4.3 Data processing

Unprocessed EMG data from all trunk muscles was transferred into frequency domain and band-pass filtered at a high-pass frequency of 10 Hz and a low-pass frequency of 500 Hz. A notch filter was applied to eliminate 60 Hz, 102.4 Hz and their aliases. The median frequency of these EMG data was computed to monitor fatigue development. The data was then transferred back to time domain for further analysis. Accordingly, filtered signals were rectified (full-wave) and averaged across data collection period. This processing occurred for both the data collected during the experimental trials, as well as data collected during the maximum voluntary contractions. The EMG signals from the MVC trials were reduced to $1/4^{th}$ second windows and the peak of the 12 windows (for the three-second exertions) for each individual muscle in each posture were identified and used as the denominator in order to normalize the EMG data from the experimental trials. The mean of the filtered and rectified EMG from the four-second, 50% MVC data collection trials was used as the numerator for the computation of the value of the NEMG. The mean of the two bilateral muscles was computed and considered for data analysis. This was deemed appropriate because of the sagittal plane symmetry of the trunk flexion postures.

4.4.4 Data analysis: First hypothesis

4.4.4.1 Assumptions of ANOVA

First, the underlying assumptions of ANOVA were tested to make sure that normality of residuals, non-correlation of residuals (i.e. independence), and constant variance of residuals are satisfied for all dependent variables (NEMG of sampled muscles) (Montgomery

2005, pp. 76-79). If any dependent variable violates one or more assumption, the variable was transformed so that the ANOVA assumptions were no longer violated (Montgomery 2005, p.80).

4.4.4.2 First hypothesis

Once ANOVA assumptions were verified, the effects of TIME, ANGLE and their interaction on the NEMG data were tested using a randomized complete block ANOVA ('subject' was the blocking variable). A significant interaction ($p<0.05$) between TIME and ANGLE for the NEMG of the iliocostalis or longissimus would indicate that the force-length relationship is affected by the fatigue that is developed over time. This analysis provides the insight necessary to modify, if necessary, the force-length modulation factor of the EMG-assisted biomechanical model so it can be used to evaluated spine loading in fatiguing lifting conditions.

4.5 Isokinetic extension phase

4.5.1 Experimental design

4.5.1.1 Independent variables

The second phase of experiment had two independent variables as well: trunk angular extension velocity at three levels (VELOCITY: 0, 5 and 15 degrees/second) and time into the fatiguing trunk extension exertion protocol (TIME: 0, 15, 30, and 45 seconds). The time duration here is shorter than that in the isometric phase because the pilot work showed that the ability of the participants to perform the experimental tasks deteriorated

much quicker in the isokinetic phase. To provide the data for the 0 degree/second condition, the data from the isometric phase was utilized (the 20 degree flexion condition). All dynamic exertions were sagittally symmetric trunk extension exertions.

4.5.1.2 Dependent variables

The dependent variables were the same as those using in the isometric extension phase trials.

4.5.2 Experimental procedure

A similar protocol was followed as that used in the isometric extension phase with two different levels of trunk extension velocity (5 and 15 degrees/second). The isokinetic trials were conducted on two different days separated by five days of rest. After a short five-minute stretching and warm up period, subjects were fitted with seven pairs of bipolar surface electrodes over the five bilateral trunk extensors (multifidus, longissimus, iliocostalis and latissimus dorsi, internal oblique) and two bilateral trunk flexors (rectus abdominis, external oblique) (Figure 27). The reference electrode will be placed over the lateral aspect of iliac crest.

Subjects then stepped into the asymmetric reference frame dynamometer and the subject's pelvis was secured to the dynamometer using a pelvic stabilizer harness system. The participant then performed a series of trunk extension and flexion maximum voluntary contractions against the static resistance provided by the dynamometer while maintaining a trunk flexion angle of 20 degrees. Two minutes of rest was provided between MVC exertions. There was a two-minute rest period prior to the start of the fatiguing muscle

protocol. In the subsequent trial, the subject was required to generate a continuous isometric extension force equal to 50% of his maximum force generation capacity (calculated in the isometric section) for 15 seconds at 30 degree trunk flexion, followed by performing a dynamic 50% MVC exertion while moving at the designated velocity from 30 to 10 degrees of trunk flexion (one trunk extension motion). The required force was graphically displayed on a computer monitor screen placed in front of subject as a red line, while exerted force by subject was displayed simultaneously on the screen as a shifting blue line. The angular velocity was controlled by the dynamometer at the designated level. After completing this test trial the subject then returned to the fatiguing isometric exertion for another 15 seconds followed by another 50% MVC dynamic exertion. This protocol was repeated until exhaustion with the EMG data being recorded during the full isokinetic concentric contraction as well as the first three seconds of the 15-second isometric contraction. Upon completion of all trials, the EMG surface electrodes were removed and the subject was free to go.

4.5.3 Data processing

As with the isometric phase, the unprocessed EMG data from all trunk muscles was transferred into frequency domain and band-pass filtered at a high-pass frequency of 10 Hz and a low-pass frequency of 500 Hz. A notch filter was applied to eliminate 60 Hz, 102.4 Hz and their aliases. The median frequency of these EMG data was computed to monitor fatigue development. The data was then transferred back to time domain for further analysis. Accordingly, filtered signals were rectified (full-wave) and averaged across data collection period. This processing occurred for both the data collected during the experimental trials, as

well as data collected during the maximum voluntary contractions. The EMG signals from the MVC trials were reduced to 1/4th second windows and the peak of the 12 windows (for the three-second exertions) for each individual muscle in each posture were identified and used as the denominator in order to normalize the EMG data from the experimental trials. For the isokinetic extension trials, EMG collected as the subject passed through a trunk flexion window of 22 to 18 degrees trunk flexion were extracted and the mean of the data collected in this trunk flexion window were used as the numerator of the normalization process. The mean of the two bilateral muscles was computed and considered for data analysis. This was deemed appropriate because of the sagittal plane symmetry of the trunk flexion postures.

4.5.4 Data Analysis: Second hypothesis

4.5.4.1 Assumptions of ANOVA

First, the underlying assumptions of ANOVA was tested to make sure that normality of residuals, non-correlation of residuals (i.e. independence), and constant variance of residuals are satisfied for all dependent variables (NEMG of sampled muscles) (Montgomery 2005, pp. 76-79). If any dependent variable violates one or more assumption, the variable was transformed so that the ANOVA assumptions were no longer violated (Montgomery 2005, p.80).

4.5.4.2 Second hypothesis

Once ANOVA assumptions were verified, the effects of TIME, VELOCITY and their interaction on the NEMG data were tested using a randomized complete block ANOVA

('subject' was the blocking variable). A significant TIME*VELOCITY interaction ($p<0.05$) for the iliocostalis or longissimus would indicate that the force-velocity relationship is affected by fatigue. This analysis provides the insight necessary to modify, if necessary, the force-velocity modulation factor of the EMG-assisted biomechanical model so it can be used to evaluated spine loading in fatiguing lifting conditions.

4.6 Development of a fatigue-modified, EMG-assisted biomechanical model

In order to fully explore the need for a fatigue-dependent gain factor in an EMG-assisted biomechanical model a full EMG-assisted biomechanical model was developed. As outlined in Section 2.3, to calculate the amount of fresh muscle tensile force, multiple factors must be considered, including muscle force-length and force-velocity modifiers, normalized EMG activity, muscle cross-sectional area, and gain factor (force per unit cross-sectional area). The value of the gain factor can be calculated such that the internal and external moments will be in equilibrium. Under conditions of fatigue, the value of this gain factor may change to reflect the electro-mechanical inefficiency and shifting load between fiber types due to the fatigue and quantifying this change will provide the data necessary to develop a novel EMG-assisted model that can function under conditions of muscle fatigue. There are several different techniques that are found in the literature to develop the factors in an EMG-assisted model and the following sections detail the approach taken in the current research.

4.6.1 Muscle force-length and force-velocity modifiers

It has been shown in the literature that muscle force capacity is not constant, but rather varies as the length and the velocity of shortening of the muscle changes. If the length of muscle in some specific trunk flexion angle is known, a regression model can be derived for predicting each muscle length change within a specific range of trunk flexion via trunk flexion angle. However, while we can calculate changing length of muscle during bending, we can furthermore compute shortening velocity of each muscle if we know the angular velocity of trunk flexion. Raschke and Chaffin (1996) provide the following figure describing the force-length modulation factor as a function of muscle length to resting length. Using this model and our own digitized data (see Section 5.1), the force-length modulation factors in the current study were 0.94, 1, and 0.94 for 10, 20, and 30 degree trunk flexion angles respectively.

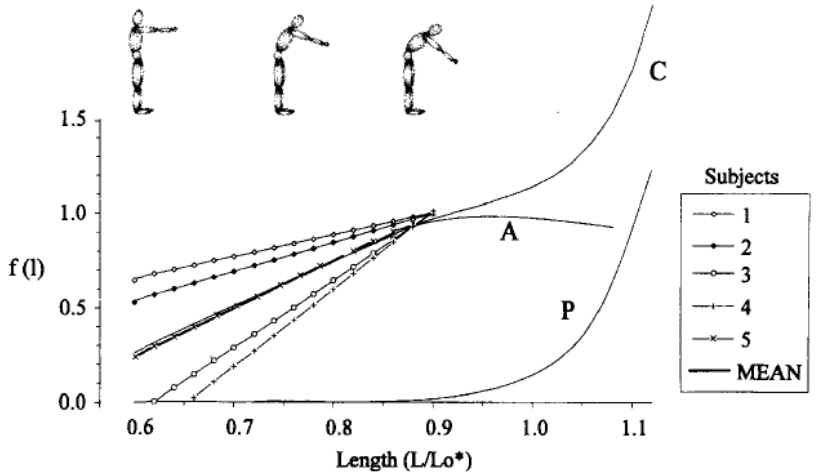

Figure 28. Force-length relationship for erector spinae (Raschke and Chaffin 1996).

L_0: Resting length of the muscle at about 20° of trunk flexion.

The force-velocity modulation factor employed in this study was taken from Raschke and Chaffin (1996) as presented in Figure 29. Accordingly, for each degree per second

increase in velocity, the maximum force of erector spinae and applied for all subjects decreased by 0.5% (Sparto and Parnianpour 1999). Using this model and our own digitized data, the force-length modulation factors in the current study were 1, 0.975, and 0.925 for 0, 5, and 15 degrees/second, respectively.

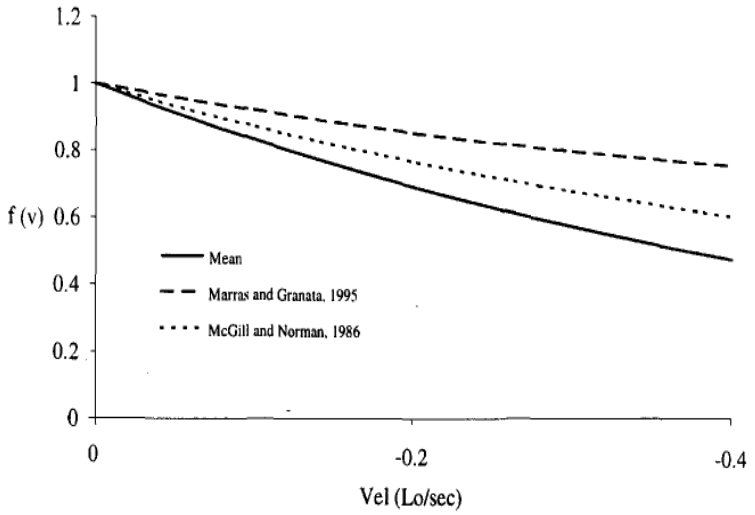

Figure 29. Change of force-velocity modulation factor while muscle length increases (Raschke and Chaffin 1996).

4.6.1.1 Digitizing origin and insertion points of sampled muscle

Tracing changes of sampled muscle length caused by change of trunk flexion angle is necessary to calculate the force-length modulation factor and the force-velocity modulation factors. Digitizing techniques help find the coordinates of origin and insertion points of the considered muscles at different trunk flexion angles (Davis and Mirka, 2000). Accordingly, changes in muscle length can be computed between different trunk flexion angles.

On the last session of experimental procedure, after removal of surface electrodes, the subjects rested for 20 minutes and then the experimenters digitized the origin and insertion locations of longissimus, latissimus dorsi, external oblique, and rectus abdominis using the FARO Arm digitization system (Figure 26). This system simply documented the three-dimensional positions of the origin and insertion of these muscles and these data were used in the biomechanical model developed through this study. Digitization was performed at a defined location, pushing the spherical probe into the skin until resistance was provided by bony landmarks under measurement points. In each of five trunk flexion angles (10, 15, 20, 25 and 30), 16 locations were measured at each angle for a total of 80 locations for each subject.

4.6.2 Muscle cross-sectional area

Muscle size plays a major role in determining the amount of force provided by a muscle (Bogduk and Macintosh 1992). Hence, considering the cross-sectional area of each muscle is necessary when using the EMG-assisted model and typically the physiological cross-sectional area (PCSA) is the value used in spinal biomechanical models. PCSA defined as the total volume of the muscle divided by the length of the muscle. In this study, the PCSA was considered as reported in Marras et al (2001) (Table1).

Table 1. The PCSA of the trunk muscles (Marras et al. 2001).

Muscle	PCSA (cm^2)
Right latissimus dorsi	20.5
Left latissimus dorsi	20.5
Right erector spinae	26
Left erector spinae	26
Right rectus abdominis	9.05
Left rectus abdominis	9.05
Right external oblique	10.6
Left external oblique	10.6

4.6.3 Moment arm

The sagittal plane moment arm of trunk muscles play significant roles in determining the contribution of a muscle to the total internal, sagittal plane moment. Jorgenson et al. (2001), using MRI techniques, recorded moment arms in sagittal and coronal planes from T8 through S1, where each moment arm was determined between vertebra centroid and muscle centroid points. Table 2 depicts the sagittal plane moment arms at the L5 level employed in the present study.

Table 2. Moment arms of sampled muscles (Jorgensen et al. 2001).

Muscle	Moment arm (cm)
Right latissimus dorsi	4.05
Left latissimus dorsi	4.05
Right erector spinae	6.1
Left erector spinae	6.1
Right rectus abdominis	7.6
Left rectus abdominis	7.6
Right external oblique	3.7
Left external oblique	3.7

4.6.4 Computation muscle gain

The force value of each individual muscle can be calculated using the following equation, in which NEMG is the normalized EMG activity of each individual muscle during extension to its MVC.

$$\text{Force} = \text{Gain}^* \text{PCSA}^*\text{NEMG}^*f(l)^*f(v) \qquad (4)$$

In this equation both gain and force are unknowns, but in the unfatigued state we can assume that the gain is constant across all trunk muscles. In doing so, we can create a moment equilibrium equation that matches the net internal moment with the external moment. This external moment can be found by measuring the force generated into the

dynamometer (and multiplying this value by the moment arm of the load cells about the axis of rotation) and then adding the estimated moment from the effect of gravity on the mass of the torso.

Net External moment = Net Internal Moment

$$\text{Net External moment} = \sum_{\textit{Summation across i muscles}} \text{Gain}^{*}\ \text{PCSA}_i{*}\text{MA}_i{*}\text{NEMG}_i{*}f(l)\ {*}f(v) \quad (5)$$

(MA_i: sagittal plane moment arm of the centroid of muscle *i* about the spine)

The gain factor (muscle stress value in N/cm^2) of each subject was calculated in this way. (Matlab code found in Appendix A). When this gain factor is applied in Equation 4, we can gain a direct estimate of the force produced by each muscle.

4.6.5 Calculation of spine reaction forces

The force vector of each individual muscle can be computed using the resulting scalar force value and action line of each muscle. The net internal moment and net spine reaction forces on the L5/S1 joint can then be computed. For example, the cross products corresponding to moment arm (r) of each individual muscle and F, was denoted as r×F, and the compression and shear joint reaction forces are computed by summing the muscle forces in the three orthogonal planes.

4.6.6 Model modification

In the present study this basic, EMG-assisted model has been modified to address the recognized problems of an altered EMG-force relationship under conditions of muscle fatigue. This approach avoids the need for frequent maximum voluntary exertions as was

seen in Sparto and Parnianpour (1999). To accomplish this we first developed an EMG-assisted model reflecting the pre-fatigue conditions to ensure that the model's estimation is appropriate. We then kept the gain factor constant (invariant gain) for all sampled muscles except the longissimus (from here on we will refer to this muscle as the erector spinae to be consistent with the exiting literature and our EMG sampling location) and we calculated the actual gain factor of erector spinae (Equation 6 – algebraic manipulation of Equation 5 with the separation of the muscles based on whether the gain is allowed to vary (erector spinae) or not (all other muscles)). This gain will tend to decrease with increased levels of fatigue.

$$Gain_{Actual} = \left[\sum \text{External Moment} - \sum \text{Internal Moment}_{\text{(Latissimus Dorsi, External Oblique, Rectus Abdominis)}}\right] / \sum \left(\text{PCSA}*\text{NEMG}*f(l)*f(v)*MA\right)_{\text{Erector Spinae}} \quad (6)$$

Ideally, we would like to estimate the dynamic actual gain value of $Gain_{Actual}$ without the need to measure the external moment at each point in time. We would prefer to calibrate the gain value with a pre-fatigue exertion and then allow the person to perform the fatiguing exertion and we can monitor the various muscle forces and the spine reaction forces. This requires that we have an independent measure of muscle fatigue that we could use to help us predict $Gain_{Actual}$. The median frequency is a standard objective parameter used to trace muscle fatigue, so we examined various functions that drew a relationship between initial gain ($Gain_{Invariant}$), initial median frequency ($MF_{Pre\text{-}fatigue}$), current median frequency (MF)

and current gain (Gain). Using a least squared analysis technique these relationships (and the corresponding Pearson correlation coefficient) were tested for a variety of gain and median frequency functions: $MF\text{-}MF_{Pre\text{-}fatigue}$ vs. $Gain\text{-}Gain_{Invariant}$ (R^2=0.63); $MF/MF_{Pre\text{-}fatigue}$ vs. $(Gain\text{-}Gain_{Invariant})$ (R^2=0.02); $(MF\text{-}MF_{Pre\text{-}fatigue})$ vs. $Gain/Gain_{Invariant}$ (R^2=0.06); $MF*MF_{Pre\text{-}fatigue}$ vs. $Gain*Gain_{Invariant}$ (R^2=0.13). Finally, we employed the ratio of post-fatigue median frequency to pre-fatigue median frequency to trace fatigue in the EMG-assisted model, and we found the best fit of $Gain_{Predicted}$ vs. $Gain_{Actual}$ for all subjects occurred when the ratio of the median frequency of the fatigued erector spinae (MF) and the unfatigued erector spinae ($MF_{Pre\text{-}Fatigue}$) was calculated ($MF/MF_{Pre\text{-}fatigue}$). The erector spinae's gain factor was therefore predicted by the following equation.

$$Gain_{Predicted} = (-\ 0.0592 + 1.046\ MF\ /MF_{pre\text{-}fatigue})*Gain_{Invariant} \quad (7)$$

The Pearson correlation coefficient describing the relationship between this predicted gain value (Equation 7) and the actual gain value (Equation 6) was 0.79.

Hence, the EMG-assisted model was modified to produce the following equation.

$$\sum \text{Internal Moment} =$$

$$\sum \text{Internal moment}_{(\text{Latissimus Dorsi, External Oblique, Rectus Abdominis})} + [\ (-\ 0.0592 + 1.046$$

$$MF/MF_{pre\text{-}fatigue})*Gain_{Invariant} * \sum (PCSA*NEMG*f(l)*f(v)*MA)_{\text{Erector Spinae}}\ ]$$

(8)

Accordingly the net internal moment, the spine compression force and the anterior-posterior spinal shear force were calculated using the actual, the invariant and the predicted gain factors applied to the sampled muscles. This technique was used to assess the ability of the invariant and the predicted gain factors to accurately predict the result using the actual gain factor. In essence this provided an assessment of the effects of varying the gain value as a function of fatigue.

4.7 Model evaluation

To evaluate the effectiveness of our approach to modifying the gain values based on fatigue level, our modified EMG-assisted model was compared with the standard EMG-assisted model developed by Marras and Granata (1997) (time invariant gain factor for all sampled muscle during the experiment). Model evaluation was accomplished by considering the mean normalized error of computed internal moment using modified gain versus mean normalized error of computed internal moment invariant gain. The goal of the model evaluation was to see if there was any significant value in adjusting the gain value as a function of fatigue level (i.e. is any additional predictive power gained).

4.7.1 Third hypothesis

The effects of fatigue and gain factor type (predicted or invariant gain factor) and the effect of the interaction between fatigue and considered gain factor on computed absolute error between measured external moment and estimated internal moment were tested using a randomized complete block ANOVA ('subject' was the blocking variable). The results found

for gain factor type support whether or not the gain factor should be modified during fatigue development. This analysis provided the insight necessary to modify the EMG-assisted biomechanical model so that it can be used to evaluated spine loading in fatiguing lifting conditions.

4.8 Model validation

The purpose of model validation was to see how accurately the modified model was able to predict internal moment for a group of new subjects under conditions of muscular fatigue. Hence new subjects were asked to perform some similar fatiguing trunk extension exertions to allow the improved accuracy of the modified model to be estimated.

4.8.1 Subjects

Two more participants were recruited from the student pool at Iowa State University. None had current/chronic low back or lower extremity problems/discomfort/pain. The basic anthropometry of the subject pool, mean (± SD), was age 31.5 (± 3.54) years, height 179 (± 8.49) cm, and whole body mass 75.5 (± 3.54) kg. They provided written informed consent before participation.

4.8.2 Isometric extension phase

Similar to section 4.3.2, upon arrival, the experiment was described and the subject was asked to sign an informed consent form. Participants' anthropometric data were then recorded. A brief (5 minute) warm up routine was provided in each session to let subjects stretch and warm up the muscles of the low back and lower extremities. Due to the required

controlled exertion for this experiment, this first session was used to train the subject to use the video feedback system of the trunk dynamometer. This experiment was conducted on two separate days, with one day of rest provided between each experimental day for recovery.

Upon completion a brief warm up, subjects were fitted with seven pairs of bipolar surface electrodes over five bilateral trunk extensors and two bilateral trunk flexors. A reference electrode was placed over the lateral aspect of iliac crest. Prior to placement, the electrode placement area was shaved and cleaned with alcohol. Subjects then stepped into the asymmetric reference frame dynamometer and the subject's pelvis was secured to the dynamometer using a pelvic stabilizer (harness around waist). The participant then performed an extension and flexion maximum voluntary contractions against the static resistance provided by the dynamometer while maintaining one of two trunk flexion postures (20, or 25 degrees, randomly chosen for that day). EMG signals were recorded for three seconds during the MVC trial, and the amount of posture specific maximum force generated by the subject was captured from the dynamometer. A two-minute rest period was provided after each maximum voluntary exertion. In the subsequent trial, the subject was instructed to generate a continuous isometric extension force equal to 50% of his maximum for 90 seconds. EMG data was recorded every 15 seconds from initiation of the trial. Upon completion of protocol, the instrumentation was removed from the subject and they were free to go. Subjects performed this protocol in each of the two trunk flexion angles (20 and 25 degrees of trunk flexion) on different days.

4.8.3 Isokinetic extension phase

A similar protocol was followed in the isokinetic extension phase with two different levels of trunk extension velocity (5 and 10 degrees/sec). These trials were conducted on two different days separated by 3 days of rest, for each subject. After a short 5 minute stretching and warm up period, subjects were fitted with seven pairs of bipolar surface electrodes over five bilateral trunk extensors and two bilateral trunk flexors. The reference electrode was placed over the lateral aspect of iliac crest.

Subjects then stepped into the asymmetric reference frame dynamometer and the subject's pelvis was secured to the dynamometer using a pelvic stabilizer. The participant then performed an extension and flexion maximum voluntary contractions against the static resistance provided by the dynamometer while maintaining a trunk flexion angle of 20 degrees. Two minutes of rest was provided between MVC exertions. There was a 2 min rest period prior to the start of the fatiguing muscle protocol. In the subsequent trial, the subject was required to generate a continuous isometric extension force equal to 50% of his maximum posture specific force generation capacity (calculated in the isometric section) for 15 seconds at 30 degree trunk flexion, followed by exerting 50% MVC from 30 to 10 degrees of trunk flexion (one trunk extension motion). They then returned to the fatiguing isometric exertion for another 15 seconds. This protocol was repeated until exhaustion, and EMG data was recorded during isokinetic concentric contraction as well as the first three seconds of 15 seconds isometric contraction. Upon completion of all trials in each session till exhaustion, the EMG surface electrodes were removed and the subject was free to go.

4.8.4 Data processing

Similar to section 4.3.3 and 4.4.3, captured EMG signals were processed. Accordingly, the filtered EMG signals during isometric and isokinetic (18 degree to 22 degree trunk flexion angle) extension were rectified and averaged to use as the numerator in the normalization process of EMG signal, which were substituted in the EMG-force relationship to calculate the tensile force of sampled muscles.

CHAPTER 5. RESULTS

5.1 FARO Arm

Results of digitization of muscle origin and insertion coordinates using the FARO Arm showed that erector spinae muscle length increased by about 12% as the subject bent from a 10 degree to a 30 degree trunk flexion angle. The measured points were achieved by placing the tip of the FARO Arm on two proposed plates (T12 and S1) as described by Marras and Granata (1995). Subject #1's data for 10 and 15 degree trunk flexion angle were not saved properly and were therefore not available.

Force-length and force-velocity modulation factors were applied on trunk extensors that were in fact elongated (Sparto and Parnianpour 1999). Digitized results for latissimus dorsi and external oblique muscles were difficult to interpret due to high variability in the results of the digitization due to experimental error during data collection. Increasing trunk flexion angle caused significant movement of bony landmarks of these muscles under the skin and therefore it was necessary to estimate points at which the FARO Arm's tip should be placed. A second factor could be the interaction between the curved shape of these muscles and the lumbar curvature that might result in data variation among subjects. Accordingly we do not present results for these other muscles here. Fortunately the erector spinae (longissimus) data was the most critical for the estimation of f(l) and f(v) modulation factors.

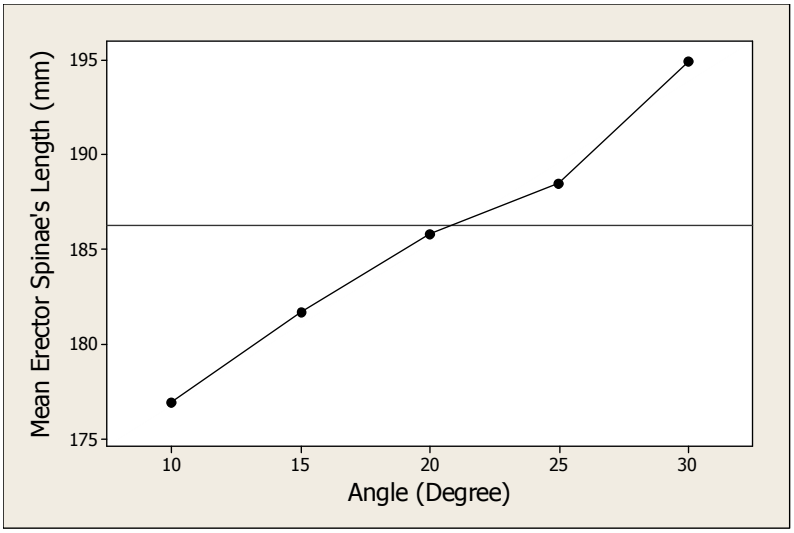

Figure 30. Mean erector spinae muscle length cross all four subjects measured from T12 to S1 in different trunk flexion angles.

Relying on present digitized data (Figure 30) and Figure 28 we considered force-length modulation factors to be 0.94, 1, and 0.94 for 10, 20, and 30 degree trunk flexion angles respectively (and 0.97 for the 25 degree condition in the model validation experiments).

5.2 Fatigue verification

5.2.1 Isometric extension phase

The aim of the current experimental design, to induce fatigue on trunk extensors under fatiguing isometric exertions was achieved. Prior to performing the statistical analysis, graphical checking of the normality of residuals and the homogeneity of variance assumptions validated the adequacy of the ANOVA model (Appendix. B). No muscle violated the condition of normality of residual assumptions. Statistical analysis showed that

there was significant difference between the NEMG value of primary trunk extensor muscles for pre-fatigue and post-fatigue trials (Table 3).

Table 3. P-values of effect of fatigue on NEMG signals of primary trunk extensors in the isometric phase trials. Analysis performed by level of ANGLE. (NS – Not Significant)

	Multifidus	Longissimus	Iliocostalis
10 Degree	NS	0.005	0.004
20 Degree	0.0001	0.0001	0.0001
30 Degree	0.0001	0.001	0.0001

Figures 31 to 33 show that EMG signals, for a given force, increased for essentially all primary trunk extensor muscles as fatigue developed. This confirms our expectation of increased EMG signals under fatiguing conditions even at constant extension moment. Initial activity was more than 35% MVC for all three trunk-flexion angles.

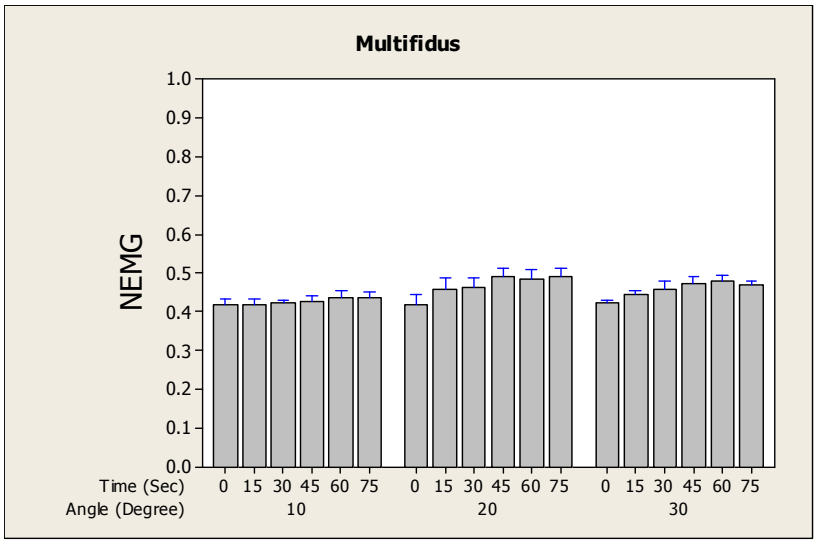

Figure 31. Mean NEMG of the bilateral multifidus under fatiguing 50% MVC isometric exertions in 10, 20, and 30 degree trunk flexion angles (The error bars on this and all subsequent figures are used to show standard error of mean for this measure. It should be noted that these error bars reflect both the between subject and within subject variability, while the statistical analysis did use subject as a blocking variable.)

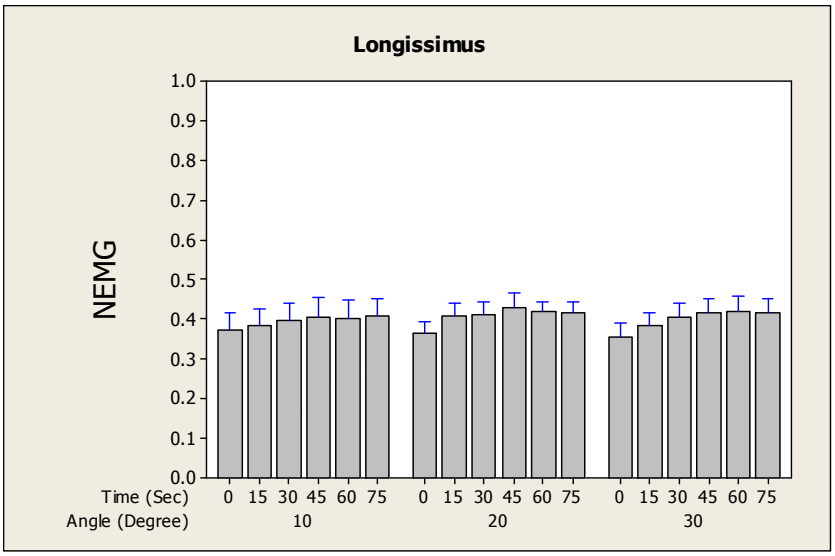

Figure 32. Mean NEMG of the bilateral longissimus under fatiguing 50% MVC isometric exertions in 10, 20, and 30 degree trunk flexion angles.

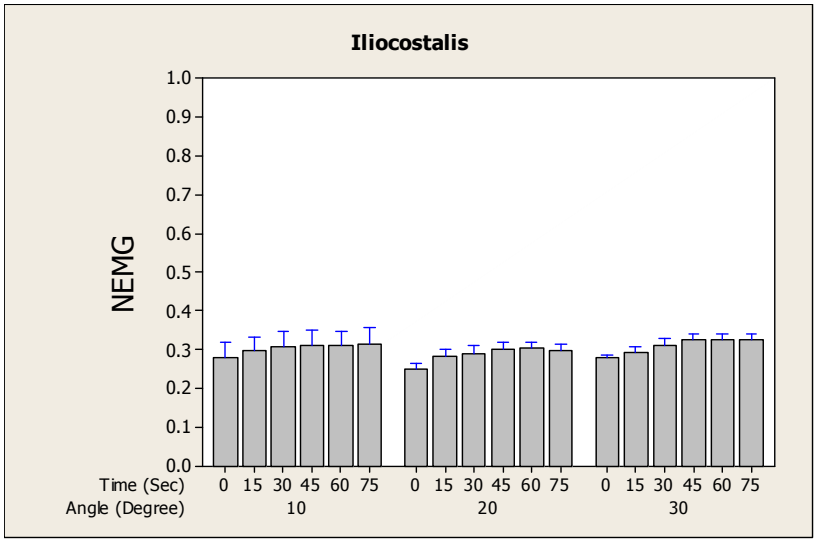

Figure 33. Mean NEMG of the bilateral iliocostalis under fatiguing 50% MVC isometric exertions in 10, 20, and 30 degree trunk flexion angles.

Initial activity of trunk flexor muscles and latissimus dorsi was less than <20% MVC (Figures 34 to 36); it is therefore assumed that significant fatigue was not developed in the 75 seconds of this experiment (Hagberg 1981). Our results showed that NEMG activity of these muscles increased during the isometric extension phase. Previous studies have shown that trunk antagonist muscle activity increases during fatiguing exertion to provide more stability (Potvin and O'Brien 1998, Granata et al. 2004).

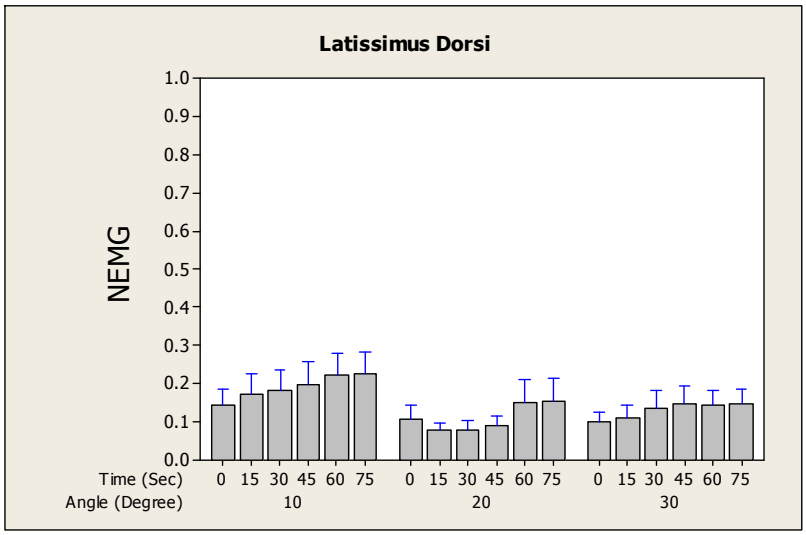

Figure 34. Mean NEMG of the bilateral latissimus dorsi under fatiguing 50% MVC isometric exertions in 10, 20, and 30 degree trunk flexion angles.

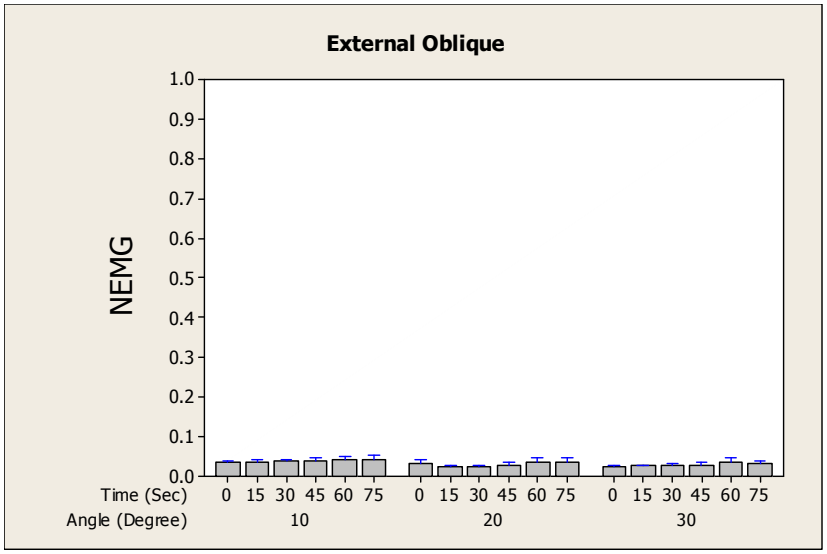

Figure 35. Mean NEMG of the bilateral external oblique under fatiguing 50% MVC isometric exertions in 10, 20, and 30 degree trunk flexion angles.

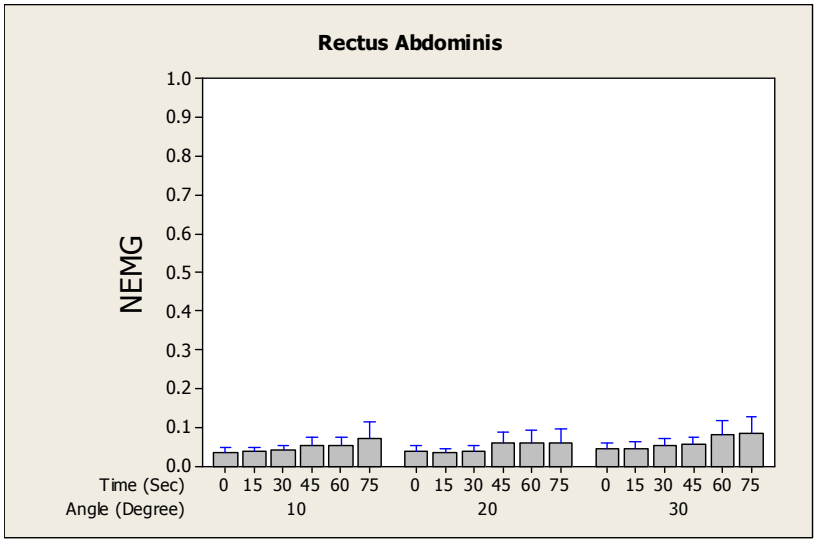

Figure 36. Mean NEMG of the bilateral rectus abdominis under fatiguing 50% MVC isometric exertions in 10, 20, and 30 degree trunk flexion angles.

The ANOVA revealed that median frequency of the erector spinae muscle group was significantly affected by TIME and ANGLE (Table 4) while interaction of TIME and ANGLE was not significant. Computing the median frequency during low EMG activity is

not reliable (O'Brien and Potvin 1997); hence we didn't present results of median frequency for other sampled muscles.

Table 4. P-values for of the ANOVA results for median frequency shift of primary trunk extensors during isometric extension phase.

	Multifidus	Longissimus	Iliocostalis
ANGLE	0.0001	0.0001	0.0001
TIME	0.0001	0.0001	0.002
ANGLE*TIME	NS	NS	NS

A drop of median frequency was associated with fatigue of the primary trunk extensor muscles. This showed that fatigued muscles recruited slow-twitch fibers to provide a given force, since the smaller size of slow-twitch fibers resulted in a smaller conduction velocity, which in turn generated a lower median frequency of the EMG power spectrum (De Luca 1993).

Moreover, results of this study confirmed a negative shift of median frequency with increased muscle elongation values as a result of increased trunk flexion angle (Mannion and Dolan 1996, Inbar et al. 1987). Because the volume of a muscle fiber is constant, during elongation the radius of a muscle fiber decreases. The conduction velocity of muscle is associated with muscle fiber radius and, accordingly, conduction velocity decreases when radius of muscle fiber decreases. The drop in median frequency at greater trunk flexion angle resulted from reduced conduction velocity under muscle elongation (Figures 37 to 39).

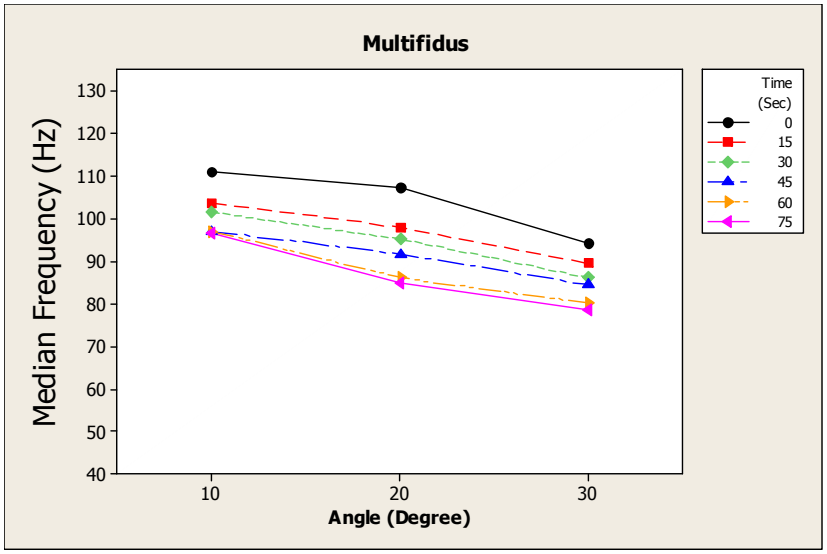

Figure 37. Interaction effect of muscle length (ANGLE) and developing fatigue (TIME) on median frequency of multifidus in the isometric phase..

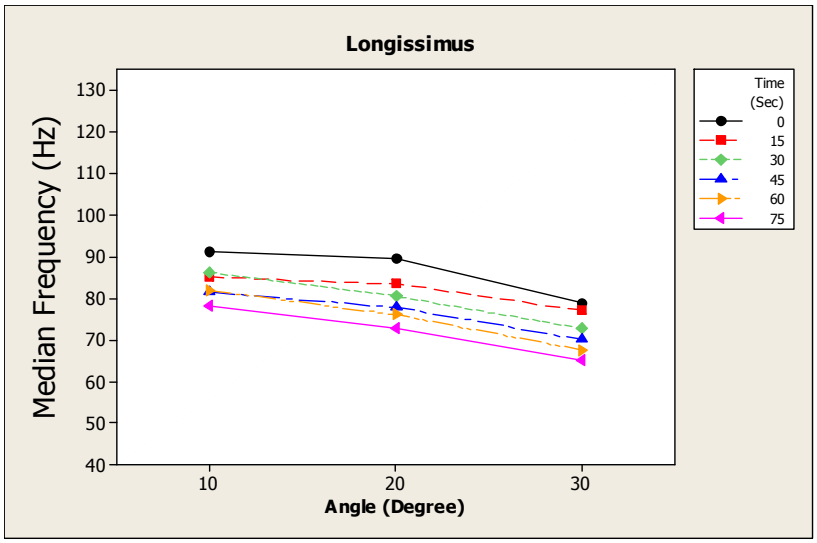

Figure 38. Interaction effect of muscle length (ANGLE) and developing fatigue (TIME) on median frequency of longissimus in the isometric phase.

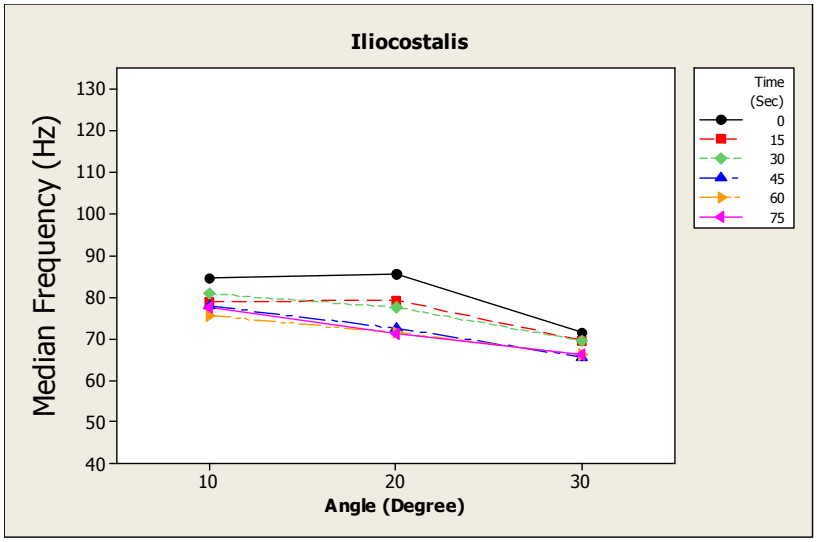

Figure 39. Interaction effect of muscle length (ANGLE) and developing fatigue (TIME) on median frequency of iliocostalis in the isometric phase.

5.2.2 Isokinetic extension phase

Prior to performing the statistical analysis, the normality of residuals and the homogeneity of variance assumptions were checked graphically to validate the adequacy of the ANOVA model. A few muscles violated normality of the residual assumptions, so Log 10 transformations were used to allow conformance with ANOVA model. Statistical analysis showed that there was significant difference among the NEMG values of the longissimus for pre-fatigue and post-fatigue trial (Table 5).

Table 5. P-values showing the effect of fatigue on NEMG signals of the primary trunk extensors in the isokinetic phase trials. Analysis performed by level of VELOCITY.

	Multifidus	Longissimus	Iliocostalis
0 Degree/Sec	0.004	0.0001	0.0001
5 Degree/Sec	NS	0.003	0.001
15 Degree/Sec	NS	NS	NS

Figures 40 to 42 demonstrate that EMG signals of primary global trunk extensor muscles increased with developing fatigue for a given force. These results confirmed our expectation of enhancement of EMG signal for fatigued muscles. In the present study only primary trunk extensor muscles were fatigued (Table 6).

Similarly to the results of the isometric extension phase, the NEMG activity of longissimus and iliocostalis increased with fatigue development for a given external moment, while NEMG activity of multifidus for 5 and 15 degree/sec didn't change that much in comparison with that for 0 degree/sec (Figure 42). Multifidus plays a major role as a local muscle in providing stability, while the global erector spinae muscle group has responsibility for trunk extension in the required concentric range of motion (Bergmark 1989).

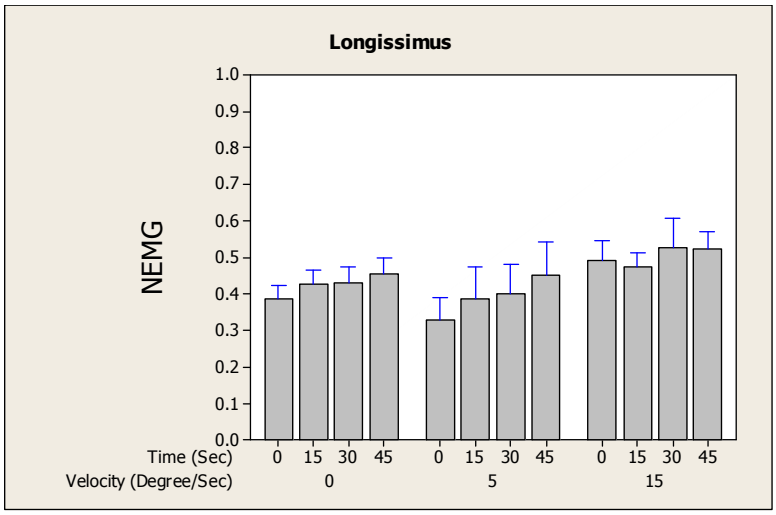

Figure 40. Mean NEMG of bilateral longissimus by developing fatigue in isokinetic extension phase.

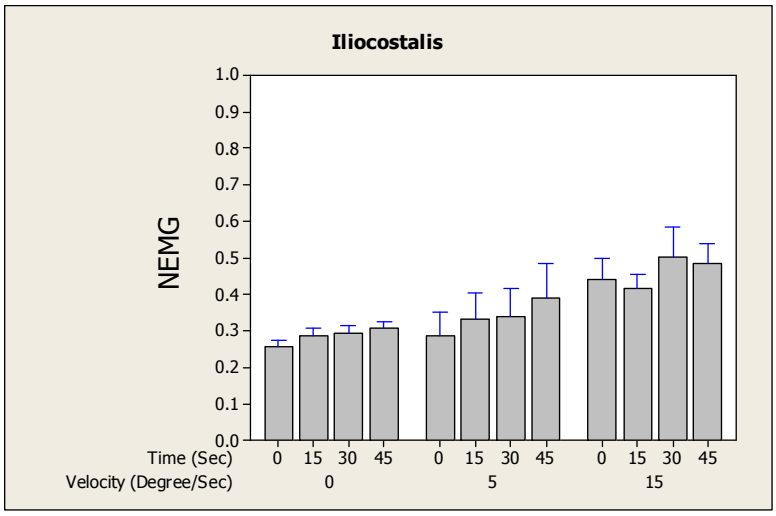

Figure 41. Mean NEMG of bilateral iliocostalis by developing fatigue in isokinetic extension phase.

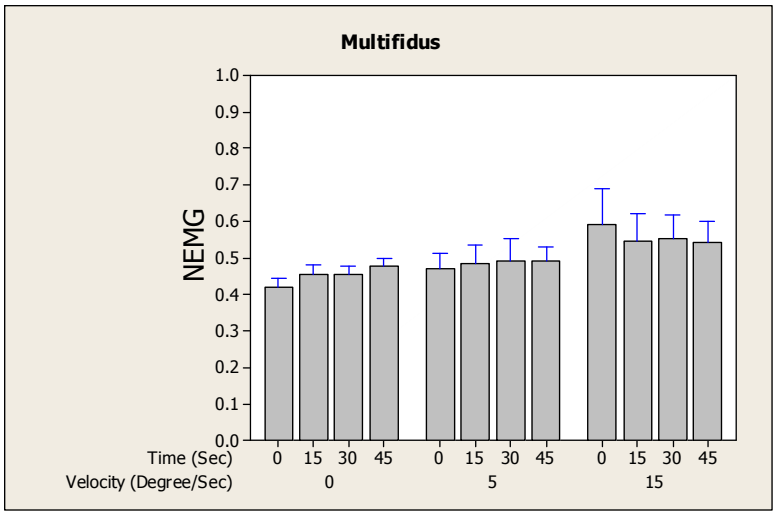

Figure 42. NEMG of bilateral multifidus by developing fatigue in isokinetic extension phase.

Similar to the isometric extension phase, it is assumed that only primary trunk extensors were fatigued, because initial muscle activity of these muscles was high enough to develop fatigue during asked force exertion for which a decrease of median frequency confirms this claim. However initial activation of trunk flexor muscles and latissimus dorsi were not that much to be able to develop fatigue in given duration force exertion.

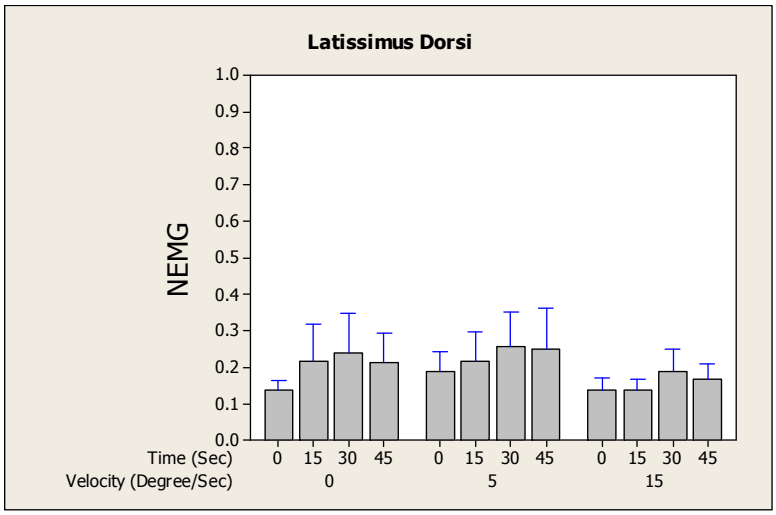

Figure 43. Mean NEMG of bilateral latissimus dorsi by developing fatigue in isokinetic extension phase.

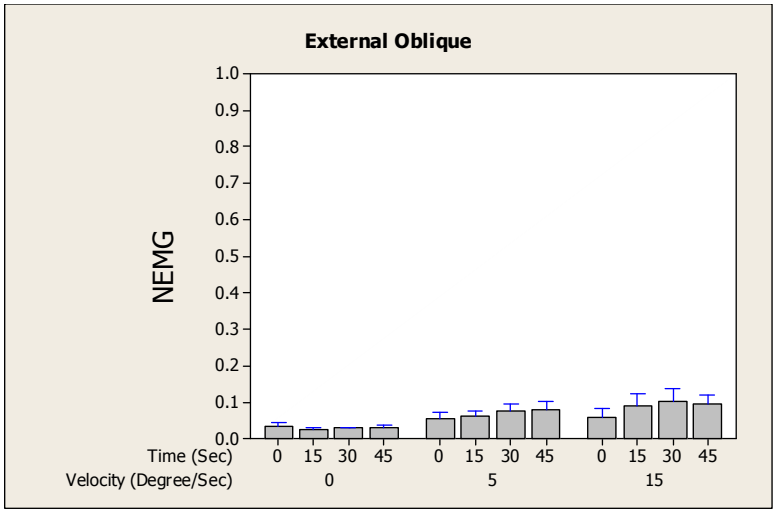

Figure 44. Mean NEMG of bilateral external oblique by developing fatigue in isokinetic extension phase.

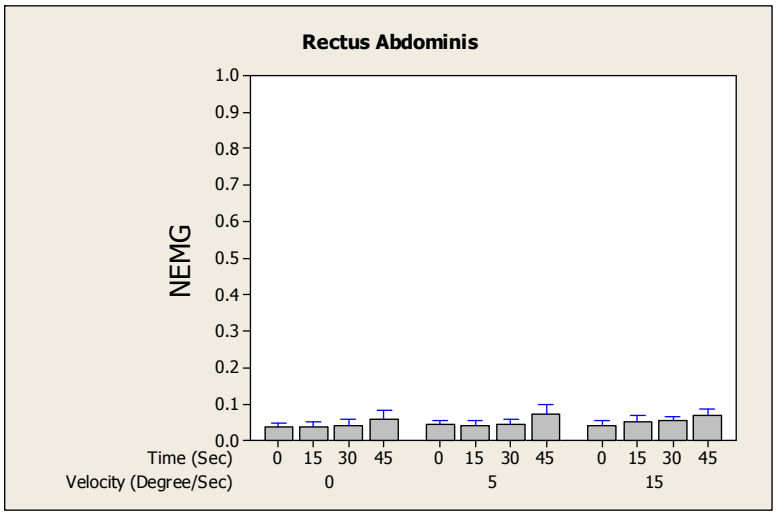

Figure 45. Mean NEMG of bilateral rectus abdominis by developing fatigue in isokinetic extension phase.

The ANOVA revealed that the median frequency of the trunk extensor muscles was significantly ($p<0.05$) affected by TIME (Table 6). It also showed that we achieved to aim of experimental design, i.e., to develop fatigue (Figures 46 to 48).

Table 6. P-values for of the ANOVA results for median frequency shift of primary trunk extensors during isokinetic extension phase.

	Multifidus	Longissimus	Iliocostalis
VELOCITY	0.0001	0.0001	0.0001
TIME	0.0001	0.0001	0.003
VELOCITY*TIME	NS	NS	NS

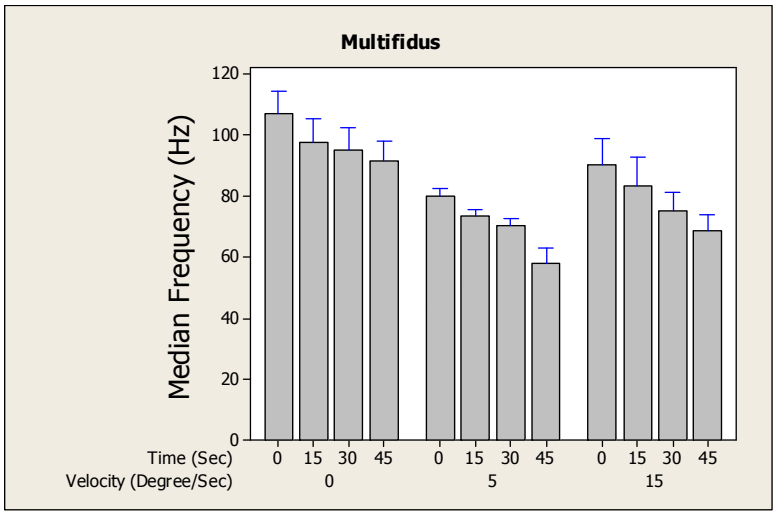

Figure 46. Median frequency of multifidus as a function of TIME in the isokinetic phase.

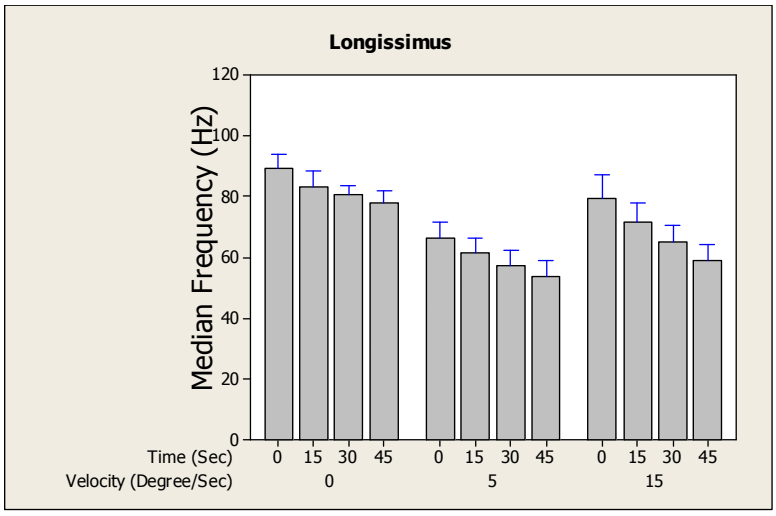

Figure 47. Median frequency of longissimus as a function of TIME in the isokinetic phase.

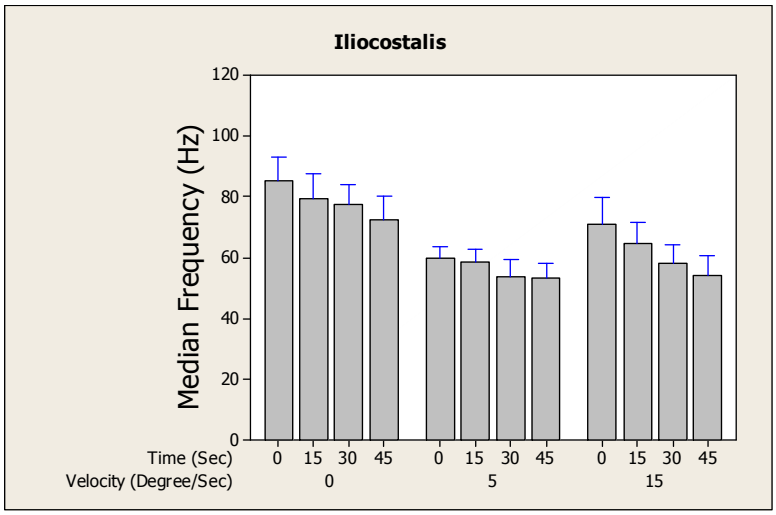

Figure 48. Median frequency of iliocostalis as a function of TIME in the isokinetic phase.

5.3 First hypothesis: Force-length modulation factor

Table 7 and Figures 49 and 50 do not support our first hypothesis regarding the need for changing the force-length modulation factor under a fatigue development condition. Increased EMG signals of sampled trunk extensor muscles under developing fatigue shifted relatively constant at each specific angle; hence it is supposed that force-length modulation factor need not be changed for sampled trunk extensor muscle (longissimus and iliocostalis) in the present modified EMG-assisted spine biomechanical model.

Table 7. P-values from ANOVA results for longissimus and iliocostalis muscle groups during isometric extension phase.

	Longissimus	Iliocostalis
ANGLE	NS	0.052
TIME	0.048	0.008
ANGLE*TIME	NS	NS

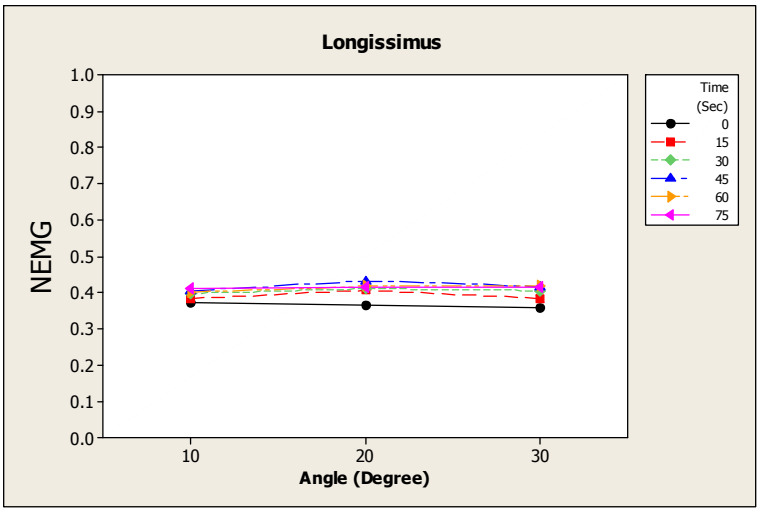

Figure 49. NEMG signal of the longissimus as a function of TIME and ANGLE in the isometric phase.

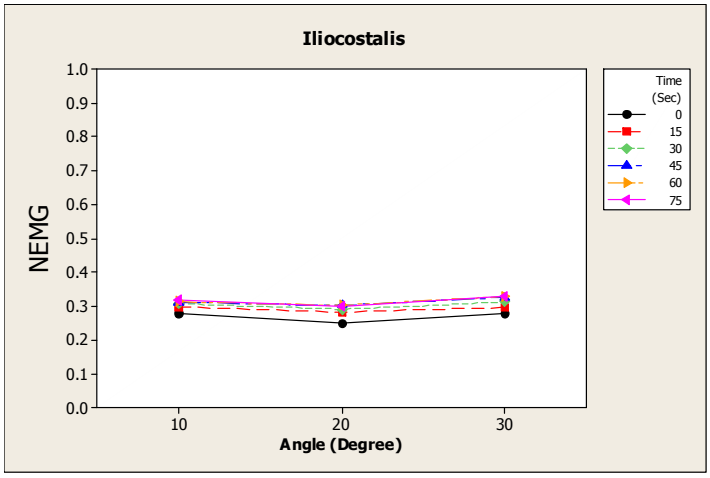

Figure 50. NEMG signal of the iliocostalis as a function of TIME and ANGLE in the isometric phase.

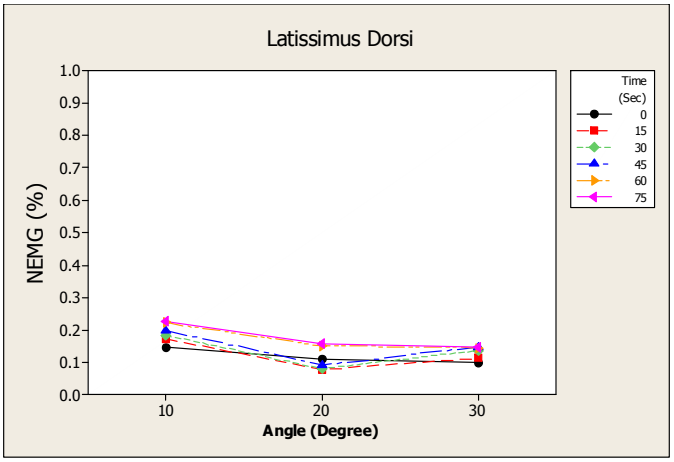

Figure 51. NEMG signal of the latissimus dorsi as a function of TIME and ANGLE in the isometric phase.

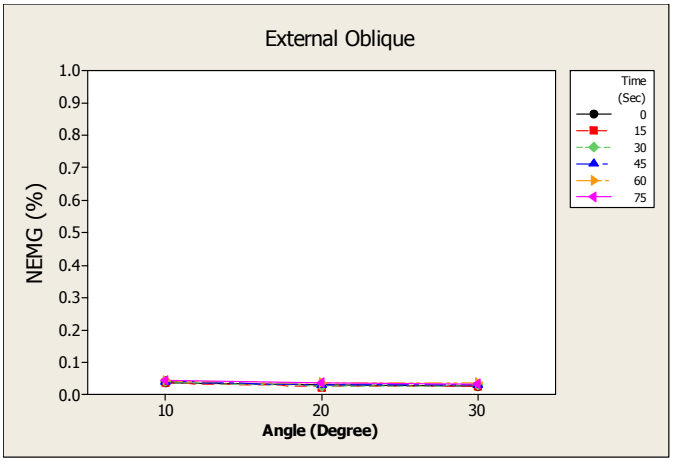

Figure 52. NEMG signal of the external oblique as a function of TIME and ANGLE in the isometric phase.

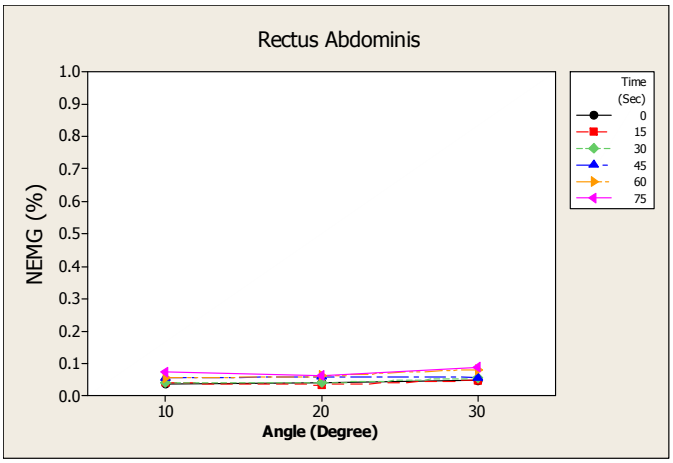

Figure 53. NEMG signal of the rectus abdominis as a function of TIME and ANGLE in the isometric phase.

Results of the pilot test (on one subject) were promising for finding a possible significant interaction effect between ANGLE and TIME. In contrast to the pilot test, the trunk flexion angle was changed from 15º, 30º, and 45º to 10º, 20º, and 30º, which might possibly have affected the data. The reason that we changed these angles was to avoid the impact of passive tissue moment on measured EMG signals.

5.4 Second hypothesis: Force-velocity modulation factor

Table 8 and Figures 54 and 55 do not support our second hypothesis regarding a need for changing the force-velocity modulation factor under conditions of fatigue development. Increased EMG signals of sampled trunk extensor muscles shifted relatively constant under fatigue development at each specific velocity; hence it is assumed that that the force-velocity modulation factor need not be changed for sampled primary trunk extensor muscle (longissimus) in the present modified EMG-assisted spine biomechanical model.

Table 8. P-values from ANOVA results for longissimus and iliocostalis muscle groups during isokinetic extension phase.

	Longissimus	Iliocostalis
VELOCITY	0.101	0.004
TIME	0.042	0.047
VELOCITY*TIME	NS	NS

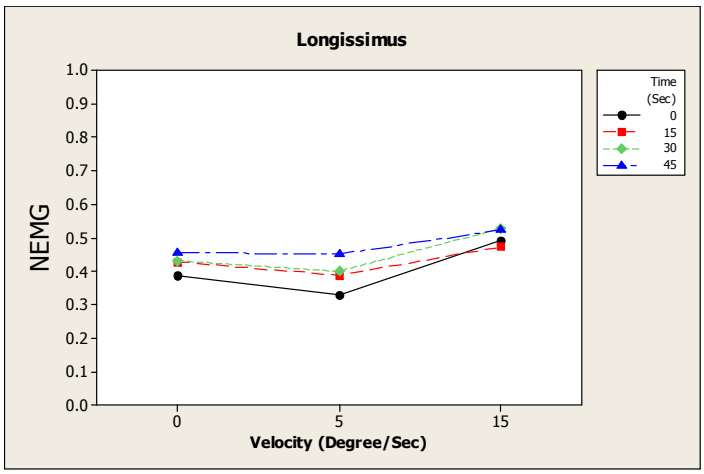

Figure 54. NEMG signal of the longissimus as a function of TIME and VELOCITY in the isokinetic phase.

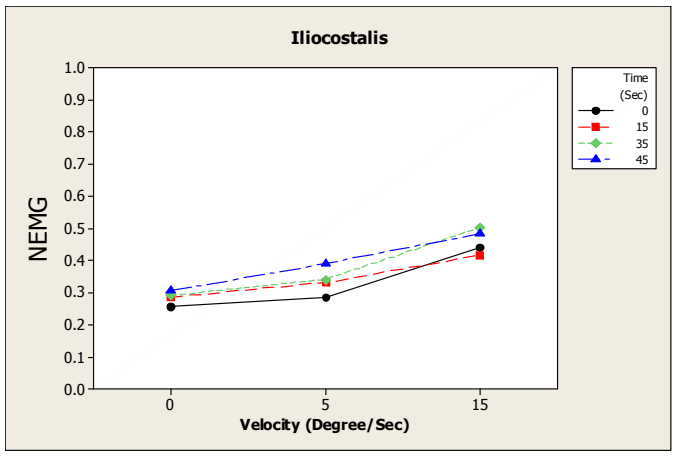

Figure 55. NEMG signal of the iliocostalis as a function of TIME and VELOCITY in the isokinetic phase.

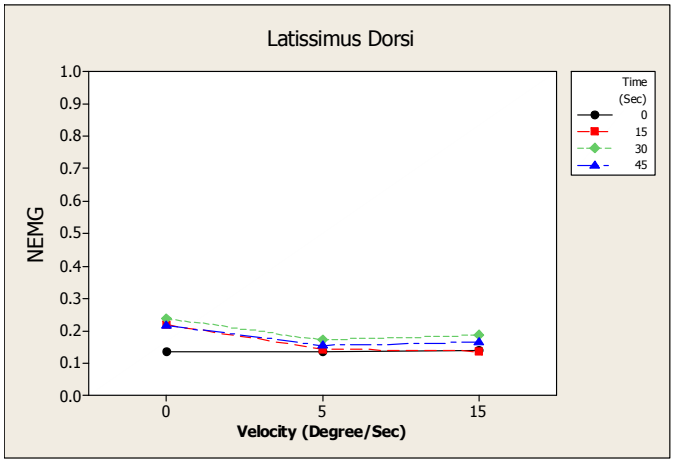

Figure 56. NEMG signal of the longissimus as a function of TIME and VELOCITY in the isokinetic phase.

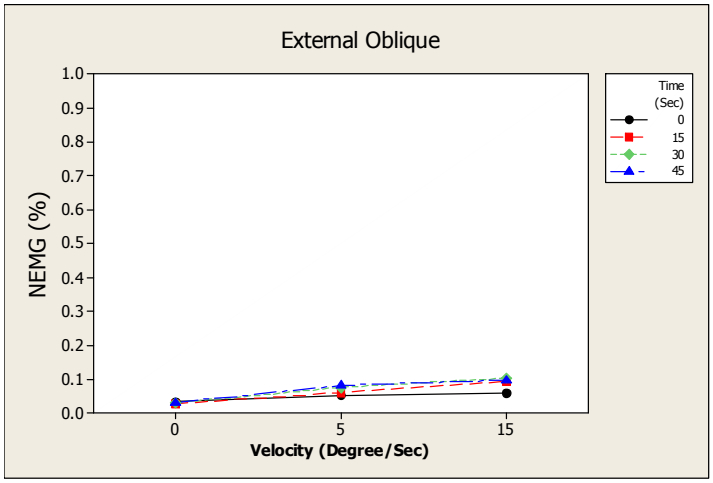

Figure 57. NEMG signal of the external oblique as a function of TIME and VELOCITY in the isokinetic phase.

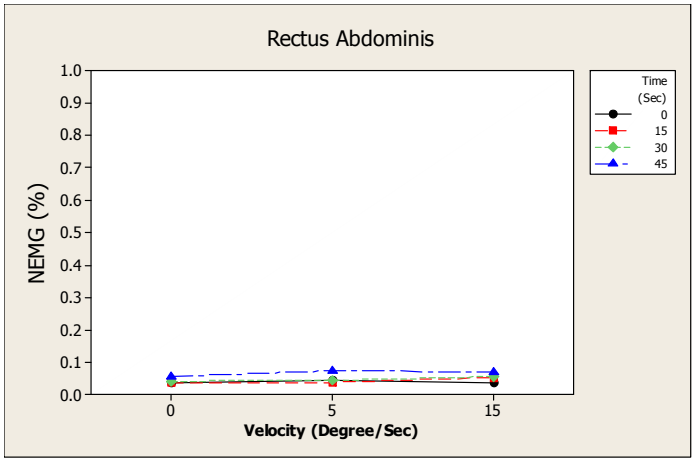

Figure 58. NEMG signal of the rectus abdominis as a function of TIME and VELOCITY in the isokinetic phase.

It must be noted that trunk muscles work together as a system and subjects may choose different muscle recruiting strategies under different conditions. The results of the present study show that the force-velocity modulation factor in EMG-assisted spine biomechanical models doesn't need to be changed in low angular velocities tested in this study during fatiguing lifting exertions while considering all superficial trunk muscles. Higher values of angular trunk extension velocity should be explored before a summative statement should be attempted.

5.5 Third hypothesis: Gain factor

5.5.1 Model evaluation

All subjects could successfully exert a consistent 50% of maximum force generation capacity through the data collection intervals (Table 9).

Table 9. Mean external moments (SD) exerted by subjects in experimental trials.

	Subject 1 (N.m)	Subject 2 (N.m)	Subject 3 (N.m)	Subject 4 (N.m)
10 Degree	75.66 (0.51)	102.55 (0.61)	88.667 (0.51)	99.167 (0.98)
20 Degree	100.50 (0.54)	117.20 (0.44)	90.800 (0.44)	116.17 (2.56)
30 Degree	114.50 (1.05)	112.00 (1.10)	89.33 (2.66)	133.17 (0.753)
5 Degree/Sec	96.62 (1.75)	100.75 (0.95)	87.500 (1.00)	113.00 (2.00)
15 Degree/Sec	101.30 (2.57)	95.75 (0.50)	86.00 (2.65)	114.50 (2.65)

To explore the impact of allowing the gain factor to vary as a function of the change in median frequency a comparison was made between the traditional EMG-assisted model (not allowing the gain to vary) and the proposed model (allowing the gain to vary as a function of fatigue (Equation 7)). Table 10 presents mean absolute error and mean

normalized error computed between estimated internal moment and measured external moment for both predicted as well as invariant gain factors.

e 10. Mean absolute error and mean normalized error between estimated internal moment and measured external moment for both predicted as well as invariant gain factors.

	Mean Absolute Error (N.m)	Mean Normalized Error (%)
Invariant Gain Factor	18.55	17.5
Predicted Gain Factor	10.20	9.67

Figure 59 depicts changes of mean absolute error computed between estimated internal moment and measured external moment using invariant versus predicted gain factor.

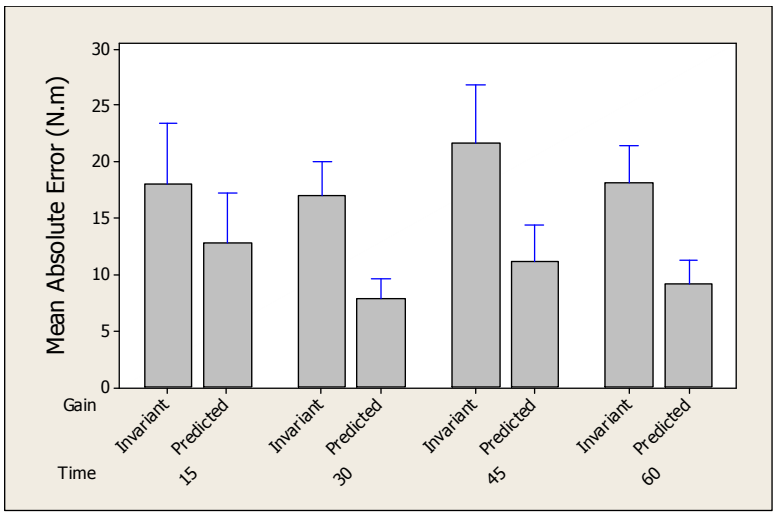

Figure 59. Changes of mean absolute error computed between internal and external moment using invariant versus predicted gain factor.

Accordingly, the mean absolute error value revealed that the internal moment has been predicted fairly well by employing the predicted gain factor without frequent

measurement of maximum force generation capacity. Moreover, the results shown in Table 11 statistically confirmed hypothesis three. The absolute error between measured external moment and estimated internal moment changed significantly while considering an invariant versus predicted gain factor for fatigued muscle. This means that, to estimate spine loading accurately, the gain factor must be modulated during fatigue development.

Table 11. ANOVA result for absolute error calculated between internal and external moments using invariant and predicted gain factors.

	Absolute Error
TIME	NS
Gain factor type (invariant vs. predicted)	0.002
TIME*Gain factor type	NS

Table 12 indicates mean absolute error and mean normalized error between actual gain and predicted gain.

Table 12. Mean absolute error and mean normalized error between predicted and actual gain factors.

	Mean Normalized Error (%)	Mean Absolute Error (N/cm^2)
Predicted Gain Factor	13.3	9.3
Model with Invariant Gain	23.1	16.5

5.5.1.1 Isometric extension phase

Figure 60 shows how accurate an EMG-assisted model could estimate internal moment using different gain factors. In this figure, the columns labeled “actual” refer to the internal moment calculated using the actual gain that equilibrates the system (i.e. this is the

"gold standard for comparison). "Invariant" refers to the internal moment using the gain found in the unfatigued condition and used on all subsequent trials. "Predicted" refers to the internal moment using the value of gain predicted from Equation 7. It shows that the estimated internal moment using a predicted gain factor was more consistent with the actual internal moment (measured external moment) than an invariant one. An estimated internal moment with invariant gain increased with time even though the exerted external moment was constant, and therefore it was not acceptable.

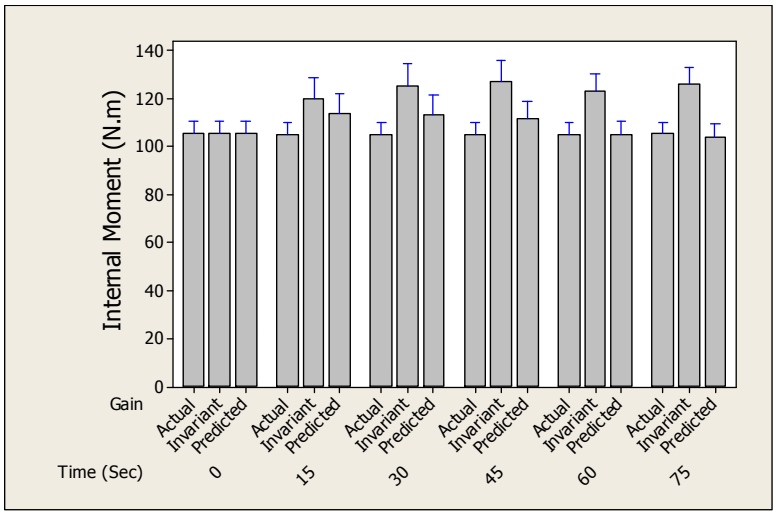

Figure 60. Changes of computed internal moment using different gain factors during developing fatigue.

Considering the impact of these results on the spinal loading variables, ANOVA test results showed anterior-posterior (A-P) shear force on L5/S1 changed significantly due to experiencing an increase in flexion angle as well as developing fatigue (Table 13). These results were generated using the gain value calculated using Equation 7. Since the external moment is constant at a given trunk angle, one would expect that the compression force and

the erector spinae muscle force would not vary as a function of TIME, but would change as a function of ANGLE. The significant effect of TIME on the A-P Shear force is likely the results of an increase in co-contraction force during fatigue development (Figure 61). The curved shape of the external oblique causes its activity to have a significant impact on A-P shear force.

Table 13. ANOVA test for resultant force of sampled muscles on L5/S1.

	Compression Force (N)	A-P Shear Force (N)	Erector Spinae Force (N)
ANGLE	0.065	0.0001	0.004
TIME	NS	0.007	NS
ANGLE*TIME	NS	NS	NS

Figure 62 presents changes of compression force on L5/S1 during fatigue development under actual, invariant, and predicted gain factors. By applying an invariant gain factor, the compression force increased under developing fatigue, while results of predicted and actual gain factors were consistent and compression force didn't changed significantly.

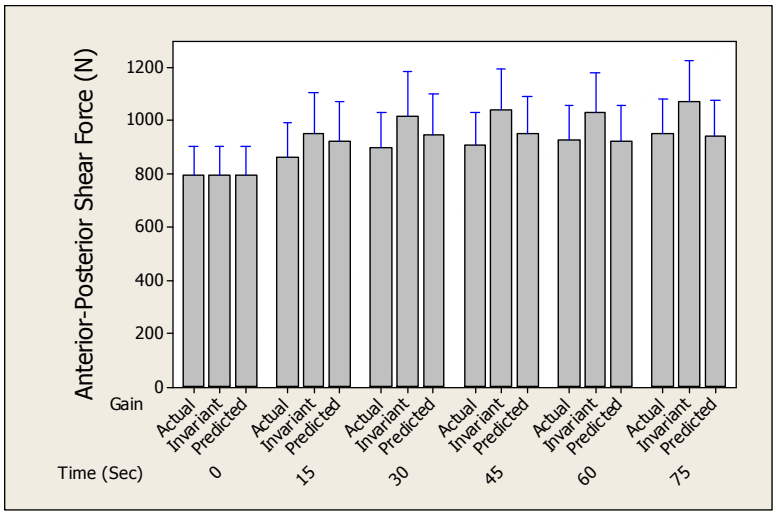

Figure 61. Changes of A-P shear force on L5/S1 by time.

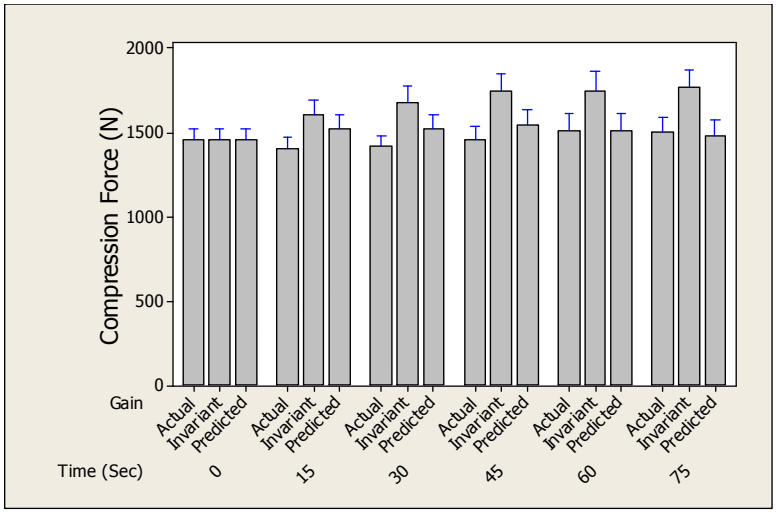

Figure 62. Changes of compression force on L5/S1 by time.

5.5.1.2 Isokinetic extension phase

Similar to section 5.5.1.1 estimated internal moment using predicted gain was more accurate than that for invariant gain (Figure 63).

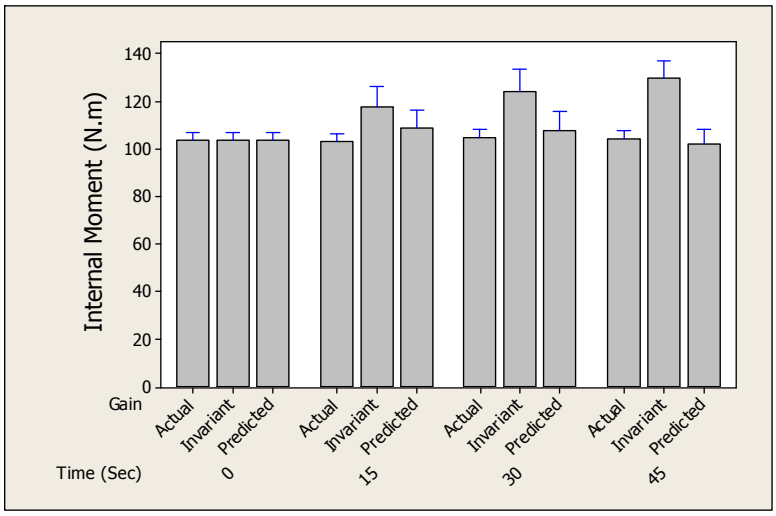

Figure 63. Changes of estimated internal moment using different gain factors during time.

The results of an ANOVA test, shown in (Table 14), indicate that A-P shear force changed significantly by VELOCITY and TIME. Both velocity and fatigue increase co-contraction force level, so shear force could increase due to increase of abdominal muscle activity (Figure 64). Increase of shear forces has been regarded as a risk factor for manual material handling, so it is important for ergonomists to have an accurate estimation of that.

Table 14. ANOVA test for internal forces provided by muscles on L5/S1.

	Compression Force (N)	A-P Shear Force (N)	Erector Spinae Force (N)
VELOCITY	0.089	0.028	NS
TIME	NS	0.021	NS
VELOCITY*TIME	NS	NS	NS

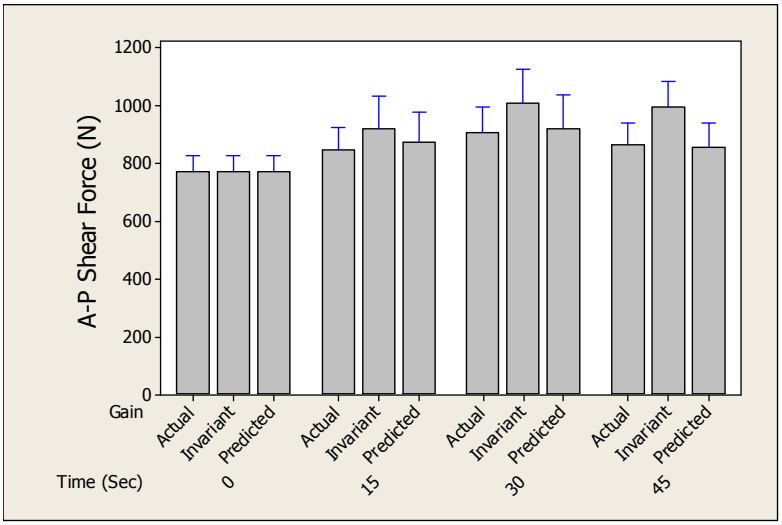

Figure 64. Changes of shear force on L5/S1 using different gain factors during time.

Figure 65 shows that estimated compression force by invariant gain, similar to internal moment, increased during developing fatigue; while estimated compression force using actual gain and predicted gain were not much affected change by fatigue.

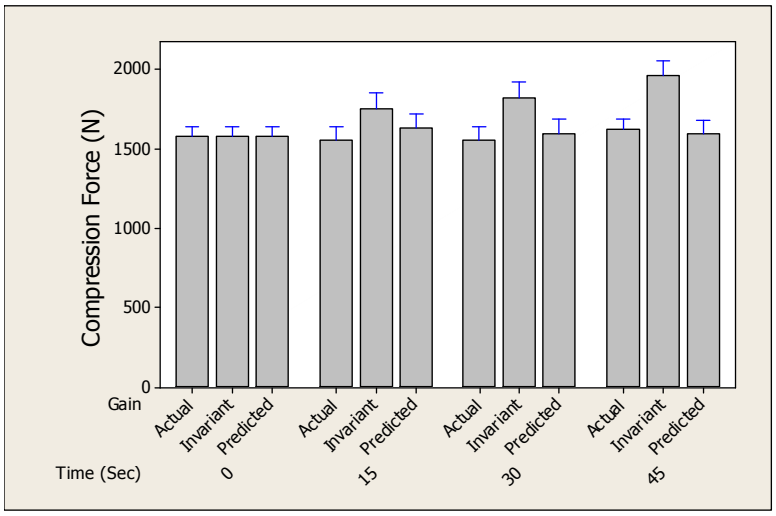

Figure 65. Changes of compression force using different gain factors during time.

Subjects exerted 50% of their maximum voluntary contraction with sagittal symmetry, so internal moment was only computed in the sagittal plane. Accordingly,

changes of compression force and internal moment for each considered gain factor were relatively consistent.

5.6 Model validation

Table 15 presents mean normalized error between estimated internal moment and measured external moment using invariant and predicted gain factors. It affirms that employing predicted gain improved mean normalized error from 21.4% to 12.9% in comparison to invariant gain factor. Moreover, Figure 66 shows that internal moment estimated using predicted gain factor is fairly consistent with measured external moment, while internal moment estimated via invariant gain factor shows fatigue-dependent increase. External moment was maintained consistently during protocol. Figures 67 and 68 confirmed similar findings to section 5.5.1 for spine loading.

Table 15. Mean absolute error and normalized absolute error between predicted internal moment and measured external moment for both modified as well as invariant gain factors.

	Mean Absolute Error (N.m)	Mean Normalized Error (%)
Invariant Gain Factor	22.49	21.40
Predicted Gain Factor	13.29	12.94

As previously mentioned, if EMG-assisted model could provide accurate estimates of internal moment, then its estimation of spine loading i.e., shear force could be reliable. These results show that a newly-developed EMG-assisted model that requires only gain factor modification, without altering force-length and force-velocity modulation factor or measuring frequent maximum force generation capacity, can lead to accurate estimates of spine loading.

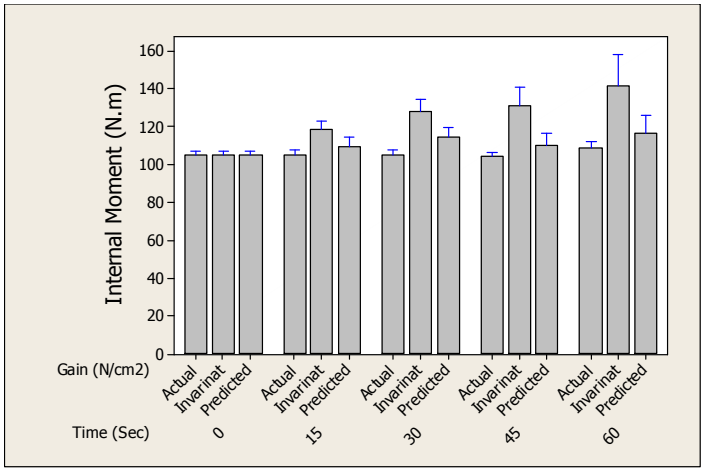

Figure 66. Changes of computed internal moment using different gain factors during time.

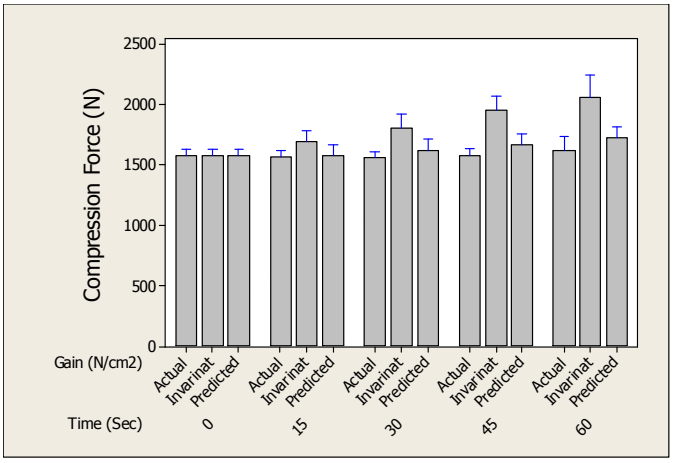

Figure 67. Changes of compression force using different gain factors during time.

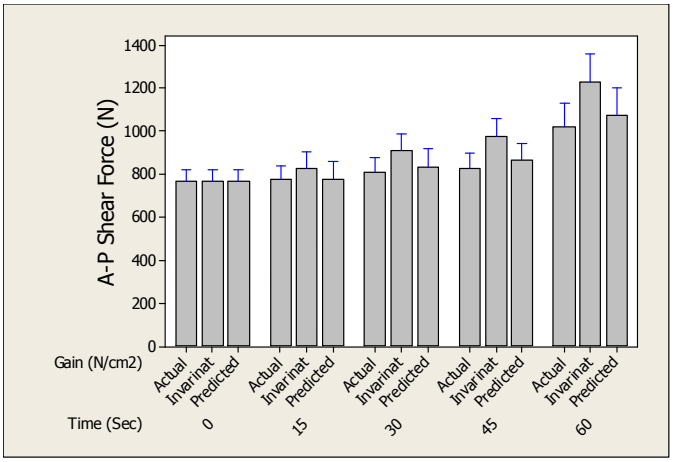

Figure 68. Changes of A-P shear force using different gain factors during time.

CHAPTER 6. DISCUSSION

The purpose of spine biomechanical approach is to determine acceptability of each task in the range of potential activities because previous studies have shown that biomechanical stresses on the lumbar spine have a direct relationship with risk of injury (Kumar 2001). The development of more accurate models will serve to ascertain knowledge of lumbar spine biomechanics, improve the ability to predict the cause and risk of injury during MMH, and provide a better basis for assessing recommendations for reducing risk factors during MMH. Accordingly, mathematical models of the lumbar spine for estimating the relevant loads during various postures have been developed. Unfortunately as these models more accurately modeled the muscular anatomy, the biomechanical system becomes indeterminate from the standpoint of mechanical equilibrium and requires other solution methods.

To overcome problems and errors associated with these simplified models, researchers have employed the EMG-assisted modeling technique. Input of EMG-assisted models are captured empirical data directly from the sampled muscles of a human subject performing a lifting task and then use these data to estimate spinal loading. In EMG-assisted models, muscle forces are predicted with captured EMG data and the accuracy of the predications could be checked by comparison of the measured external moment and estimated internal moment provided by muscles. To increase the accuracy of these EMG-assisted models, several other known physiological factors have been addressed by developing force-length and force-velocity modulation factors. These models have proven very effective at estimating muscle forces and spinal loads under a variety of conditions.

It is important to note, however, that all previous validated EMG-assisted models except Sparto and Parnianpour (1999) have considered fresh (i.e. unfatigued) muscles. The muscles during fatiguing recruit slow twitch fibers instead of fast twitch fibers to increase endurance. This leads to different EMG responses at various contraction lengths and velocities in comparison to those of fresh muscles because of different mechanical features used by slow and fast twitch fibers to provide a given force. Sparto and Parnianpour (1999) addressed this challenge by asking subjects to exert repeated maximum voluntary contractions throughout a fatiguing protocol so that the normalized EMG would reflect an accurate estimate of the percent of maximum force generated by that muscle at that instant in time. They demonstrated that this did, in fact, provide a reliable method for addressing these EMG artifacts that occur as a result of muscle fatigue. It is not practical, or wise, to have subjects perform a large number of MVC exertions during an experimental trial, and it is impossible in an industrial environment. Accordingly, the goal of this study was to develop an EMG-assisted model that is able to accurately assess spinal loads during fatiguing exertions. This led to a detailed investigation of the impact of muscle fatigue on 1) the force-length modulation factor, 2) the force-velocity modulation factor and 3) the gain factor (maximum muscle stress value).

6.1 First hypothesis: Force-length modulation factor

Previous studies have shown that muscle length has a significant impact on median frequency as well as on EMG amplitude (Inbar et al. 1987; Dolan et al. 1995). Therefore a force-length modulation factor was introduced to modulate impact of muscle length on EMG

signals for a given force. It was unknown, however, whether the determined force-length modulation factor for fresh muscle should be different for fatigued muscles or not. The opportunity of cross-bridge formation plays a major role at different lengths, and is greatest at resting muscle length. However, whether or not the likelihood of this formation is equivalent for both slow and fast twitch fibers was a motivation for this study in evaluating the interaction effects of TIME and ANGLE on EMG signals.

The results of the isometric extension phase showed that interaction effects between TIME and ANGLE were not significant in EMG signals. Relying on ANOVA test results, it was found that force-length modulation factor need not be changed during fatigue development in the presented range of motion. The results of the pilot test (performed for only one subject) were promising with respect to finding a significant impact of TIME and ANGLE interaction on EMG signals. However patterns of EMG signals found in the full study simply did not show a significant interaction between TIME and ANGLE (Figures 49-51) as was seen in the pilot work (Figures 14-15). There was very little data in the basic muscle physiology literature indicating that this interaction might be expected, but because of some promising pilot results, it was pursued.

One important difference between the present study and the pilot test was that we considered 10, 20, and 30 rather than 15, 30, and 45 degree trunk flexion angles to avoid possible effects related to passive tissue moment. Dolan et al. (1994) showed that passive tissues, i.e., intervertebral ligaments, the lumbodorsal fascia, and even the disc itself, can generate extensor moments during lifting and thereby partially compensate for external moments at extreme flexion angles. The impact of passive tissue in generating such internal moments within the range considered in the present study was negligible because the passive

tissues could not be elongated enough when moving between a fully upright and a 30 degree trunk flexion angle to make a significant contribution to the extensor moment (Marras and Granata 1997). It is unlikely therefore that this is the source of the non-significant effect.

6.2 Second hypothesis: Force-velocity modulation factor

It was expected that collected EMG signals under fatigue development and resulting recruitment of slow twitch fibers would differ from those of fresh muscle, since the capability to provide the required shortening velocity and force differs from that of fast twitch fibers. It is believed that the reduction in maximum shortening velocity is due to an alteration in cross-bridge kinetics due to recruiting of slow-twitch fibers rather than fast-twitch fibers in fatiguing muscle (Chaffin 1999) as a result of fast twitch units reaching their peak tension and relaxing more rapidly than slow units. De Ruiter et al. (2000) showed that the drop in the force generation capability of human adductor pollicis muscle during developing fatigue is affected by changes in angular velocity. By reviewing various factors that affect EMG signals, it is apparent that factors that could potentially introduce physiological artifacts must be recognized and controlled when using EMG signals to compute muscle contraction forces for fatigued muscle. However the results of this study suggested that force-velocity modulation factors for low velocities need not be changed. Achievement of a high confidence level with respect to experimental control and to the EMG-assisted model's assumptions required that we choose low velocity values (0, 5, and 15 degree/sec) in the present study (Granata and Marras 1993; Marras and Granata 1997). De Ruiter et al. (2000) evaluated the impact of fatigue on the force-velocity relationship at

angular velocities larger than 100 deg/sec for human adductor pollicis muscle. We do not preclude the possibility that alteration of the force-velocity modulation factor may be required at these higher velocities. The EMG-assisted model is valid for smooth lifting exertion, during which the time delay between the muscle contraction force and onset of EMG signals is negligible (Granata and Marras 1995). Accordingly, selected angular velocity levels were fairly low in the present experimental design in which subjects were asked to maintain only 50% MVC during extension. Although EMG amplitude increased with fatigue development, interactive effects between TIME and VELOCITY were not significant on captured EMG signals. However, to better understand effects of interaction between TIME and VELOCITY, it might be necessary to perform studies with higher velocity limits. Moreover, co-contraction antagonist muscles play a major role in increasing trunk stability and trunk extensor muscles' activity changes to satisfy mechanical equilibrium. Accordingly, response of a simple individual muscle might be different to that during interaction between velocity and fatigue.

6.3 Third hypothesis: Gain factor

The present study was conducted to achieve an accurate estimation of spine loading occurring during fatiguing lifting exertions. Previous studies have affirmed that an EMG-assisted biomechanical spine model is the most accurate spine model for predicting spine loading by considering inter-subject variability and muscle co-activation force (Marras and Granata 1995; Marras and Granata 1997). The contributions provided by different trunk muscle groups such as the agonist, antagonist, and even lower extremity muscles, might differ in spine loading to satisfy a given force during fatiguing lifting exertions. Hence,

captured the EMG signals of these muscle groups could lead to a more accurate estimation of spine loading.

Trunk-based muscular fatigue produced by overexertion, prolonged isometric exertion, or during repetitive bending, has been identified as having significant impact on occurrence of spinal injuries, specifically those related to manual material handling (Adams et al. 2000), but to our knowledge except for Sparto and Parnianpour (1999), no studies have addressed validation of the EMG-assisted spine biomechanical model under fatiguing lifting exertions. The purpose of using the EMG-assisted model in present study was to employ major muscles with EMG signals measured directly by surface electrodes to estimate spine loading under such exertions. This contributed to understanding of impact of fatigue on agonist and antagonist muscle activities for a given external moment to determine changes in spinal load distribution.

The primary advantage of the present modified EMG-assisted biomechanical model of the spine is that its outputs are reliable under conditions of fatigue without frequently measuring maximum voluntary contraction or even a need to change force-length or force-velocity modulation factors. One major assumption for EMG-assisted biomechanical spine model is use of the same gain factor for all contributing muscles (Granata and Marras 1993; Granata and Marras 1995; Marras and Granata 1997), although as fatigue develops, force generation capability of fatigued muscle declines and thereby gain factor must be reconsidered (Sparto and Parnianpour 1999). The results of the current study using predicted gain factor approved gain factor for fatigued muscle must be modified to produce an accurate estimation of spine loading because of fatigue artifacts on EMG signals.

During fatiguing lifting exertions, a shift of power spectrum to lower frequencies occurs and this has historically been monitored by finding the median frequency of collected EMG during contraction. The median frequency has been known to represent a reliable technique for objectively tracing fatigue during isometric lifting exertion. However, median frequency is not a reliable technique when a muscle has a low activation level (Potvin and Bent 1997). Initial muscle activation level can indicate what particular muscle has become fatigued in a short time (Hagberg 1981). If the muscle's initial activation level is less than 15-20% of MVC (Hagberg 1981), it is assumed that the muscle's endurance time would be infinite. The pre-fatigue activation of the erector spinae muscle group was much greater than the 15% MVC value and its EMG signal median frequency declined significantly in time. It is therefore reasonable to assume that only the erector spinae muscle group was fatigued, and that the observed enhancement in its EMG signal could not be related to increase of tensile force for a given force. The muscle's force-generation capability decreases under developing fatigue (Sparto and Parnianpour 1999) and the muscle must recruit new slow-twitch fibers to provide a given force. Slow-twitch fibers are weaker than fast-twitch fibers (Burke et al. 1973); hence the muscle must recruit a larger number of slow-twitch fibers. This causes the EMG signal amplitude of fatigued muscles to increase, but this increase is not due to tensile force and is rather a fatigue artifact that must be modulated. Sparto and Parnianpour (1999) measured maximum force generation capacity frequently to modulate the gain factor of the erector spinae, since force generation capacity of fatigued muscle herein erector spinae, decline by developing fatigue therefore its gain factor cannot be as same as the pre-fatigue gain factor.

During fatigue, membrane depolarization leads to reduction in action potential (AP) amplitude and a subsequent decrease in the amount of Ca^{+2} released from the sarcolemma reticulum (Allen and Lamb 2008). The effects of AP size and propagation differ among different muscle fiber types. Slow-twitch fibers are more easily excitable than fast-twitch fibers, and therefore a decrease in AP size leads to a reduction in the number of fast-twitch fibers activated (Westerblad et al. 1991). Since fast-twitch fibers are stronger than slow-twitch fibers, a muscle must recruit a larger number of slow-twitch fibers to provide a given force. From other standpoint, during high-intensity exercise, oxygen delivery is impeded and muscle cells must instead rely on anaerobic pathways such as that involving creatine phosphate anaerobic glycolysis to maintain ATP levels required for contraction (Hargreaves and Spriet 2006). Oxygen availability may be limited during both dynamic and static exercise. During dynamic exercise, delivery levels may not meet demand; while during static exercise insufficient blood flow brought on by elevated intramuscular pressure can be a limiting factor (Hargreaves and Spriet 2006). As oxygen delivery is impeded, muscle cells must rely on anaerobic mechanisms to restore ATP supply. Breakdown of ATP in fast-twitch fibers occurs at a faster rate than its regeneration (Burke et al. 1973). Slow-twitch fibers use less ATP and accumulate metabolites at a slower rate than fast-twitch fibers, so their endurance time is greater than that of other muscle fiber types (Katz et al 1986). The recruitment of new slow-twitch fibers could be confirmed by an increase in EMG signal of the erector spinae muscle group while developing fatigue for a given force. Meanwhile the rate of EMG increase of trunk extensor muscles depends on experimental design and the particular manner of fatigue development. In addition, when an increase in EMG amplitude of a fatiguing muscle is observed under a given force, it could be assumed that a decrease in

its maximum force generation capacity has occurred, so enhancement of EMG signals during a fatiguing exertion includes recruitment of more slow-twitch fibers to compensate for a decline in force capability. Therefore part of the observed fatigued muscle EMG signals are errors (artifacts) that should be modulated.

Sparto and Parnianpour (1999) indicated that gain factor declined as fatigue developed. The results of the present study confirmed this behavior, although we predicted the gain factor of a fatigued muscle using the ratio of median frequency and the pre-fatigue gain factor (Equation 7). The maximum muscle stress per square centimeter of cross-sectional area (gain factor) that can be provided by fresh muscle is greater than that of fatigued muscle. Burke et al. (1973) showed that the fast-twitch fibers recruited when muscle is fresh are physically stronger than the slow-twitch fibers recruited in the state of muscle fatigue. Hence, gain factor is dependent on recruitment of these fast or slow-twitch fibers, and declines during recruitment of slow-twitch fibers when muscles undergo fatigue. Accordingly, diminished muscle capability is compensated via recruitment of greater numbers of slow-twitch fibers for a given force. Indeed, it can be ascertained that observed enhancements of the EMG signals of fatigued muscle for a given force do not result from increasing muscle tensile force, and it needs to be modulated by considering correct gain factors. Results showed that estimation of internal moment with invariant gain leads to an increase of over 20% of its initial value over TIME, even as the exerted external moment maintained is constant, and therefore this result is not correct. It occurs because gain factor is not modulated for fatigued muscle as the protocol progresses and artificial enhancement of EMG signals of fatigued muscle are erroneously considered and treated as increases in muscle tensile force. The improvement of the mean absolute error and normalized error

affirmed the necessity of considering use of a time-variable gain factor when studying fatiguing lifting exertions. Estimation of internal moment as well as post-fatigue gain factor for new subjects (in the model validation phase of this study) using the modified EMG-assisted model showed that the model estimated spine loading well without changing force-length or force-velocity modulation factors while only performing maximum voluntary contractions in the unfatigued condition. Frequent maximum voluntary contractions employed by Sparto and Parnianpour (1999) can accelerate the development of fatigue, de-motivate the participants, and increase the risk of injury. Hence, while using the present modified EMG-assisted model, the subject was not asked to perform frequent maximum voluntary exertions

Clark et al. (2003) have shown that, by performing prolonged submaximal isometric extension, the EMG amplitudes of erector spinae group increase by up to about 55% of endurance time for a given force, and then decrease while EMG activity of hip extensor muscles increases. San Juan et al. (2005) indicated that, to attain optimum recruitment of the trunk extensor muscles, a pelvic stabilizer must be used. The present study confirmed results of these studies even including pelvic restriction (San Juan et al. 2005). This systematic contribution of lower-extremity muscles suggests that, as fatigue develops in trunk extensors, and their force generation capability decreases, the musculature control system recruits lower-extremity extensor muscles to prevent pelvic rotation and to provide the moment needed to increase endurance time. Accordingly, to evaluate the impact of fatigue on trunk extensor muscles, we examined EMG signals over the first 75 seconds of the isometric-extension phase (about 50% of subject's endurance time). It is believed that, even if a fatiguing muscle exhibits an EMG signal decrease, the captured EMG signals also contain

fatigue artifacts and should be modulated. This could most likely happen in free dynamic fatiguing lifting exertion. For instance, a greater contribution of other trunk extensor or even lower extremity to provide some of the required moment by developing fatigue in the erector spinae muscle group might cause the erector spinae EMG to decline. However captured EMG signals of fatigued muscle still contain fatigue artifact and need to be modulated.

It is acknowledged that muscle geometry i.e., action line and moment arm, has significant impact on modeled spinal loading. In the present study, subjects were trained during the first session to maintain constant posture under all conditions; therefore possible errors relevant to consideration of detailed muscle geometry were consistent. On the other hand, the lifting exertions were performed in sagittally symmetric postures and data were measured during concentric range of motion; hence, the impact with respect to the modeling action line for abdomen muscles is negligible. In the present lifting exertions, antagonist muscles only work as stabilizers, so their activation levels are usually small.

Potvin and O'Brien (1998) indicated that, during fatiguing contraction, antagonist muscle activation level and resulting co-contraction force increases. The present study confirmed increasing levels of abdominal muscle activation as fatigue progressed. Although the compression forces on L5/S1 didn't change significantly using predicted gain factor similar to actual gain factor, the invariant gain factor led to an increase of over 20% in the compression force compared to its initial value. The A-P shear force increased due to developing fatigue for all three gain factors, for a given force. This result might due to the curved shape of the external oblique having a significant impact on A-P shear force component. However, use of invariant gain factor led to about 15% overestimation in comparison with actual gain factor, while it was less than 5% for predicted gain factor. The

present model could be useful for exploration of differences in the trunk musculoskeletal control system of healthy workers or workers with lower-back disorders. The stochastic features of agonist and antagonist muscle activities (Mirka and Marras 1993) required researchers to pay special attention to variability of compression and shear forces on L5/S1 under different conditions in order to trace possible risk factors for low-back disorders. Hence, the present model would be capable of estimating the pre-fatigue and post-fatigue spinal loads simultaneously; thus, it could be more reliable in predicting muscle forces during the performance of repeated lifting and might provide valuable information for discovery of the potential source of low-back disorders. Variability in spinal loading during repetitive-lifting exertions could affect the risk of LBDs. Most biomechanical models, i.e., optimization models, estimate indistinguishable spine loads during repeated biomechanical performance even though the depicted shear force in the present study changed markedly during fatiguing exertion for a given force. Clarifying biomechanical variability associated with MMH could therefore help in understanding of the etiology of occupational risk factors, possibly leading to an improved criteria task design. However some studies using EMG-assisted model have attempted to estimate biomechanical variability in repetitive-lifting exertion while failing to consider decline in force-generation capacity of fatigued muscle (Marras and Granata 1997; Granata et al. 1999). It is believed that, during repetitive lifting exertion, fatigue could easily occur and therefore the gain factor for fatigued muscle should be modified to accurately estimate spine loading.

6.4 Limitation and future work

It is acknowledged that more detailed models are needed under certain specific conditions like those in various fatigue-developing protocols. Lower-extremity muscles such as gluteus maximus, bicep femoris, and semitendinosus control pelvic rotation and therefore, like passive tissue moments, they can provide moments to extend the spine. It is suggested that, for future studies, the function of these muscles be monitored in free fatiguing lifting exertions, or even by developing an EMG-assisted model that consider lower extremity components.

The internal oblique's deeper location makes it hard to collect EMG signals using surface EMG electrodes. McGill et al. (1996) described the capture of internal oblique EMG signals by using surface electrodes, resulting in 10 to 15 % of MVC difference in comparison with what would be captured with fine wire electrodes, so such signals captured by surface electrodes could not be reliably applied in EMG-assisted spine biomechanical models. In fact the measured surface EMG signal for this muscle could come from the latissimus dorsi therefore it was not modeled in present study. During lateral bending and twisting exertions, the internal oblique is employed as one of primary extensors whose behavior must be captured with fine-wire electrodes. Moreover, in this study only sagittally-symmetric lifting exertions were considered. It might be useful to measure just how abdominal muscle activity changes under twisting-fatiguing or asymmetrical-lifting exertions.

In the present model, latissimus dorsi is counted as an effective extensor muscle in L5/S1 (Marras and Granata; 1997) although Bogduk et al. (1998) reported that the possible contribution of latissimus dorsi to lumbar spine extension is small. While some researchers believe that the latissimus dorsi and posterior aspect of internal oblique muscles share the

extension moment during repetitive lifting exertion (Granata et al. 1999; Marras and Granata 1995) other studies have shown that the main function of the latissimus dorsi is on actions like pulling and providing required force for shoulder movement (Bogduk et al. 1998; Bergmark 1989). The maximum contribution of the latissimus dorsi is to provide an extensor moment on the lumbar spine whose value is less than 5% of the total external moment (Bogduk et al. 1998). Hence the latissimus dorsi doesn't belong to the lumbar spine and considering it only increases spine-modeling complexity without gaining any extra accuracy. The latissimus dorsi must, however, be modeled in shoulder-based or pulling tasks (Bogduk et al. 1998). In the current EMG-assisted model, the function of latissimus dorsi became more significant through developing fatigue due to its increased activity in providing the aforementioned force required using shoulders when the force generation capability of the erector spinae decreased. It seems necessary to determine the actual impact of the latissimus dorsi on spine loading in L5/S1 level, whether through sampling or some other means. Moreover, the internal oblique muscle is known to be a flexor with its centroid point in the anterior side of the spinal column. We believe deep trunk muscles such as the quadratus lumborum share a required moment with the erector spinae and, when the erector spinae is fatigued, these muscles try to compensate for declining force in the erector spinae. The smaller moment arm of these muscles in comparison with the erector spinae leads to a dramatically higher activation of them to provide the required internal moment. These muscles have a smaller cross-sectional area, and so are more likely to produce an overexertion trauma in order to provide needed internal moment (Marras and Mirka 1992). Granata et al. 1999 reported that muscle recruitment strategy used by an expert manual material handler is different than for novice workers. Interaction variability among

superficial and deep trunk muscles during lifting exertions is a possible item of interest in distinguishing between expert and novice workers.

Employing an accurate spine biomechanical model is very helpful for ergonomists and biomechanical engineers to know with a level of high confidence the distribution of spine loading during muscular fatigue development. This high level of confidence will assist them to clarify the variability of spine loading associated with fatigue induced by MMH and possibly also help in the understanding of the etiology of occupational risk factors. Finally it may lead to the establishment of better safety criteria for task design and duty cycles in order to avoid low back injuries.

CHAPTER 7. CONCLUSIONS

The present study develops and validates an EMG-assisted biomechanical spinal model under fatiguing lifting exertions. This novel EMG-assisted model can lead to accurate estimates of spine loading, and requires only gain factor modification. Our results indicate that, for the levels of trunk flexion angle and trunk extension velocity considered in this study, no force-length or force-velocity modulation factors or measurement of frequent maximum voluntary contractions are necessary. In this study, the gain factor is modified by the ratio of median frequency (value at pre-fatigue and value at a fatigued state). The developed EMG-assisted model was validated by estimation of spine loading for two new subjects. The mean normalized error between external moment and internal moment using invariant gain factor was 22% while it was improved to 11% using the modified gain factor for fatigued muscle.

Using this novel EMG-assisted biomechanical model to assess spinal load, our results showed that an increase in co-activation force of antagonist muscles under fatigued conditions led to an increase in shear force on L5/S1, while compression force didn't change significantly. This is in direct contrast to previous studies that have shown an increase in compression and we feel that this increase is a result of inaccuracies in the way the fatigued muscle forces were modeled. The results are very helpful for ergonomists and biomechanics engineers to know with a level of high confidence the distribution of spine loading during fatigue development as it will help in the establishment of better safety criteria for task design in order to avoid possible risk factors.

REFERENCES

Adam, A., De Luca, C. J (2003). Recruitment order of motor units in human vastus lateralis muscle is maintained during fatiguing contractions. J Neurophysiol 90:2919-27.

Adriane, E. D., Bronk, D. W (1929). The discharge of impulses in motor nerve fibres, Part II. The frequency of discharge in reflex and voluntary contractions. J. Physiol 67:119-.

Allen, D. G., Lamb, G. D (2008). Westerblad H. Skeletal muscle fatigue: cellular mechanisms. Physiol Rev 88: 287-332.

Arendt-Nielsen, L., Mills, K. R (1985).The relationship between mean power frequency of the EMG spectrum and muscle fiber conduction velocity. Clin. Neurophysiol. 60: 130-6.

Aspden, R. M (1989). The spine as an arch: A new mathematical model. Spine 14:266-74.

Bean, J.C., Chaffin, D.B., Schultz, A.B (1988). Biomechanical model calculation of muscle contraction forces: a double linear programming method. Journal of Biomechanics 21: 59-66.

Bergmark, A (1989). Stability of the lumbar spine. A study in mechanical engineering. Acta Orthop Scand. 230: (Suppl 60):20-4.

Bernard, B. P (1997). Musculoskeletal disorders and workplace factors: a critical review of epidemiologic evidence for work related musculoskeletal disorders of the neck, upper extremity, and low back. Cincinnati (OH): National Institute for Occupational Safety and Health, US.

Bigland, B., Lippold, C. J (1954). The relation between force, velocity and integrated electrical activity in human muscles. J. Physiol 123: 214- 24.

Bogduk, N., Johnson, G., Spalding, D (1998). The morphology and biomechanics of latissimus dorsi. Clin Biomech 13:377-85.

Bogduk, N., Macintosh, J.E., Pearcy, M.J (1992a). A universal model of the lumbar back muscles in the upright position. Spine 17: 897-913.

Burke, R. E., Levine, D. N., Tsairis, P. Zajac, F. E (1973). Physiological types and histochemical profiles in motor units of the cat gastrocnemius. J. Physiol. (Lond.) 234: 723-48.

Chaffin, D. B (1969). A computerized biomechanical model-development of and use in studying gross body actions. J biomech. 2429-41.

Chaffin, D. B., Andersson, G. B. J., Martin B. J (1999).Occupational Biomechanics, John WILEY & Sons, Inc (3rd Edition).

Cholewicki, J., McGill, S.M (1994). EMG assisted optimization: a hybrid approach for estimating muscle forces in an indeterminate biomechanical model. J of Biomechanics 27:1287-1289.

Cholewicki, J, McGill, S.M., Norman, R.W (1995). Comparison of muscle forces and joint load from an optimization and EMG assisted lumbar spine model: towards development of a hybrid approach. Journal of Biomechanics 28: 321-31.

Curtin, N. A., Edman, K. A (1994). Force-velocity relation for frog muscle fibres: effects of moderate fatigue and of intracellular acidification. J Physiol 475: 483-94.

Crowninshield, R. D., Brand, R. A (1981). A Physiologically Based Criterion of Muscle Force Prediction in Locomotion. J. Biomech 14: 793-801.

Davis, J.R., Mirka, G.A (2000). Transverse-contour modeling of trunk muscle-distributed forces and spinal loads during lifting and twisting. Spine 25: 180-189.

Delp, S.L., Suryanarayanan, S., Murray, W.M., Uhlir, J., Triolo, R.J (2001). Architecture of the rectus abdominis, quadratus lumborum, and erector spinae.J Biomech. 34:371-5.

De Luca, C. J (1993). Use of the surface EMG signal for performance evaluation of back muscles. Muscle Nerve.16:210-216.

De Luca, C. J., Lefeverrs, Mccue M. P., Xenakis, A. P (1982). Behaviour of human motor units in different muscles during linearly varying contractions. J Physiol (Lond) 329: 113-28.

De Luca, C. J (1997). The use of surface electromyography in biomechanics. J Appl Biomech 13: 135-63.

Dempsey, P.G., Hashemi, L (1999). Analysis of workers 'compensation' claims associated with manual material handling. Ergonomics 42 (1): 183 -95.

De Ruiter, C.J., Didden, W.J.M., Jones, D.A. and De Haan, A (2000). The force-velocity relationship of human adductor pollicis muscle during stretch and the effects of fatigue. Journal of Physiology 526: 671 –681.

De Ruiter, C. J., De Haan, A (2001). Similar effects of cooling and fatigue on eccentric and concentric force-velocity relationships in human muscle. J Appl Physiol 90: 2109–16.

Dolan, P., Mannion, A.F., Adams, M.A (1994). Passive tissues help the back muscles to generate extensor moments during lifting. J Biomech 27:1077-85.

Dolan, P., Mannion, A.F. and Adams, M.A (1995). Fatigue of the erector spinae muscles a quantitative assessment using 'frequency banding' of the surface EMG signal. Spine 20: 149-59.

Dolan, P., Kingman, I., De Looze, M. P, et al (2001). An EMG technique for measuring spinal loading during asymmetric lifting. Clin Biomech; 16: S17-24.

Doud, J. R., Walsh, J. M (1995). Muscle fatigue and muscle length interaction: effect on the EMG frequency components. Electromyogr. Clin. Neurophysiol 35: 331-9.

Drewes, C. D (1999c). Electromyography: Recording electrical signals from human muscle. Tested Studies for Laboratory Teaching, Association for Biology Laboratory Education (ABLE), 21: 248-70.

Duggan, P. F., Martonosi, A (1970). Sarcoplasmic reticulum. IX. The permeability of sarcoplasmic reticulum membranes. J. gen. Phy8iol. 56:147-67.

Ebashi, S (1991). Excitation-contraction coupling and the mechanism of muscle contraction. Ann. Rev. Physiol 53: 1-16.

Fathallah, F. A, Marras, W. S., Parnianpour, M., Granata, K. P (1997). A method for measuring external spinal loads during unconstrained free-dynamic lifting. J Biomech 30: 975-8.

Freivalds, A., Chaffin, D. B., Garg, A., et al (1984). A dynamic biomechanical evaluation of lifting maximum acceptable loads. J Biomech. 17:251-62.

Gardner-Morse, MG, Stokes IA (1998). The effects of abdominal muscle coactivation on lumbar spine stability. Spine 23: 86-91

Gagnon, D., Lariviere, C., Loisel, P (2001). Comparative ability of EMG, optimization, and hybrid modelling approaches to predict trunk muscle forces and lumbar spine loading during dynamic sagittal plane lifting, Clin. Biomech. 16 (5):359-72.

Gracovetsky, S., Farfan, H (1986). The optimum spine. Spine 11:543-73.

Granata, K. P., Marras, W. S (1993). An EMG-assisted model of loads on the lumbar spine during asymmetric trunk extensions. J Biomech 26:1429-38.

Granata, K. P., Marras, W. S (1995). An EMG assisted model of biomechanical trunk loading during free-dynamic lifting. J Biomech 28:1309-17.

Granata, K. P., Marras, W. S. and Davis, K. G (1999). Variation in spinal load and trunk dynamics during repeated lifting exertions, Clinical Biomechanics, 14: 367 -375.

Granata, K.P., Slota, G.P., Wilson, S.E (2004b). Influence of fatigue in neuromuscular control of spinal stability. Hum Factors 46:81-91.

Hagberg, M (1981). Muscular endurance and surface electromyogram in isometric and dynamic exercise. J Appl Physiol 51:1-7.

Hargreaves, M., Spriet, L. L (2006). Exercise Metabolism, 2nd edition. Champaign, Illinois: Human Kinetics.

Heckathorne, C. W., Childress, D. S (1981). Relationship of the surface electromyogram to the force, length, velocity, and contraction rate of the cineplastic arm. American Journal of Physical Medicine 60:1-19.

Hoogendoorn, W.E., Van Poppel, M.N.M., Bongers, P.M., Bouter, B.W., Bouter, L.M (1999). Physical load during work and leisure time as risk factors for back pain, Scandinavian Journal of Work Environment and Health 25 (5): 387-403.

Hughes, R.E (1995). Choice of optimization models for predicting spinal forces in a three-dimensional analysis of heavy work. Ergonomics 38 (12): 2476-84.

Huxley, A. F., Niedergerke, R (1954). Structural changes in muscle during contraction. Interference microscopy of living muscle fibers. Nature 173: 971-3.

Huxley, A. F (1957). Muscle structure and theories of contraction. Prog. Biophy8. biophy8. Chem 7: 255-318.

Huxley. A. F. 1974. Muscular contraction. J. Physiol 243:1-43.

Hüppe, A., Müller, K., Raspe, H (2007). Is the occurence of back pain in Germany decreasing? Two regional postal surveys a decade apart. Eur J Public Health17:318-22.

Inbar, G.F., Allin, J., Kranz, H (1987). Surface EMG spectral changes with muscle length. Med Biol Eng Comput 25(6):683-9.

Jorgenson, M.J., Marras, W.S., Granata, K.P., Wiand, J.W (2001). MRI-derived moment-arms of the female and male spinal loading muscles. Clinical Biomechanics 16:182-93.

Jorgensen, M.J., Marras, W.S., Gupta, P., Waters, T.R (2003a). The effect of torso flexion on the lumbar torso extensor muscle sagittal plane moment arms. The Spine J 3: 363-9.

Jorgensen, M.J., Marras, W.S., Gupta, P (2003b). Cross-sectional area of the lumbar back muscles as a function of torso flexion. Clin. Biomech 18: 280-286.

Katz, J. N (2006). Lumbar disc disorders and low-back pain: Socioeconomic factors and consequences. J Bone Joint Surg Am 88:S21-4.

Katz, A., Sahlin, K., Henriksson, J. (1986). Muscle ATP turnover rate during isometric contraction in humans. Journal of Applied Physiology 60: 1839-42.

Kumar, S (2001). Theories of musculoskeletal injury causation. Ergonomics 44: 17-47.

Lamb, R., Hobart, D (1992). Anatomic and Physiologic Basis for Surface Electromyography., Selected Topics in Surface Electromyography for Use in the Occupational Setting: Expert Perspectives 6-21.

Lawrence, R. C., Helmick, C. G., Arnett, F. C., et al (1998). Estimates of the prevalence of arthritis and selected musculoskeletal disorders in the United States. Arthritis Rheum 41:778-99.

Lippold, O (1952). The relation between integrated action potentials in the human muscle and its isometric tension. J Physiol 117:492-9.

Lloyd, D.G., Besier, T.F (2003). An EMG-driven musculoskeletal model to estimate muscle forces and knee joint moments in vivo.J. Biomech. 36: 765-76.

Mamaghani, N. K., Shimomura, Y., Iwanaga, K., Katsuura, T (2002). Mechanomyogram and electromyogram responses of upper limb during sustained isometric fatigue with varying shoulder and elbow postures. J Physiol Anthropol Appl Human Sci; 21(1):29-43.

Mannion, A.F., Connolly, B., Wood, K., Dolan, P (1997). The use of surface EMG power spectral analysis in the evaluation of back muscle function. J Rehabil Res Dev 34:427-39.

Mannion, A.F., Dolan, P (1994). Electromyographic median frequency changes during isometric contraction of the back extensors to fatigue. Spine 19(11) :1223-9.

Mannion, A. F., Dolan, P (1996). The effects of muscle length and force output on the EMG power spectrum of the erector spinae. J Electromyogr Kinesiol 6: 159-68.

Manchikanti, L., Singh, V., Smith, H. S., Hirsch, J. A (2009). Evidence-based medicine, systematic reviews, and guidelines in interventional pain management: Part 4: Observational studies. Pain Physician 12:73-108.

Merletti, R., Parker PA (2004). Electromyography: Physiology, Engineering, and Noninvasive Applications. Hoboken, NJ: Wiley.

Marras, W.S., Jorgenson, M.J, Granata, K.P., Wiand, B (2001). Female and male trunk geometry: Size and prediction of the spine loading trunk muscles derived from MRI. Clinical Biomechanics16:38-46.

Marras, W. S., Lavender, S. A., Leurgans, S. E., Fathallah, F. A., Ferguson, S. A., Allread, W. G., Rajulu, S. L. (1995). Biomechanical risk factors for occupationally related low-back disorders, Ergonomics 38: 377- 410.

Marras, W. S., Lavender, S. A., Leurgans, S. E., Rajulu, S. L., Allread, W. G., Fathallah, F. A. and Ferguson, S. A (1993). The role of dynamic three-dimensional motion in occupationally-related low-back disorders, Spine 18: 617 - 28.

Marras, W. S., Granata, K. P (1996). Spine loading during trunk lateral bending motions. J Biomech 30:697-703.

Marras, W.S., Granata, K. P (1997). Changes in trunk dynamics and spinal loading during repeated trunk exertions. Spine 22:2564-70.

Marras, W.S (1990). Guidelines: industrial electromyography. International Journal of Industrial Ergonomics, 6, 89-93.

Marras, W.S., Sommerich, C. M (1991). A three-dimensional motion model of loads on the lumbar spine: I. Model structure. Human Factors 33:123-37.

Marras, W.S., Sommerich, C, M (1991). A three-dimensional motion model of loads on the lumbar spine: II. Model validation. Human Factors 33:139-49.

Marras, W.S., Granata, K. P (1995). A biomechanical assessment and model of axial twisting in the thoraco-lumbar spine. Spine 20:1440-51.

Marras, W.S., Granata, K.P (1997). The development of an EMG-assisted model to assess spine loading during whole-body free-dynamic lifting. J Electromyogr Kinesiol 7:259-68.

Marras, W.S., Mirka, G. A (1992). A comprehensive evaluation of trunk response to asymmetric trunk motion. Spine. 17: 318-26.

Marras, W.S (2000). Occupational low back disorder causation and control. Ergonomics. 43: 880-902.

McGill, S.M (1997). The biomechanics of low back injury: implications on current practice in industry and the clinic. Journal of Biomechanics 30: 465-75.

McGill, S.M., Norman, R.W (1986). Partitioning of the L4-L5 dynamic moment into disc, ligamentous, and muscular components during lifting. Spine 11, 666-78.

McGill, S.M., Norman, R. W (1985). Dynamically and statically determined low back moments during lifting. J Biomech 8:877- 85.

McGill, S.M., Norman, R. W (1987). Effects of an anatomically detailed erector spinae model on L4/L5 disc compression and shear. J Biomechanics 20: 591-600.

McGill, S.M., Hoodless, K (1990). Measured and modelled static and dynamic axial trunk torsion during twisting in males and females. J. Biomed. Engng12: 403-09.

McGill, S.M (1992). A myoelectrically based dynamic three-dimensional model to predict loads on lumbar spine tissues during lateral bending. Journal of Biomechanics 25: 395-414.

McGill, S.M., Santiguida, L., Stevens, J (1993). Measurement of the trunk musculature from T5 to L5 using MRI scans of 15 young males corrected for muscle fiber orientation. Clin Biomech 8:171-8.

McGill, S.M., Juker, D., Kropf, P (1996). Appropriately placed surface EMG electrodes reflect deep muscle activity (psoas, quadratus lumborum, abdominal wall) in the lumbar spine. J Biomech. 29:1503-1507.

McGill, S.M., Juker, D., Kropf, P (1996). Quantitative intramuscular myoelectric activity of quadratus lumborum during a wide variety of lift tasks. Clin Biomech (Bristol, Avon)11:170-2.

Milner-Brown, H. S., Stein, R. B., Yemm, R (1973 a). The contractile properties of human motor units during voluntary isometric contractions. J. Physiol. 228: 285-306.

Milner-Brown, H. S., Stein, R. B., Yemm, R (1973b). Changes in firing rate of human motor units during linearly changing voluntary contractions. J. Physiol 230: 371-90.

Mirka, G. A., Marras, W. S (1993). A stochastic model of trunk muscle coactivation during trunk bending. Spine 1811:1396-409.

Moritani, T., Nagata, A., Muro, M (1982). Electromyographic manifestations of muscular fatigue. Med Sci Sports Exerc 14:198–202.

Morris, J.M., Lucas, D.B., Bresler, B (1961). Role of the trunk in stability of the spine. Journal of Bone and Joint Surgery 43: 327-52.

O'Brien, P.R., Potvin, J, R (1997). Fatigue–related EMG responses of trunk muscles to a prolonged, isometric twist exertion. Clin Biomech. 12:306-13.

Petrofsky, J. S., Glaser, R. M., Phillips, C. A., Lind, A. R. Williams, C (1982). Evaluation of the amplitude and frequency components of the surface EMG as an index of muscle fatigue. Ergonomics 25: 213-23.

Potvin, J. R., Bent, L. R (1997). A validation of techniques using surface EMG signals from dynamic contractions to quantify muscle fatigue during repetitive tasks. J Electromyo Kinesiol 7:131-9.

Potvin, J. R., O'Brien, P.R (1998). Trunk muscle co-contraction increases during fatiguing, isometric, lateral bend exertions. Spine.23:774–81.

Punnett L, Fine LJ, Keyserling WM, Herrin GD, Chaffin DB (1991). Back disorders and nonneutral trunk postures of automobile assembly workers. Scand J Work Environ Health 17: 337-46.

Punnett, L., Wegman, D. H (2004). Work-related musculoskeletal disorders: the epidemiologic evidence and the debate. J Electromyogr Kinesiol 14:13–23.

Redfern, M (1992). Functional muscle: effects on electromyographic output. In: Soderberg GL, editor. Selected Topics in Surface Electromyography for the Use in the Occupational Setting: Expert Perspectives. Cincinnati, OH: US Department of Health and Human Services, Public Health Service.

Reilly, C. H., Marras, W. S (1989). Simulift: A simulation model of the human trunk motion. Spine 14:5-11.

Raschke U., Chaffin, D.B (1996). Support for a linear length–tension relation of the torso extensor muscles: An investigation of the length and velocity EMG– force relationship. J Biomech 29:1597-604.

Rassier, D.E., Macintosh, B.R., Herzog, W (1999). Length dependence of active force production in skeletal muscle. J Appl Physiol 86: 1445-57.

San Juan, J.G., Yaggie, J.A., Levy, S.S., Mooney, V., Udermann, B.E, Mayer, J.M (2005). Effects of pelvic stabilization on lumbar muscle activity during dynamic exercise. J. Strength Cond. Res 19(4):903-07.

Schultz, A. B., Andersson, G.B.J (1981). Analysis of loads on the lumbar spine. Spine 6(1):76-82.

Schultz, A. B., Andersson, G. B. I., Haderspeck, K (1982). Analysis and measurement of lumbar trunk loads in tasks involving bends and twists, J Biomech 15: 669-75.

Schultz, A. B., Andersson, G. B. J., Ortengern, R (1982). Loads on the lumbar spine. J Bone joint surgery 64 (5): 713-20.

Sparto, P. J., Parnianpour, M (1999). An electromyography-assisted model to estimate trunk muscle forces during fatiguing repetitive trunk exertions. J. Spinal Disorders 12:509-18.

Sparto, P.J., Parnianpour, M., Marras, W.S., Granata, K.P., Reinsel, T.E., Simon, S (1998). Effect of electromyogram–force relationships and method of gain estimation on the prediction of an electromyogram-driven model of spinal loading. Spine 23(4): 423-9.

Sparto, P.J., Parnianpour, M (1998). Estimation of trunk muscle force and spinal loads during fatiguing repetitive trunk exertions. Spine 22: 2563-73.

Van Dieën J. H., Kingma, I (2005). Effects of antagonistic co-contraction on differences between electromyography based and optimization based estimates of spinal forces. Ergonomics 48:411-26.

Verhaak, P. F., Kerssens, J. J., Dekker, J., Sorbi, M. J., Bensing, J. M (1998). Prevalence of chronic benign pain disorder among adults: a review of the literature. Pain 77: 231-9.

Westerblad, J., Lee J. A., Lannergren, J., Allen, D. G. (1991). Cellular mechanisms of fatigue in skeletal muscle. Am. J. Physiol 261:C195-209.

Wilkie, D. R (1950). The relation between force and velocity in human muscle. J. Physiol 110: 249-80.

APPENDIX A. MATLAB CODE

```
close all
clear all

[file1, text1] = xlsread('Directory',1,'a1:k5');%READ MVC file
     MVC=file1;
 for kk=1;% Subjects #

          directory1=['Directory' num2str(kk) '.xlsx'];
 [file, text] = xlsread(directory1,1, 'c9:p4133');
  q=kk;

[m,z]=size(file);
freq = 1024; %Sampling Frequency
n=floor(m/1024); %n=4; %duration (sec)
N = n*freq/2; % number of samples in half of FFT
f = freq*(0:N)/2/N;
nn = n*1024;
file=file(1:nn,:);
EMG(:,1:10)=file(:,5:14);
[m2,ch]=size(EMG);
loadcell1=file(:,1)*20.055-12.566; % Read amount of force exerted on right
loadcell of ARF
loadcell2=file(:,2)*19.179+12.551; % Read amount of force exerted on left
loadcell of ARF
arfload=(loadcell1+loadcell2)*-9.81; % Total external force measured by
ARF
Voltage=file(:,3); % Read amount of voltage associated to trunk flexion
angle
Angle=185-30.3*Voltage;

for k=1:ch
    data=EMG(:,k);
    data=data-mean(data);
```

```
X = fft(data);
power = abs(X(1:N+1)).^2;

%Filters 0-10 Hz
X((n*0+1):(n*(10)+1))=0;
X(length(X)-(n*(10)-1):length(X)-(n*1-1))=0;
%Filters 59-61 Hz
X((n*59+1):(n*(61)+1))=0;
X(length(X)-(n*(61)-1):length(X)-(n*59-1))=0;
%Filters 119-121 Hz
X((n*119+1):(n*(121)+1))=0;
X(length(X)-(n*(121)-1):length(X)-(n*119-1))=0;
%Filters 179-181 Hz
X((n*179+1):(n*(181)+1))=0;
X(length(X)-(n*(181)-1):length(X)-(n*179-1))=0;
%Filters 239-241 Hz
X((n*239+1):(n*(241)+1))=0;
X(length(X)-(n*(241)-1):length(X)-(n*239-1))=0;
%Filters 102-103 Hz
X((n*102+1):(n*(103)+1))=0;
X(length(X)-(n*(103)-1):length(X)-(n*102-1))=0;
%Filters 203-207 Hz
X((n*203+1):(n*(207)+1))=0;
X(length(X)-(n*(207)-1):length(X)-(n*203-1))=0;
%Filters 306-308 Hz
X((n*305+1):(n*(309)+1))=0;
X(length(X)-(n*(309)-1):length(X)-(n*305-1))=0;
    %Filters 409-410 Hz
X((n*408+1):(n*(411)+1))=0;
X(length(X)-(n*(411)-1):length(X)-(n*408-1))=0;
    %Filters 500-512 Hz
X((n*500+1):(n*(512)+1))=0;
X(length(X)-(n*(512)-1):length(X)-(n*500-1))=0;

power = abs(X(1:N+1)).^2;
```

```
    filtarray = real(ifft(X));
    datafilted(:,k) = filtarray;

end

afilt=abs(datafilted);
for i=1:m2
    arfload1(i,:)=mean(arfload(1:m2,:));
end

    for j=1:m2
        afilt1(j,:)=mean(afilt(1:m2,:));
    end

for i=1:m2
    Angle1(i,:)=mean(Angle(1:m2,:),1);
end

for i=1:m2
    NEMG(i,:)=afilt1(i,1:10)./MVC(q,1:10); % calculate normalized EMG
end

       M=71; % Body mass
       H=1.73; % Height

if q==1  % 10 degree isometric trunk flexion angle
           for i=1:m2
             Vel(i,1)=1;
             L(i,1)=0.94;
           end

end
```

```
if q==2 % 20 degree isometric trunk flexion angle
            for i=1:m2
              Vel(i,1)=1;
              L(i,1)=1;
            end

end

if q==3      % 30 degree isometric trunk flexion angle
            for i=1:m2
              Vel(i,1)=1;
              L(i,1)=0.94;
            end

end

if q==4       % 5 degree per second
            for i=1:m2
            Vel(i,1)=0.975;
            L(i,1)=1;
            end
end



if q==5 % 15 degree per second
            for i=1:m2
                Vel(i,1)=0.925;
                L(i,1)=1;
            End
end



for i=1:m2;
```

```
bodymoment(i,1)=sind(Angle1(i,1))*0.0966*H*0.468*M*9.81+sind(Angle1(i,1))*
(0.277*H+0.135)*0.084*M*9.81; % Body moment
end

        Aexternalmoment=arfload1*0.23+bodymoment; % Total external moment

        for i=1:m2
        originrla(i,:)=[0.25*waistwidth -0.3*waistdepth 0];
        end
        for i=1:m2
        originlla(i,:)=[-0.25*waistwidth -0.3*waistdepth 0];
        end
         for i=1:m2
        originrer(i,:)=[0.2*waistwidth -0.3*waistdepth 0];
         end
         for i=1:m2
        originler(i,:)=[-0.2*waistwidth -0.3*waistdepth 0];
         end
         for i=1:m2
        originrre(i,:)=[0.1*waistwidth 0.55*waistdepth 0];
         end
         for i=1:m2
        originlre(i,:)=[-0.1*waistwidth 0.55*waistdepth 0];
         end
         for i=1:m2
        originrex(i,:)=[0.1*waistwidth 0.55*waistdepth 0];
         end
         for i=1:m2
        originlex(i,:)=[-0.1*waistwidth 0.55*waistdepth 0];
         end
         for i=1:m2
        originrin(i,:)=[0.45*waistwidth -0.3*waistdepth 0];
         end
         for i=1:m2
        originlin(i,:)=[-0.45*waistwidth -0.3*waistdepth 0];
         end
```

```
        for i=1:m2
      origin(i,:)=[-0.061 -0.061 -0.0405 -0.0405 0 0 0.037 0.037 0.076
0.076];
        end

insertionz=0.0275*H;
   for i=1:m2
   insertionrla(i,:)=[waistwidth*0.6
waistdepth*0.1+sind(Angle1(i,1))*insertionz cosd(Angle1(i,1))*insertionz];
   end
   for i=1:m2
   insertionlla(i,:)=[waistwidth*-0.6
waistdepth*0.1+sind(Angle1(i,1))*insertionz cosd(Angle1(i,1))*insertionz];
   end
   for i=1:m2
   insertionrer(i,:)=[waistwidth*0.3 waistdepth*-
0.3+sind(Angle1(i,1))*insertionz cosd(Angle1(i,1))*insertionz];
   end
   for i=1:m2
   insertionler(i,:)=[waistwidth*-0.3 waistdepth*-
0.3+sind(Angle1(i,1))*insertionz cosd(Angle1(i,1))*insertionz];
   end
   for i=1:m2
   insertionrre(i,:)=[waistwidth*0.1
waistdepth*0.55+sind(Angle1(i,1))*insertionz
cosd(Angle1(i,1))*insertionz];
   end
   for i=1:m2
   insertionlre(i,:)=[waistwidth*-0.1
waistdepth*0.55+sind(Angle1(i,1))*insertionz
cosd(Angle1(i,1))*insertionz];
   end
   for i=1:m2
   insertionrex(i,:)=[waistwidth*0.45 waistdepth*-
0.19+sind(Angle1(i,1))*insertionz cosd(Angle1(i,1))*insertionz];
   end
for i=1:m2
```

```
   insertionlex(i,:)=[waistwidth*-0.45 waistdepth*-
0.19+sind(Angle1(i,1))*insertionz cosd(Angle1(i,1))*insertionz];
end

for i=1:m2
 insertionrin(i,:)=[waistwidth*0.45
waistdepth*0.2+sind(Angle1(i,1))*insertionz cosd(Angle1(i,1))*insertionz];
end

for i=1:m2
   insertionlin(i,:)=[waistwidth*-0.45
waistdepth*0.2+sind(Angle1(i,1))*insertionz cosd(Angle1(i,1))*insertionz];
end
   insertionreraction=insertionrer-originrer;
for i=1:m2
   valuerer(i)=norm(insertionreraction(i,:));
end

for i=1:m2
   Valuerer(i,:)=[valuerer(i) valuerer(i) valuerer(i)];
end
   unitvectorrer=insertionreraction./Valuerer;
   insertionleraction=insertionler-originler;
for i=1:m2
   valueler(i)=norm(insertionleraction(i,:));
end
for i=1:m2
   Valueler(i,:)=[valueler(i) valueler(i) valueler(i)];
end
   unitvectorler=insertionleraction./Valueler;
   insertionrlaaction=insertionrla-originrla;
for i=1:m2
   valuerla(i)=norm(insertionrlaaction(i,:));
end
for i=1:m2
   Valuerla(i,:)=[valuerla(i) valuerla(i) valuerla(i)];
```

```
end
   unitvectorrla=insertionrlaaction./Valuerla;
   insertionllaaction=insertionlla-originlla;
for i=1:m2
   valuella(i)=norm(insertionllaaction(i,:));
end
for i=1:m2
   Valuella(i,:)=[valuella(i) valuella(i) valuella(i)];
end
   unitvectorlla=insertionllaaction./Valuella;
   insertionrexaction=insertionrex-originrex;
for i=1:m2
   valuerex(i)=norm(insertionrexaction(i,:));
end
for i=1:m2
   Valuerex(i,:)=[valuerex(i) valuerex(i) valuerex(i)];
end
   unitvectorrex=insertionrexaction./Valuerex;
   insertionlexaction=insertionlex-originlex;
   for i=1:m2
   valuelex(i)=norm(insertionlexaction(i,:));
   end
   for i=1:m2
   Valuelex(i,:)=[valuelex(i) valuelex(i) valuelex(i)];
   end
   unitvectorlex=insertionlexaction./Valuelex;
   insertionrinaction=insertionrin-originrin;
   for i=1:m2
   valuerin(i)=norm(insertionrinaction(i,:));
   end
   for i=1:m2
   Valuerin(i,:)=[valuerin(i) valuerin(i) valuerin(i)];
   end
   unitvectorrin=insertionrinaction./Valuerin;
   insertionlinaction=insertionlin-originlin;
   for i=1:m2
   valuelin(i)=norm(insertionlinaction(i,:));
```

```
    end
    for i=1:m2
    Valuelin(i,:)=[valuelin(i) valuelin(i) valuelin(i)];
    end
    unitvectorlin=insertionlinaction./Valuelin;
    insertionrreaction=insertionrre-originrre;
    for i=1:m2
    valuerre(i)=norm(insertionrreaction(i,:));
    end
    for i=1:m2
    Valuerre(i,:)=[valuerre(i) valuerre(i) valuerre(i)];
    end
    unitvectorrre=insertionrreaction./Valuerre;
    insertionlreaction=insertionlre-originlre;
    for i=1:m2
    valuelre(i)=norm(insertionlreaction(i,:));
    end
    for i=1:m2
    Valuelre(i,:)=[valuelre(i) valuelre(i) valuelre(i)];
    end
    unitvectorlre=insertionlreaction./Valuelre;
unitvectori=[unitvectorrer(:,1) unitvectorler(:,1) unitvectorrla(:,1)
unitvectorlla(:,1) unitvectorrin(:,1) unitvectorlin(:,1)
unitvectorrex(:,1) unitvectorlex(:,1) unitvectorrre(:,1)
unitvectorlre(:,1)];
   unitvectorj=[unitvectorrer(:,2) unitvectorler(:,2) unitvectorrla(:,2)
unitvectorlla(:,2) unitvectorrin(:,2) unitvectorlin(:,2)
unitvectorrex(:,2) unitvectorlex(:,2) unitvectorrre(:,2)
unitvectorlre(:,2)];
   unitvectorz=[unitvectorrer(:,3) unitvectorler(:,3) unitvectorrla(:,3)
unitvectorlla(:,3) unitvectorrin(:,3) unitvectorlin(:,3)
unitvectorrex(:,3) unitvectorlex(:,3) unitvectorrre(:,3)
unitvectorlre(:,3)];

pcsa1=[26 26 20.5 20.5 0 0 10.6 10.6 9.05 9.05]; %Physiological cross
sectional area
   for i=1:m2
```

```
   NEMG1(i,1:4)=L(i)*Vel(i)*NEMG(i,1:4).*pcsa1(1,1:4);
    NEMG1(i,5:10)=NEMG(i,5:10).*pcsa1(1,5:10);
   end
   figure(13), plot(NEMG1),title('NEMG1');
  for G=1:200 % Find the best gain factor
           internalmoment=sum((G*NEMG1.*origin)');
          momentinternal=(internalmoment)';
           er=Aexternalmoment+momentinternal;
           mse(G,1)=mean(er.*er);
  end

gain(q)=find(mse==min(mse));
emgforcevalue=gain(q)*NEMG1;
AER=(emgforcevalue(1,1)+emgforcevalue(1,2))/2; % Erector spinae's tensile
force
       forcei=emgforcevalue.*unitvectori;
       forcej=emgforcevalue.*unitvectorj;
       AShearforce=sum((forcej')); % Anterior-Posterior shear force
       forcez=emgforcevalue.*unitvectorz;
       Acompressionforce=sum((forcez')); % Compression force
       Ainternal=(sum((gain(q)*NEMG1.*origin)'))';% Internal moment


   figure(1),plot(forcei), title('force-x'), ylabel(q);
   figure(2),plot(forcej), title('force-y'), ylabel(q);
   figure(3),plot(forcez), title('force-z'), ylabel(q);
   figure(4),plot(Ainternal), title('Internal-moment'), ylabel(q);

    end
```

APPENDIX B. ADDITIONAL RESULTS OF ISOMETRIC AND ISOKINETIC EXTENSION PHASES

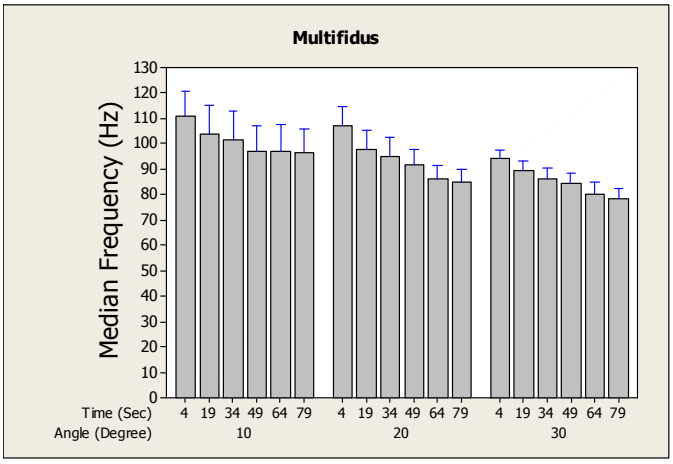

Figure 69. Median frequency of EMG for multifidus as a function of TIME in the isometric phase.

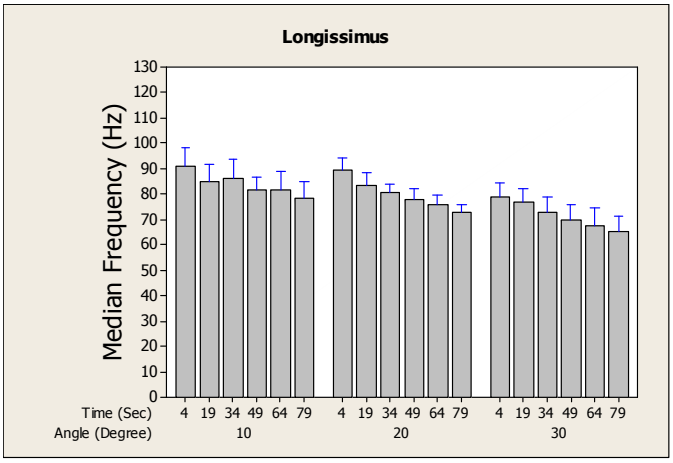

Figure 70. Median frequency of EMG for longissimus as a function of TIME in the isometric phase.

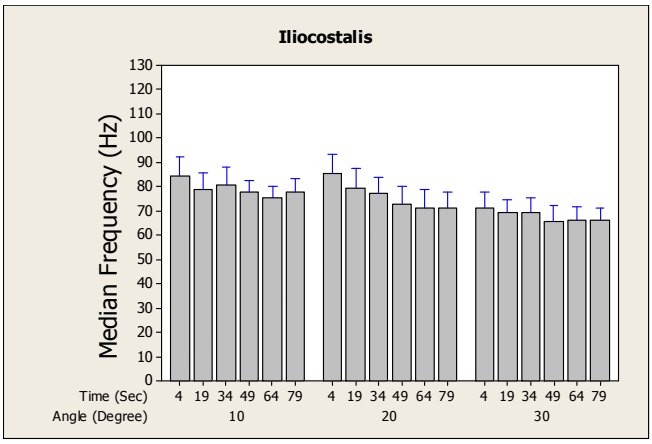

Figure 71. Median frequency of EMG for iliocostalis as a function of TIME in the isometric phase.

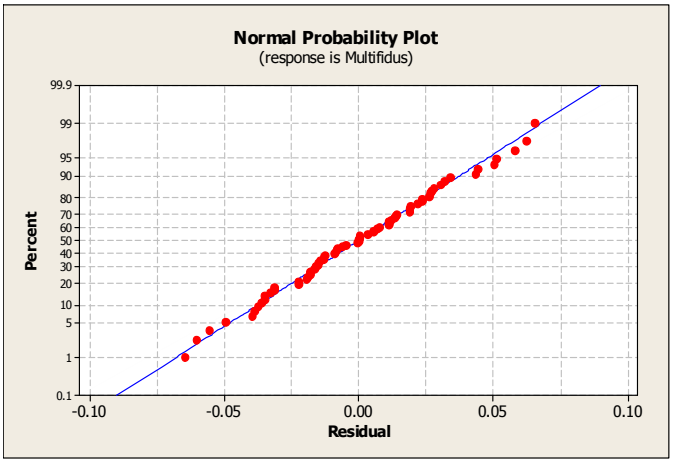

Figure 72. Normal probability plot of the residuals of the NEMG for multifidus.

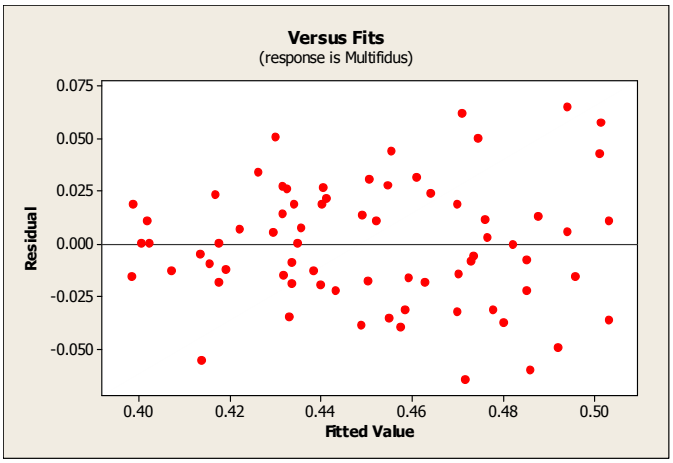

Figure 73. Residuals vs. measured values of the NEMG for multifidus.

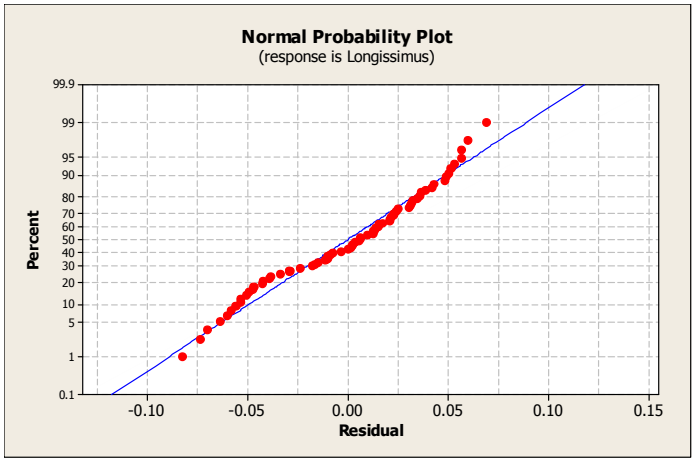

Figure 74. Normal probability plot of the residuals of the NEMG for longissimus.

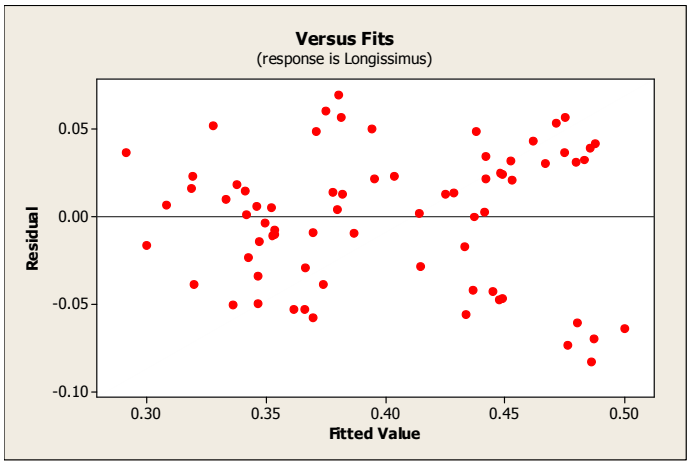

Figure 75. Residuals vs. measured values of the NEMG for longissimus.

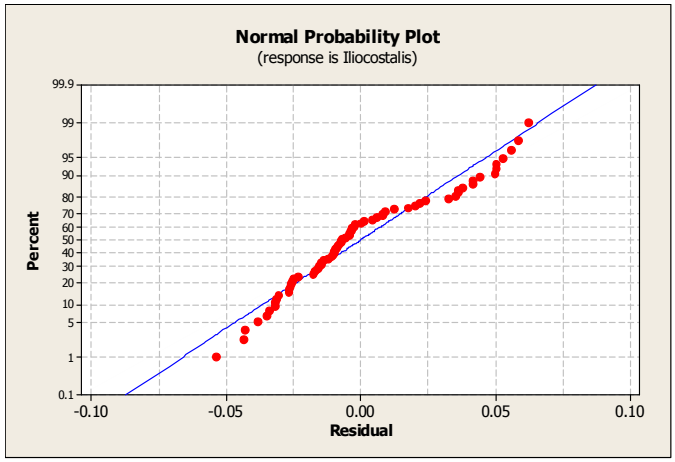

Figure 76. Normal probability plot of the residuals of the NEMG for iliocostalis.

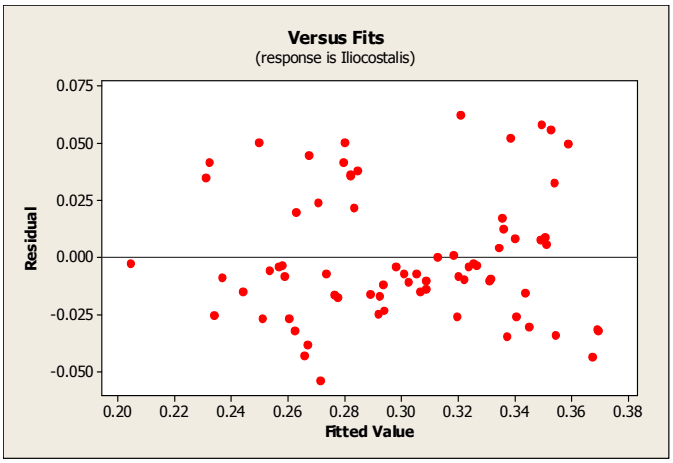

Figure 77. Residuals vs. measured values of the NEMG for iliocostalis.

APPENDIX C. ADDITIONAL RESULTS FOR MODIFIED EMG-ASSISTED MODEL

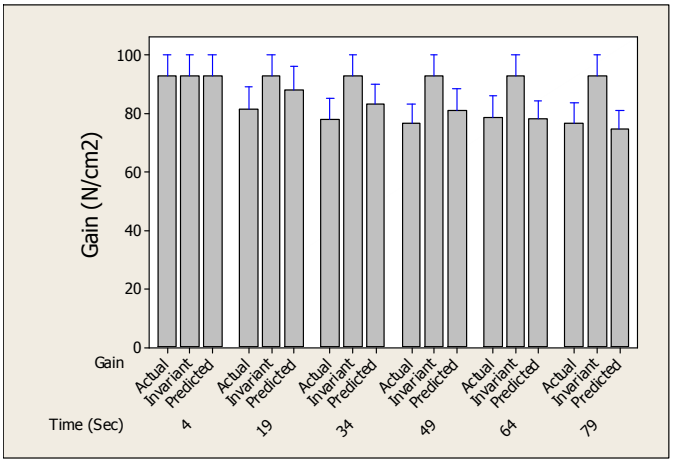

Figure 78. Changes of different gain factors by developing fatigue during isometric extension phase.

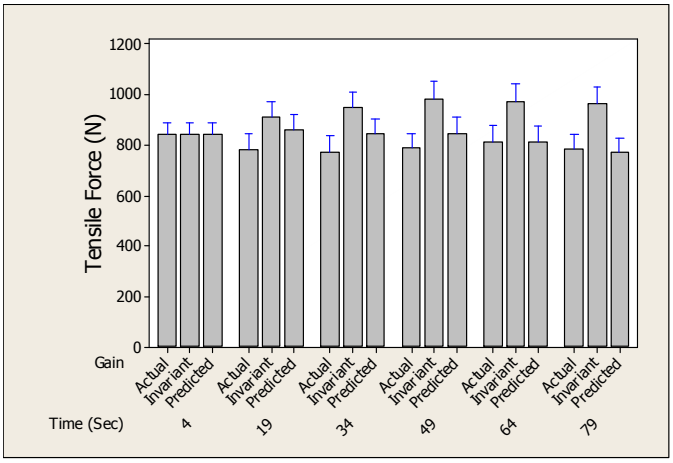

Figure 79. Changes of erector spinae's tensile force for different considered gain factors during developing fatigue in isometric extension phase.

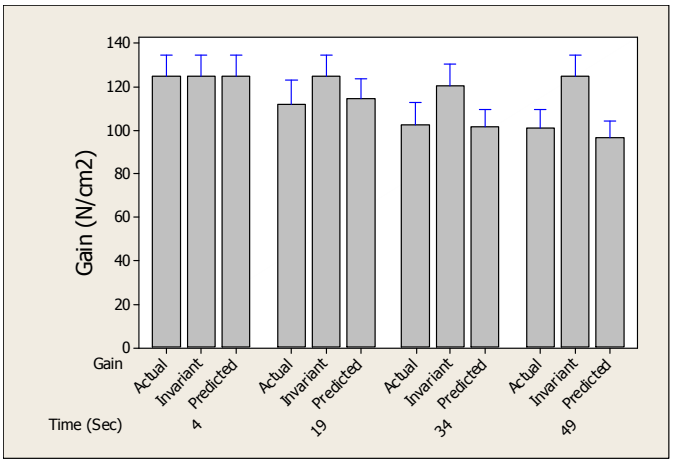

Figure 80. Changes of different considered gain factors by developing fatigue during isokinetic extension phase.

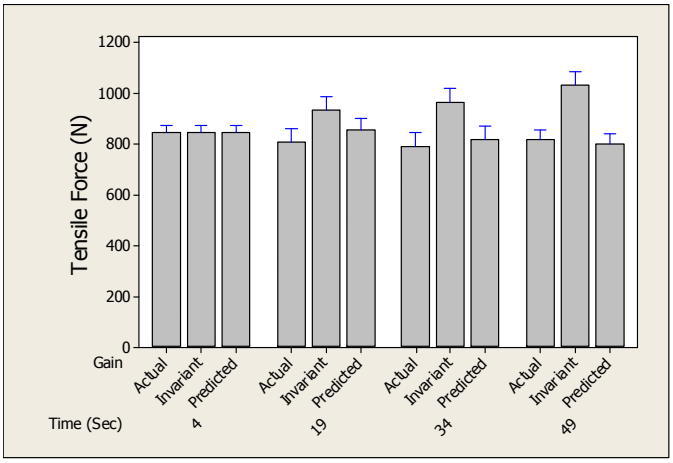

Figure 81. Changes of erector spinae's tensile force for different considered gain factors during developing fatigue in isokinetic extension phase.